Mathematical Derivation of a Homogenized Bidomain Model for Pulsed Field Ablation

Simon Bihoreau-Duchemin, Annabelle Collin, Michael Leguèbe, Clair Poignard

Mathematical Derivation of a Homogenized Bidomain Model for Pulsed Field Ablation

Simon Bihoreau Duchemin[a,b], Annabelle Collin[c], Michael Leguèbe[a,b,d], Clair Poignard[e]

[a] *Centre Inria de l'Université de Bordeaux, Talence, F-33400, France*
[b] *Institut de Mathématiques de Bordeaux, Université de Bordeaux, Talence, F-33400, France*
[c] *Laboratoire de Mathématiques Jean Leray, Nantes Université, Nantes, F-44100, France*
[d] *IHU Liryc, Fondation Bordeaux Université, Pessac, F-33600, France*
[e] *AIMOKA: Inria, Assistance Publique-Hôpitaux de Paris, Université Sorbonne-Paris Nord, Rennes, F-35042, France*

Abstract

Pulsed Field Ablation (PFA) is an emerging technology for the treatment of cardiac arrhythmias, relying on irreversible electroporation to selectively destroy cardiac cells while sparing surrounding structures. Despite its rapid clinical adoption, the mathematical modeling of electroporation in cardiac tissue remains challenging due to the nonlinear interplay between microscopic membrane processes and tissue-scale electrical conduction.

In this work, we derive a multiscale mathematical model for PFA grounded in a microscopic description that explicitly accounts for intra- and extracellular media. Through a rigorous high-order homogenization procedure, we obtain a macroscopic bidomain-type system in which the nonlinearity involves both the electric field magnitude and the macroscopic transmembrane potential. This feature contrasts with the classical bidomain model for electrophysiology, where only the transmembrane potential appears, and reflects the different mechanisms driving electroporation at the cell scale (transmembrane potential increase) and at the tissue scale (electric field intensity).

We establish well-posedness and energy estimates for the microscopic problem, prove convergence of the asymptotic expansion at arbitrary order, and provide numerical evidence supporting the accuracy of the homogenized model. Our results offer a mathematically justified and physically interpretable macroscopic framework for simulating PFA, paving the way for clinically relevant computational studies.

Keywords: Nonlinear high-order homogenization, Bidomain model, Pulsed Field Ablation, Electroporation modeling

1. Introduction

Cardiac ablation is a widespread therapy for the treatment of cardiac arrhythmias. It consists in destroying cardiac cells in targeted areas responsible for the disruption of the electrophysiological current pattern which drives heart contraction. A thin and flexible tube, called catheter, is inserted inside the heart through a blood vessel. The catheter contains

a device, which depends on the technology used, that delivers energy into the region to ablate. The most common ablation technologies are Radio-Frequency Ablation (RFA) [1] relying on heat, cryoablation [2] relying on cold and Pulsed Field Ablation (PFA) relying on a phenomenon called irreversible electroporation.

Recent research focuses on PFA, a promising technology that drastically reduces the risks of damaging adjacent structures as lungs during the ablation while improving the clinical performance [3, 4, 5, 6]. PFA consists in delivering short and intense electric pulses in the cardiac tissue, which induces cell death through irreversible electroporation. Under the effect of the intense electric field, pores appear on the cell membranes which become permeable and are destroyed as a result of excessive exchanges between intra- and extracellular media. Electroporation has been in use for oncology for approximately two decades in superficial tumors, and for about one decade in deep-seated tumor ablations, and its use in cardiology is now increasing [7].

Given the complexity of the electroporation phenomenon and of the cardiac tissue, modeling electrical conduction at tissue scale during PFA - which is the central objective of our work - remains a major challenge for improving both its understanding and its clinical applicability. Several models have already been developed for electrically passive tissues. In most cases, an electrostatic model is used to compute a single electric potential u which satisfies $-\nabla \cdot \sigma \nabla u = f$, where electroporation is modeled through a conductivity σ that depends nonlinearly on the electric field $\|\nabla u\|$ [8, 9, 10]. This approach, that we call standard in the following, is phenomenological: the nonlinearity of σ is not based on a detailed description of the physics on the cell membranes.

Several variations of the standard model for electrically passive tissues have been proposed in the literature: either with a dynamical response of the conductivity with the intensity of the electric field [11], or, more commonly, by adding a dependence on temperature for irreversible electroporation (see for instance Supp. Material 3 of [12] for a collection of standard model variations). Concerning cardiac tissue specifically, some studies use directly the standard model as for passive tissue [13, 14, 15], while others focus on the anisotropic property of muscle fibers [16, 17]. Another approach was proposed earlier in [18], where the authors propose a two dimensional bidomain model - which models cardiac electrical activity and results from the periodic homogenization of microscopic bidomain model accounting for the ionic exchanges at cell membranes - with an electric conductivity that depends solely on the transmembrane voltage instead of $\|\nabla u\|$. Simply plugging an electroporation model into cardiac bidomain equations may not be physically justified, for at least two reasons. First, there is a large magnitude difference between the physiological ionic currents and PFA pulses, which should not lead to the classical bidomain equations after the homogenization process. Secondly, in the case of two electrodes at opposite potentials of the same intensity, the transmembrane voltage in the middle of the electrodes is zero while the electroporated region clearly includes this point [19].

Here, we derive a physically inspired model specifically for PFA, consistent with a microscopic description that explicitly includes intra- and extracellular media. While our approach is conceptually related to the cardiac bidomain model, our microscopic problem is drastically

different in the sense that we focus on the static problem, which is tailored to capture the effects of electroporation for typical microsecond long electroporating pulses, see for instance [20] and references therein. It is worth noting that this change of view point requires also different tools for the mathematical analysis of the model. Starting from this microscopic static PFA problem, which was previously presented in [20], we rigorously carry out the non linear homogenization process with appropriate scaling of the physical quantities involved. Our goal is to derive a macroscopic static bidomain model for PFA that is both mathematically justified and physically interpretable, and that accurately captures the effects of electroporation.

The microscopic model from which we start is itself of great interest, as it provides a detailed description of the physical processes at the cellular scale as shown in the literature [21, 20, 22]. However, due to the extremely high computational cost of microscopic model - see for instance [23] in a cardiac electrophysiology context - it is impractical for large-scale simulations and would be completely intractable in any realistic clinical setting. Deriving a macroscopic homogenized model is therefore essential for enabling clinically relevant numerical studies.

From a mathematical standpoint, several homogenization techniques can be used to derive a macroscopic model from a microscopic one. In the context of cardiac electrophysiology, notable approaches include periodic unfolding methods [24], Γ-convergence [25], and two-scale convergence as introduced by Nguetseng [26] and Allaire [27] and applied in various contexts, including cardiac models [28]. In this work, we will carry out the expansion to high orders, since the classical zero-order limit, obtained by two-scale convergence, is not sufficient in our setting. While such higher-order expansions have not yet been developed for cardiac bidomain models to our knowledge, they have been studied in other contexts; see for instance [29, 30, 31, 32, 33, 34].

Although this is not the main focus of the paper, we provide proofs of well-posedness for all the models appearing in this paper, both at the microscopic and macroscopic scales. These static models differ from the classical microscopic, and therefore also from macroscopic, models of cardiac electrophysiology, which are time-dependent. Consequently, the existence and uniqueness proofs are also different and the numerous studies that have addressed existence and uniqueness of both cardiac micro- and macroscopic models (see for instance [35, 36, 37, 38, 39, 40, 28, 41]) do not apply.

The paper is organized as follows. In Section 2, we introduce the model which accounts for the cell scale, and its nondimensionalization in the context of PFA. We then provide a mathematical analysis including the proof of well-posedness of the equations and the derivation of energy estimates with respect to the small parameter ε corresponding to the ratio between the cellular and tissue scales. Before presenting the full asymptotic analysis, we first focus on the first two orders by using a classical two-scale convergence argument for the limit problem. More precisely, in Section 3, we study the limit problem as ε tends to zero, and formally derive the equation satisfied by the next-order asymptotic term. Together, these constitute the proposed tissue-scale model for PFA, which is the main result of this work and is summarized in Section 3.4 along with an effective model for means of comparison with

the classical bidomain for electrophysiology. Our homogenized model and then its effective version (25) differs from the bidomain model by involving both the electric field magnitude and the macroscopic transmembrane potential in the nonlinearity, while at the microscopic scale only the transmembrane potential matters. This shows that electroporation is driven by transmembrane potential at the cell scale but by the electric field at the tissue scale. We then present numerical evidence of the convergence of the cell-scale model towards this macroscopic model, and introduce a quantity to assess electroporation at the tissue scale, supported by numerical illustrations. Encouraged by the observed numerical convergence rates, we provide a rigorous justification of the asymptotic expansion to any order n in Section 4. This final step makes it possible to derive optimal error estimates and to reveal the influence of the geometry on the higher-order terms.

2. Microscopic modeling and analysis

This section is devoted to the microscopic model considered in this work. We first introduce the geometrical setup, then present the model itself and its nondimensionalization, and finally establish existence and uniqueness results along with energy estimates.

2.1. Geometrical setup

Let $d = 2$ or 3. Let $Y = [0,1]^d$ be the unit mathematical cell with boundary ∂Y. Consider two subdomains Y_i and Y_e of Y, representing the intra- and extracellular media, such that $\overline{Y_\mathrm{i}} \cup \overline{Y_\mathrm{e}} = Y$ and $\mathring{Y}_\mathrm{i} \cap \mathring{Y}_\mathrm{e} = \emptyset$. The interface between these subdomains, corresponding to the cardiac cell membrane, is noted $\Gamma = \partial\overline{Y_\mathrm{i}} \cap \partial\overline{Y_\mathrm{e}}$ (see Figure 1).

To represent the tissue, let $\Omega := \prod_{i=1}^{d}]a_i, b_i[\subset \mathbb{R}^d$, composed of multiple periodically arranged cardiac cells. We assume that there exists a parameter $\varepsilon > 0$ and an index set $N_\varepsilon \subset \mathbb{Z}^d$ such that

$$\overline{\Omega} = \bigcup_{n \in N_\varepsilon} \varepsilon(Y + n).$$

It is worth noting that ε represents the ratio between the characteristic length scale of the cells and that of the macroscopic tissue domain.

We then define the intra- and extracellular subdomains of Ω, and their interface by

$$\overline{\Omega_\mathrm{i}^\varepsilon} := \bigcup_{n \in N_\varepsilon} \varepsilon(\overline{Y_\mathrm{i}} + n), \quad \overline{\Omega_\mathrm{e}^\varepsilon} := \bigcup_{n \in N_\varepsilon} \varepsilon(\overline{Y_\mathrm{e}} + n), \quad \Gamma_\mathrm{m}^\varepsilon := \bigcup_{n \in N_\varepsilon} \varepsilon(\Gamma + n),$$

so that they are unions of rescaled and translated unit-cell subdomains and interfaces. We assume that $\Omega_\mathrm{e}^\varepsilon$ is connected, which is necessary for the Poincaré-Wirtinger inequality in Lemma A.1 to hold, and that $\Gamma_\mathrm{m}^\varepsilon$ is infinitely smooth.

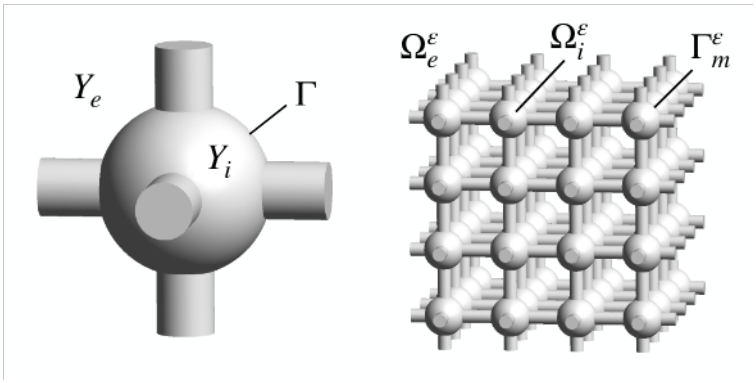

Figure 1: Example of unit cell Y (left) and macroscopic domain Ω (right)

2.2. Microscopic bidomain equations

2.2.1. Model statement

We consider the following static microscopic bidomain model in which the intra- and extra-cellular electric potentials $u_{\mathrm{i}}^\varepsilon$ and $u_{\mathrm{e}}^\varepsilon$ satisfy

$$-\nabla\cdot(\sigma_{\mathrm{i}}^\varepsilon\nabla u_{\mathrm{i}}^\varepsilon) = f^\varepsilon|_{\Omega_{\mathrm{i}}^\varepsilon}, \qquad \text{in } \Omega_{\mathrm{i}}^\varepsilon, \tag{1a}$$

$$-\nabla\cdot(\sigma_{\mathrm{e}}^\varepsilon\nabla u_{\mathrm{e}}^\varepsilon) = f^\varepsilon|_{\Omega_{\mathrm{e}}^\varepsilon}, \qquad \text{in } \Omega_{\mathrm{e}}^\varepsilon, \tag{1b}$$

$$\sigma_{\mathrm{i}}^\varepsilon\nabla u_{\mathrm{i}}^\varepsilon\cdot n_{\mathrm{i}} = \sigma_{\mathrm{e}}^\varepsilon\nabla u_{\mathrm{e}}^\varepsilon\cdot n_{\mathrm{i}}, \qquad \text{on } \Gamma_{\mathrm{m}}^\varepsilon, \tag{1c}$$

$$-\sigma_{\mathrm{i}}^\varepsilon\nabla u_{\mathrm{i}}^\varepsilon\cdot n_{\mathrm{i}} = I_{\mathrm{m}}^\varepsilon(u_{\mathrm{i}}^\varepsilon - u_{\mathrm{e}}^\varepsilon), \qquad \text{on } \Gamma_{\mathrm{m}}^\varepsilon, \tag{1d}$$

where $\sigma_{\mathrm{i}}^\varepsilon > 0$ and $\sigma_{\mathrm{e}}^\varepsilon > 0$ are the scalar conductivities of the intra- and extra-cellular media (in $\mathrm{S\,m^{-1}}$) and f^ε (in $\mathrm{A\,m^{-3}}$) is a source term representing the electric pulses. System (1) is complemented with a gauge condition $\int_{\Omega_{\mathrm{e}}^\varepsilon} u_{\mathrm{e}}^\varepsilon = 0$, and with periodic boundary conditions.

Electroporation is taken into account in System (1) by choosing an appropriate current function $I_{\mathrm{m}}^\varepsilon$. Indeed, the pulsed electric field generates pores on the membrane surface, which is normally a highly resistive barrier. This results in a significant increase of cell membrane conductance and, consequently, of the transmembrane current $I_{\mathrm{m}}^\varepsilon$. In cardiac electrophysiology, this transmembrane current, which depends on time, originates mainly from complex ionic exchanges across the cell membrane, driven by the transmembrane potential $v_{\mathrm{m}}^\varepsilon := u_{\mathrm{i}}^\varepsilon - u_{\mathrm{e}}^\varepsilon$ and gating variables, and described by physiological [42, 43] or phenomenological [44, 45] models. However, in the context of pulsed electric fields, the electroporation current is several orders of magnitude larger than physiological ionic currents, which justifies neglecting these [46]. In this work, we adopt the modeling approach proposed in [22, 47], where the transmembrane current is simplified as a purely resistive flux across the membrane. The membrane surface conductance is then modeled by a nonlinear function $S_{\mathrm{m}}^\varepsilon$, which depends on the transmembrane voltage as proposed in [20]:

$$I_{\mathrm{m}}^\varepsilon(v) := S_{\mathrm{m}}^\varepsilon(v)\,v. \tag{2}$$

At rest, the cell membranes have a high resistive effect, which is reduced by electropora-

tion. As consequence, $S_{\mathrm{m}}^{\varepsilon}$, which is the inverse of the surface resistance, always take values that are strictly positive, although very low when the cell is at rest. Since electroporation is triggered by a voltage threshold V^{ep}, a typical profile for $S_{\mathrm{m}}^{\varepsilon}$ is a increasing sigmoid with a transition around V^{ep}. Several temporal models of electroporation at the cellular scale exist [46, 22], but we chose here a static model, primarily to avoid complicating the mathematical analysis and also because it remains the current standard in tissue modeling for PFA.

The well-posedness of the above nonlinear problem in a single cell has been derived previously in [20] under Assumption 2 (see below). The novelty here resides on the analysis of the assembly of a large number of cells, what we call "microscopic model" and the convergence towards limit homogenized problems at any order, what we call "macroscopic model".

2.2.2. Nondimensionalization

In order to highlight the relative amplitudes of the different quantities that are involved, in the specific use of electroporation ablation on cardiac tissue, we proceed by nondimensionalizing System (1). A piece of tissue considered in cardiac ablation is smaller than the whole heart (around $10^{-1}\,\mathrm{m}$), typically its characteristic size is $L_0 = 10^{-2}\,\mathrm{m}$ [48]. The characteristic cardiac cell size is $10^{-4}\,\mathrm{m}$ [49], therefore the ratio between the two scales at stake is $\varepsilon = 10^{-2}$. An electrical pulse for PFA leads to a potential that is around $U_0 = 10^2\,\mathrm{V}$ [48]. At the cell level, electroporation occurs after the transmembrane potential reaches a threshold of characteristic value $V_0^{\mathrm{ep}} = 1\,\mathrm{V}$ [50]. A significant increase in membrane conductance is then observed, with the baseline value being on the order of $1\,\mathrm{S\,m^{-2}}$. According to [9, 51], the exact maximum value of this conductance has little influence on the overall dynamics. We therefore choose to model the characteristic electroporated membrane conductance S_0 as substantially above the baseline, and set $S_0 = 10^2\,\mathrm{S\,m^{-2}}$. As in every cell scale electroporation model, we assume that the increase of $S_{\mathrm{m}}^{\varepsilon}$ is located around V_0^{ep}. In consequence, $S_{\mathrm{m}}^{\varepsilon}$ can be rewritten in the electroporation regime as $S_{\mathrm{m}}^{\varepsilon}(\lambda V_0^{\mathrm{ep}})$, where λ is a unitless variable of order 1. The physiological value of the intra- and extra-cellular conductivities is around $\Sigma_0 = 1\,\mathrm{S\,m^{-1}}$ [49]. The injected current is of order $1\,\mathrm{A}$ $(= \Sigma_0 L_0 U_0)$ so the volume current source f^{ε} has a characteristic value $F_0 = \frac{1}{L_0^3}\,\mathrm{A} = 10^6\,\mathrm{A\,m^{-3}}$.

Using these normalization constants, we define the following unitless quantities

$$\tilde{u}_{\mathrm{i,e}}^{\varepsilon}\left(\frac{\cdot}{L_0}\right) = \frac{1}{U_0} u_{\mathrm{i,e}}^{\varepsilon}(\cdot), \qquad \tilde{\sigma}_{\mathrm{i,e}} = \frac{1}{\Sigma_0}\sigma_{\mathrm{i,e}}^{\varepsilon},$$
$$\tilde{S}_{\mathrm{m}}\left(\frac{\cdot}{V_0^{\mathrm{ep}}}\right) = \frac{1}{S_0} S_{\mathrm{m}}^{\varepsilon}(\cdot), \qquad \tilde{f}\left(\frac{\cdot}{L_0}\right) = \frac{1}{F_0} f^{\varepsilon}(\cdot),$$

where we assumed that the dependence relatively to ε only lies implicitly in the characteristic

quantities. By substituting these quantities in System (1), we obtain

$$-\tilde{\nabla}\cdot(\tilde{\sigma}_i\tilde{\nabla}\tilde{u}_i^\varepsilon) = \frac{L_0^2F_0}{\Sigma_0U_0}\tilde{f}|_{\tilde{\Omega}_i^\varepsilon}, \qquad \text{in } \tilde{\Omega}_i^\varepsilon, \tag{3a}$$

$$-\tilde{\nabla}\cdot(\tilde{\sigma}_e\tilde{\nabla}\tilde{u}_e^\varepsilon) = \frac{L_0^2F_0}{\Sigma_0U_0}\tilde{f}|_{\tilde{\Omega}_e^\varepsilon}, \qquad \text{in } \tilde{\Omega}_e^\varepsilon, \tag{3b}$$

$$\tilde{\sigma}_i\tilde{\nabla}\tilde{u}_i^\varepsilon\cdot n_{\mathrm{i}} = \tilde{\sigma}_e\tilde{\nabla}\tilde{u}_e^\varepsilon\cdot n_{\mathrm{i}}, \qquad \text{on } \tilde{\Gamma}_m^\varepsilon, \tag{3c}$$

$$-\tilde{\sigma}_i\tilde{\nabla}\tilde{u}_i^\varepsilon\cdot n_{\mathrm{i}} = \frac{S_0L_0}{\Sigma_0}\frac{V_0^{\mathrm{ep}}}{U_0}\tilde{S}_m\left(\frac{U_0}{V_0^{\mathrm{ep}}}(\tilde{u}_i^\varepsilon-\tilde{u}_e^\varepsilon)\right)\frac{U_0}{V_0^{\mathrm{ep}}}(\tilde{u}_i^\varepsilon-\tilde{u}_e^\varepsilon), \qquad \text{on } \tilde{\Gamma}_m^\varepsilon, \tag{3d}$$

where the domains $\tilde{\Omega}_{i,e}^\varepsilon$ and $\tilde{\Gamma}_m^\varepsilon$ are obtained by rescaling $\Omega_{i,e}^\varepsilon$ and $\Gamma_{\mathrm{m}}^\varepsilon$ by L_0. We express the dimension factors as powers of ε:

$$\frac{L_0^2F_0}{\Sigma_0U_0} = 1, \quad \frac{S_0L_0}{\Sigma_0}\frac{V_0^{\mathrm{ep}}}{U_0} = 10^{-2} = \varepsilon, \quad \frac{U_0}{V_0^{\mathrm{ep}}} = 10^2 = \frac{1}{\varepsilon}.$$

This leads to the following nondimensionalized system by omitting the tilde notation for better readability and denoting $I_{\mathrm{m}}(v) := S_{\mathrm{m}}(v)v$,

$$-\nabla\cdot(\sigma_{\mathrm{i}}\nabla u_{\mathrm{i}}^\varepsilon) = f|_{\Omega_{\mathrm{i}}^\varepsilon}, \qquad \text{in } \Omega_{\mathrm{i}}^\varepsilon, \tag{4a}$$

$$-\nabla\cdot(\sigma_{\mathrm{e}}\nabla u_{\mathrm{e}}^\varepsilon) = f|_{\Omega_{\mathrm{e}}^\varepsilon}, \qquad \text{in } \Omega_{\mathrm{e}}^\varepsilon, \tag{4b}$$

$$\sigma_{\mathrm{i}}\nabla u_{\mathrm{i}}^\varepsilon\cdot n_{\mathrm{i}} = \sigma_{\mathrm{e}}\nabla u_{\mathrm{e}}^\varepsilon\cdot n_{\mathrm{i}}, \qquad \text{on } \Gamma_{\mathrm{m}}^\varepsilon, \tag{4c}$$

$$-\sigma_{\mathrm{i}}\nabla u_{\mathrm{i}}^\varepsilon\cdot n_{\mathrm{i}} = \varepsilon I_{\mathrm{m}}\left(\frac{u_{\mathrm{i}}^\varepsilon-u_{\mathrm{e}}^\varepsilon}{\varepsilon}\right), \qquad \text{on } \Gamma_{\mathrm{m}}^\varepsilon, \tag{4d}$$

which is the starting point of the homogenization process.

Remark 2.1. When performing this nondimensionalization in the cardiac electrophysiology context and in a static framework (see [28]), the current continuity condition in the cellular problem reads

$$-\sigma_{\mathrm{i}}\nabla u_{\mathrm{i}}^\varepsilon\cdot n_{\mathrm{i}} = \varepsilon I_{\mathrm{ion}}(u_{\mathrm{i}}^\varepsilon-u_{\mathrm{e}}^\varepsilon), \quad \text{on } \Gamma_{\mathrm{m}}^\varepsilon,$$

where I_{ion} denotes the ionic current. The difference with electroporation lies in the dependence on ε in the nonlinearity. This plays a crucial role and, as we will see later, leads to a different behavior.

2.3. Analysis of the microscopic problem

2.3.1. Periodic spaces definition.

We introduce several notations for periodic spaces. Let $D = \Omega$ or Y and let $\mathcal{D}$ be a subset of D, typically $\mathcal{D} = \Omega_{\mathrm{i}}^\varepsilon$, $\Omega_{\mathrm{e}}^\varepsilon$ or Ω if $D = \Omega$ and $\mathcal{D} = Y_{\mathrm{i}}$, Y_{e}, Y or Γ if $D = Y$. We denote by

$$\mathcal{C}_{\mathrm{per}}^\infty(\mathcal{D}) = \left\{u|_{\mathcal{D}},\ u\in\mathcal{C}^\infty(\mathbb{R}^d),\ u \text{ is } D\text{-periodic}\right\},$$

and $H^1_{\rm per}(\mathcal{D})$ its completion for the $H^1(\mathcal{D})$-norm. We also define, for $\mathcal{D}$ a subset of Y,

$$\mathcal{C}^\infty_{\rm per}(\Omega\times\mathcal{D}) = \left\{u|_{\Omega\times\mathcal{D}},\ u\in\mathcal{C}^\infty(\mathbb{R}^d\times\mathbb{R}^d),\ u \text{ is } \Omega\times Y\text{-periodic}\right\}.$$

For $E(\mathcal{D})$ being any of these spaces, we denote by

$$\overline{E}(\mathcal{D}) := \left\{u\in E(\mathcal{D}),\ \int_{\mathcal{D}} u = 0\right\}.$$

2.3.2. Existence, uniqueness and energy estimates.

In this section, we prove the well-posedness of the microscopic system and the energy estimates satisfied by the solution. The analysis is done under the following mathematical assumptions.

Assumption 1 (Source term)**.** $f\in\overline{\mathcal{C}^\infty_{\rm per}}(\Omega)$.

Assumption 2 (nonlinearity)**.** As in [20], we assume the following properties for $S_{\rm m}$. $S_{\rm m}\in\mathcal{C}^\infty(\mathbb{R})$ is even on $\mathbb{R}$, non-decreasing on $\mathbb{R}^+$ and there exist $S^0_{\rm m}$, $S^1_{\rm m}$, L and M positive constants such that

$$\begin{aligned}\forall\lambda\in\mathbb{R},\ 0<S^0_{\rm m}\le S_{\rm m}(\lambda)\le S^1_{\rm m},\\ \forall(\lambda,\mu)\in\mathbb{R}^2,\ |S_{\rm m}(\lambda)-S_m(\mu)|\le L\,|\lambda-\mu|\,,\\ \forall\lambda\in\mathbb{R},\ |I'_{\rm m}(\lambda)| = \left|(S_{\rm m}(\cdot)\cdot)'(\lambda)\right|\le M.\end{aligned}$$

Remark 2.2. We can show that Assumption 2 implies that for all $(\lambda,\mu)\in\mathbb{R}^2$,

$$(S_{\rm m}(\lambda)\lambda - S_{\rm m}(\mu)\mu)\,(\lambda-\mu)\ge S^0_{\rm m}(\lambda-\mu)^2. \tag{5}$$

Indeed, since $S_{\rm m}\in\mathcal{C}^\infty(\mathbb{R})$ is non-decreasing on $\mathbb{R}^+$, its derivative satisfies $S'_{\rm m}(\lambda)\ge 0$ for all $\lambda>0$. Moreover, as $S_{\rm m}$ is even, $S'_{\rm m}$ is odd, which implies $\lambda\,S'_{\rm m}(\lambda)\ge 0$ for all $\lambda\in\mathbb{R}$. Consequently,

$$I'_{\rm m}(\lambda) = S_{\rm m}(\lambda)+\lambda\,S'_{\rm m}(\lambda)\ge S_{\rm m}(\lambda)\ge S^0_{\rm m}$$

showing that $I_{\rm m}(\lambda)$ is strongly monotone. The conclusion then follows directly from the mean value theorem: $\forall\lambda,\mu\in\mathbb{R}$, there exists ξ between λ and μ such that

$$I_{\rm m}(\lambda)-I_{\rm m}(\mu) = I'_{\rm m}(\xi)(\lambda-\mu)$$

as multiplying by $(\lambda-\mu)$ yields

$$(S_{\rm m}(\lambda)\lambda - S_{\rm m}(\mu)\mu)(\lambda-\mu) = I'_{\rm m}(\xi)(\lambda-\mu)^2\ge S^0_{\rm m}(\lambda-\mu)^2,$$

Theorem 2.3. *Under Assumptions 1 and 2, System* (4) *has a unique solution* $(u^\varepsilon_{\rm i},u^\varepsilon_{\rm e})$ *in*

$\mathcal{C}^\infty_{\mathrm{per}}(\Omega^\varepsilon_{\mathrm{i}}) \times \overline{\mathcal{C}^\infty_{\mathrm{per}}}(\Omega^\varepsilon_{\mathrm{e}})$. *Moreover, the following estimates hold for all* $\varepsilon > 0$ *small enough,*

$$\begin{aligned}
\|u^\varepsilon_{\mathrm{e}}\|_{H^1(\Omega^\varepsilon_{\mathrm{e}})} &\leq C \|f\|_{L^2(\Omega)} \\
\|u^\varepsilon_{\mathrm{i}}\|_{H^1(\Omega^\varepsilon_{\mathrm{i}})} &\leq C \|f\|_{L^2(\Omega)} \\
\|v^\varepsilon_{\mathrm{m}}\|_{L^2(\Gamma^\varepsilon_{\mathrm{m}})} &\leq C \|f\|_{L^2(\Omega)},
\end{aligned}$$

where C *does not depend on* ε*, and* $v^\varepsilon_{\mathrm{m}} := u^\varepsilon_{\mathrm{i}} - u^\varepsilon_{\mathrm{e}}$ *in the sense of trace operators on the interface* $\Gamma^\varepsilon_{\mathrm{m}}$*.*

Proof. This proof relies on Lemmas A.1 and A.2, originally established in [52] and recalled in Appendix A for completeness. We begin the proof by establishing existence and uniqueness. First, we show the existence of a solution to the variational formulation, then we prove its regularity in $\mathcal{C}^\infty_{\mathrm{per}}$, and finally we conclude with the proof of energy estimates.
Existence and uniqueness of the variational formulation. We first show that the following variational formulation has a unique solution: find $(u^\varepsilon_{\mathrm{i}}, u^\varepsilon_{\mathrm{e}}) \in H^1_{\mathrm{per}}(\Omega^\varepsilon_{\mathrm{i}}) \times \overline{H^1_{\mathrm{per}}}(\Omega^\varepsilon_{\mathrm{e}})$ such that for all $(\phi_{\mathrm{i}}, \phi_{\mathrm{e}}) \in H^1_{\mathrm{per}}(\Omega^\varepsilon_{\mathrm{i}}) \times \overline{H^1_{\mathrm{per}}}(\Omega^\varepsilon_{\mathrm{e}})$,

$$\begin{aligned}
&\int_{\Omega^\varepsilon_{\mathrm{i}}} \sigma_{\mathrm{i}} \nabla u^\varepsilon_{\mathrm{i}} \cdot \nabla \phi_{\mathrm{i}} + \int_{\Omega^\varepsilon_{\mathrm{e}}} \sigma_{\mathrm{e}} \nabla u^\varepsilon_{\mathrm{e}} \cdot \nabla \phi_{\mathrm{e}} \\
&\qquad + \int_{\Gamma^\varepsilon_{\mathrm{m}}} \varepsilon I_{\mathrm{m}} \left(\frac{u^\varepsilon_{\mathrm{i}} - u^\varepsilon_{\mathrm{e}}}{\varepsilon} \right) (\phi_{\mathrm{i}} - \phi_{\mathrm{e}}) \quad = \int_{\Omega^\varepsilon_{\mathrm{i}}} f \phi_{\mathrm{i}} + \int_{\Omega^\varepsilon_{\mathrm{e}}} f \phi_{\mathrm{e}}.
\end{aligned} \tag{6}$$

Let us first prove the uniqueness. Assume that $(u_{\mathrm{i}}, u_{\mathrm{e}})$ and $(U_{\mathrm{i}}, U_{\mathrm{e}})$ are two solutions. The difference $(\nu_{\mathrm{i}}, \nu_{\mathrm{e}}) := (u_{\mathrm{i}} - U_{\mathrm{i}}, u_{\mathrm{e}} - U_{\mathrm{e}})$ satisfies

$$\begin{aligned}
&\sigma_{\mathrm{i}} \|\nabla \nu_{\mathrm{i}}\|^2_{L^2(\Omega^\varepsilon_{\mathrm{i}})} + \sigma_{\mathrm{e}} \|\nabla \nu_{\mathrm{e}}\|^2_{L^2(\Omega^\varepsilon_{\mathrm{e}})} \\
&+ \varepsilon \int_{\Gamma^\varepsilon_{\mathrm{m}}} \left(I_{\mathrm{m}} \left(\frac{u_{\mathrm{i}} - u_{\mathrm{e}}}{\varepsilon} \right) - I_{\mathrm{m}} \left(\frac{U_{\mathrm{i}} - U_{\mathrm{e}}}{\varepsilon} \right) \right) (\nu_{\mathrm{i}} - \nu_{\mathrm{e}}) = 0.
\end{aligned}$$

Using Assumption 2 to bound the third term, we show that $\|\nabla \nu_{\mathrm{i}}\|_{L^2(\Omega^\varepsilon_{\mathrm{i}})} = \|\nabla \nu_{\mathrm{e}}\|_{L^2(\Omega^\varepsilon_{\mathrm{e}})} = \|\nu_{\mathrm{i}} - \nu_{\mathrm{e}}\|_{L^2(\Gamma^\varepsilon_{\mathrm{m}})} = 0$. Thanks to the gauge condition, it implies that $\nu_{\mathrm{e}} = 0$ in $\Omega^\varepsilon_{\mathrm{e}}$. Therefore $0 = \|\nu_{\mathrm{i}} - \nu_{\mathrm{e}}\|_{L^2(\Gamma^\varepsilon_{\mathrm{m}})} = \|\nu_{\mathrm{i}}\|_{L^2(\Gamma^\varepsilon_{\mathrm{m}})}$, and $\nu_{\mathrm{i}} = 0$ in $\Omega^\varepsilon_{\mathrm{i}}$ because it is constant.

Let us now prove the existence of the solution. Consider the following functional defined for all $(v_{\mathrm{i}}, v_{\mathrm{e}}) \in H^1_{\mathrm{per}}(\Omega^\varepsilon_{\mathrm{i}}) \times \overline{H^1_{\mathrm{per}}}(\Omega^\varepsilon_{\mathrm{e}})$ by

$$\begin{aligned}
\mathcal{F}(v_{\mathrm{i}}, v_{\mathrm{e}}) = &\frac{1}{2} \int_{\Omega^\varepsilon_{\mathrm{i}}} \sigma_{\mathrm{i}} |\nabla v_{\mathrm{i}}|^2 + \frac{1}{2} \int_{\Omega^\varepsilon_{\mathrm{e}}} \sigma_{\mathrm{e}} |\nabla v_{\mathrm{e}}|^2 \\
&+ \varepsilon^2 \int_{\Gamma^\varepsilon_{\mathrm{m}}} \int_0^{\frac{(v_{\mathrm{i}} - v_{\mathrm{e}})(x)}{\varepsilon}} I_{\mathrm{m}}(s) \, \mathrm{d}s \mathrm{d}x - \int_{\Omega^\varepsilon_{\mathrm{i}}} f v_{\mathrm{i}} - \int_{\Omega^\varepsilon_{\mathrm{e}}} f v_{\mathrm{e}}.
\end{aligned}$$

The Fréchet derivative $\mathcal{F}'$ of $\mathcal{F}$ is given by

$$\mathcal{F}'(v_\mathrm{i}, v_\mathrm{e}) \cdot (\phi_\mathrm{i}, \phi_\mathrm{e}) = \int_{\Omega_\mathrm{i}^\varepsilon} \sigma_\mathrm{i} \nabla v_\mathrm{i} \cdot \nabla \phi_\mathrm{i} + \int_{\Omega_\mathrm{e}^\varepsilon} \sigma_\mathrm{e} \nabla v_\mathrm{e} \cdot \nabla \phi_\mathrm{e} + \varepsilon \int_{\Gamma_\mathrm{m}^\varepsilon} I_\mathrm{m}\left(\frac{v_\mathrm{i} - v_\mathrm{e}}{\varepsilon}\right)(\phi_\mathrm{i} - \phi_\mathrm{e}) - \int_{\Omega_\mathrm{i}^\varepsilon} f\phi_\mathrm{i} - \int_{\Omega_\mathrm{e}^\varepsilon} f\phi_\mathrm{e}.$$

We show in the following that $\mathcal{F}$ is strictly convex and coercive, thus it admits a unique critical point (see Corollary 1.4 of Chapter 3 of [53]), which is exactly the solution of the variational formulation.

We first show that $\mathcal{F}$ is convex. Let $(v_\mathrm{i}, v_\mathrm{e})$ and $(w_\mathrm{i}, w_\mathrm{e})$ in $H^1_\mathrm{per}(\Omega_\mathrm{i}^\varepsilon) \times \overline{H^1_\mathrm{per}}(\Omega_\mathrm{e}^\varepsilon)$, we have

$$\begin{aligned}
&(\mathcal{F}'(v_\mathrm{i}, v_\mathrm{e}) - \mathcal{F}'(w_\mathrm{i}, w_\mathrm{e})) \cdot ((v_\mathrm{i}, v_\mathrm{e}) - (w_\mathrm{i}, w_\mathrm{e})) = \\
&\int_{\Omega_\mathrm{i}^\varepsilon} \sigma_\mathrm{i} \left|\nabla(v_\mathrm{i} - w_\mathrm{i})\right|^2 + \int_{\Omega_\mathrm{e}^\varepsilon} \sigma_\mathrm{e} \left|\nabla(v_\mathrm{e} - w_\mathrm{e})\right|^2 \\
&+ \varepsilon \int_{\Gamma_\mathrm{m}^\varepsilon} \left(I_\mathrm{m}\left(\frac{v_\mathrm{i} - v_\mathrm{e}}{\varepsilon}\right) - I_\mathrm{m}\left(\frac{w_\mathrm{i} - w_\mathrm{e}}{\varepsilon}\right)\right)(v_\mathrm{i} - v_\mathrm{e} - (w_\mathrm{i} - w_\mathrm{e})) \geq 0,
\end{aligned}$$

because every term is positive, thanks to Assumption 2. The strict convexity is immediate thanks to the Gauge condition.

We then show the coercivity of $\mathcal{F}$. Let $(v_\mathrm{i}, v_\mathrm{e}) \in H^1_\mathrm{per}(\Omega_\mathrm{i}^\varepsilon) \times \overline{H^1_\mathrm{per}}(\Omega_\mathrm{e}^\varepsilon)$ and $\alpha > 0$, we get

$$\begin{aligned}
\mathcal{F}(v_\mathrm{i}, v_\mathrm{e}) &\geq \frac{1}{2}\left(\sigma_\mathrm{i} \left\|\nabla v_\mathrm{i}\right\|^2_{L^2(\Omega_\mathrm{i}^\varepsilon)} + \sigma_\mathrm{e} \left\|\nabla v_\mathrm{e}\right\|^2_{L^2(\Omega_\mathrm{e}^\varepsilon)}\right) + \frac{S^0_\mathrm{m}}{2} \left\|v_\mathrm{i} - v_\mathrm{e}\right\|^2_{L^2(\Gamma_\mathrm{m}^\varepsilon)} \\
&\qquad - \int_{\Omega_\mathrm{i}^\varepsilon} f v_\mathrm{i} - \int_{\Omega_\mathrm{e}^\varepsilon} f v_\mathrm{e}, \\
&\geq C\left(\left\|v_\mathrm{i}\right\|^2_{H^1(\Omega_\mathrm{i}^\varepsilon)} + \left\|v_\mathrm{e}\right\|^2_{H^1(\Omega_\mathrm{e}^\varepsilon)}\right) - \int_{\Omega_\mathrm{i}^\varepsilon} f v_\mathrm{i} - \int_{\Omega_\mathrm{e}^\varepsilon} f v_\mathrm{e}, \\
&\geq C\left(\left\|v_\mathrm{i}\right\|^2_{H^1(\Omega_\mathrm{i}^\varepsilon)} + \left\|v_\mathrm{e}\right\|^2_{H^1(\Omega_\mathrm{e}^\varepsilon)}\right) - \frac{\alpha}{2}\left\|v_\mathrm{i}\right\|^2_{L^2(\Omega_\mathrm{i}^\varepsilon)} - \frac{\alpha}{2}\left\|v_\mathrm{e}\right\|^2_{L^2(\Omega_\mathrm{e}^\varepsilon)} \\
&\qquad - \frac{1}{2\alpha}\left\|f\right\|^2_{L^2(\Omega_\mathrm{i}^\varepsilon)} - \frac{1}{2\alpha}\left\|f\right\|^2_{L^2(\Omega_\mathrm{e}^\varepsilon)}, \\
&\geq C\left(\left\|v_\mathrm{i}\right\|^2_{H^1(\Omega_\mathrm{i}^\varepsilon)} + \left\|v_\mathrm{e}\right\|^2_{H^1(\Omega_\mathrm{e}^\varepsilon)}\right) - C'\frac{\alpha}{2}\left\|v_\mathrm{i}\right\|^2_{H^1(\Omega_\mathrm{i}^\varepsilon)} - C'\frac{\alpha}{2}\left\|v_\mathrm{e}\right\|^2_{H^1(\Omega_\mathrm{e}^\varepsilon)} \\
&\qquad - \frac{1}{2\alpha}\left\|f\right\|^2_{L^2(\Omega_\mathrm{i}^\varepsilon)} - \frac{1}{2\alpha}\left\|f\right\|^2_{L^2(\Omega_\mathrm{e}^\varepsilon)}.
\end{aligned}$$

First line uses Assumption 2, second line uses norm equivalence given in Lemma A.2, third line uses Young inequality and finally fourth line uses Poincaré-Wirtinger inequality given in Lemma A.1. By choosing α such that $C - C'\frac{\alpha}{2} > 0$, we obtain that $\lim \mathcal{F}(v_\mathrm{i}, v_\mathrm{e}) = +\infty$ when $\left\|v_\mathrm{i}\right\|_{H^1(\Omega_\mathrm{i}^\varepsilon)} + \left\|v_\mathrm{e}\right\|_{H^1(\Omega_\mathrm{e}^\varepsilon)} \to +\infty$.

Regularity. We identify Ω with a torus, so that the boundaries of $\Omega_\mathrm{i}^\varepsilon$ and $\Omega_\mathrm{e}^\varepsilon$ consist solely of the membrane interface $\Gamma_\mathrm{m}^\varepsilon$, which is assumed to be infinitely smooth.

First step: Prove that $u_{\mathrm{i}}^{\varepsilon} \in H^2(\Omega_{\mathrm{i}}^{\varepsilon})$ and $u_{\mathrm{e}}^{\varepsilon} \in H^2(\Omega_{\mathrm{e}}^{\varepsilon})$.
The quantity $(u_{\mathrm{i}}^{\varepsilon} - u_{\mathrm{e}}^{\varepsilon})/\varepsilon$ belongs to $H^{\frac{1}{2}}(\Gamma_{\mathrm{m}}^{\varepsilon})$ so there exists $v \in H^1(\Omega_{\mathrm{i}}^{\varepsilon})$ such that $v|_{\Gamma_{\mathrm{m}}^{\varepsilon}} = (u_{\mathrm{i}}^{\varepsilon} - u_{\mathrm{e}}^{\varepsilon})/\varepsilon$. By denoting ∇v its gradient in the sense of distributions and as $I_{\mathrm{m}} \in \mathcal{C}^{\infty}(\mathbb{R})$ (Assumption 2), we then have:

$$\nabla \left(I_{\mathrm{m}}(v) \right) = I_{\mathrm{m}}'(v) \nabla v.$$

Since $I_{\mathrm{m}}'(v) \in L^{\infty}(\Omega_{\mathrm{i}}^{\varepsilon})$ (always by Assumption 2) and $\nabla v \in L^2(\Omega_{\mathrm{i}}^{\varepsilon})$, we have $I_{\mathrm{m}}(v) \in H^1(\Omega_{\mathrm{i}}^{\varepsilon})$ and therefore

$$\varepsilon I_{\mathrm{m}} \left(\frac{u_{\mathrm{i}}^{\varepsilon} - u_{\mathrm{e}}^{\varepsilon}}{\varepsilon} \right) \in H^{\frac{1}{2}}(\Gamma_{\mathrm{m}}^{\varepsilon}).$$

Since the intracellular potential $u_{\mathrm{i}}^{\varepsilon}$ satisfies the following problem:

$$\begin{array}{rll} -\nabla \cdot (\sigma_{\mathrm{i}} \nabla u_{\mathrm{i}}^{\varepsilon}) = & f & \in L^2(\Omega_{\mathrm{i}}^{\varepsilon}), \\ -\sigma_{\mathrm{i}} \nabla u_{\mathrm{i}}^{\varepsilon} \cdot n_{\mathrm{i}} = & \varepsilon I_{\mathrm{m}} \left(\frac{u_{\mathrm{i}}^{\varepsilon} - u_{\mathrm{e}}^{\varepsilon}}{\varepsilon} \right) & \in H^{\frac{1}{2}}(\Gamma_{\mathrm{m}}^{\varepsilon}), \end{array} \tag{7}$$

we have $u_{\mathrm{i}}^{\varepsilon} \in H^2(\Omega_{\mathrm{i}}^{\varepsilon})$ (by elliptic regularity, see Proposition 2.5.2.3 of [54]).
With the same reasoning, we show that $u_{\mathrm{e}}^{\varepsilon} \in H^2(\Omega_{\mathrm{e}}^{\varepsilon})$.
Second step: Prove that $u_{\mathrm{i}}^{\varepsilon} \in H^k(\Omega_{\mathrm{i}}^{\varepsilon})$ and $u_{\mathrm{e}}^{\varepsilon} \in H^k(\Omega_{\mathrm{e}}^{\varepsilon})$ for any $k \geq 2$.
We proceed by induction on $k \geq 2$. The two main arguments are the Sobolev embedding in any bounded domain Ω of $\mathbb{R}^d$, from $H^s(\Omega)$ into $L^{\infty}(\Omega)$ for $s > d/2$, and from $H^s(\Omega)$ into $W^{s-1,4}(\Omega)$ if $s \geq 1$ (see for instance [55], Section 5.6, and recall that we work in $\mathbb{R}^d$, with $d = 2$ or 3).

More precisley, at step k, we assume $u_{\mathrm{i}}^{\varepsilon} \in H^k(\Omega_{\mathrm{i}}^{\varepsilon})$ and $u_{\mathrm{e}}^{\varepsilon} \in H^k(\Omega_{\mathrm{e}}^{\varepsilon})$. The quantity $(u_{\mathrm{i}}^{\varepsilon} - u_{\mathrm{e}}^{\varepsilon})/\varepsilon$ belongs to $H^{k-\frac{1}{2}}(\Gamma_{\mathrm{m}}^{\varepsilon})$ so there exists $v \in H^k(\Omega_{\mathrm{i}}^{\varepsilon})$ such that $v|_{\Gamma_{\mathrm{m}}^{\varepsilon}} = (u_{\mathrm{i}}^{\varepsilon} - u_{\mathrm{e}}^{\varepsilon})/\varepsilon$. If we show that $I_{\mathrm{m}}(v) \in H^k(\Omega_{\mathrm{i}}^{\varepsilon})$, then $\varepsilon I_{\mathrm{m}}\left((u_{\mathrm{i}}^{\varepsilon} - u_{\mathrm{e}}^{\varepsilon})/\varepsilon\right) \in H^{k-\frac{1}{2}}(\Gamma_{\mathrm{m}}^{\varepsilon})$ and, as $f \in \mathcal{C}^{\infty}(\Omega_{\mathrm{i}}^{\varepsilon})$ and $u_{\mathrm{i}}^{\varepsilon}$ still satisfies Equation (7), we would get $u_{\mathrm{i}}^{\varepsilon} \in H^{k+1}(\Omega_{\mathrm{i}}^{\varepsilon})$, using for instance Theorem 2.5.1.1 of [54]. Following the same reasoning, we would also get $u_{\mathrm{e}}^{\varepsilon} \in H^{k+1}(\Omega_{\mathrm{e}}^{\varepsilon})$.
To demonstrate that $I_{\mathrm{m}}(v) \in H^k(\Omega_{\mathrm{i}}^{\varepsilon})$, we show that $\partial^{\alpha} I_{\mathrm{m}}(v) \in L^2(\Omega_{\mathrm{i}}^{\varepsilon})$ for any multi-index α such that $|\alpha| = k$. Let $\alpha \in \mathbb{N}^d$ and $\beta \in \mathbb{N}^d$, such that $|\alpha| = k$, $|\beta| = 2$ (we denote by β_1 and β_2 the two non-zero components of β) and $\beta \leq \alpha$, we have

$$\partial^{\alpha} \left(I_{\mathrm{m}}(v) \right) = \partial^{\alpha-\beta} \partial^{\beta} \left(I_{\mathrm{m}}(v) \right) = \partial^{\alpha-\beta} \left(I_{\mathrm{m}}''(v) \partial^{\beta_2} v \, \partial^{\beta_1} v + I_{\mathrm{m}}'(v) \partial^{\beta} v \right),$$

which gives, by Leibniz formula,

$$= \sum_{\nu \leq \alpha - \beta} \binom{\alpha - \beta}{\nu} \left(\partial^{\nu} \left(\partial^{\beta_2} v \, \partial^{\beta_1} v \right) \partial^{\alpha-\beta-\nu} \left(I_{\mathrm{m}}''(v) \right) + \partial^{\nu+\beta} v \partial^{\alpha-\beta-\nu} \left(I_{\mathrm{m}}'(v) \right) \right).$$

We show that each term in the above sum belongs to $L^2(\Omega_{\mathrm{i}}^{\varepsilon})$. Let $\nu \leq \alpha - \beta$. We first consider the term

$$\partial^{\nu} \left(\partial^{\beta_2} v \, \partial^{\beta_1} v \right) \partial^{\alpha-\beta-\nu} \left(I_{\mathrm{m}}''(v) \right) \in L^2(\Omega_{\mathrm{i}}^{\varepsilon}).$$

We prove that it belongs to $L^2(\Omega_{\rm i}^\varepsilon)$ by showing that $\partial^\nu(\partial^{\beta_2} v\, \partial^{\beta_1} v) \in L^2(\Omega_{\rm i}^\varepsilon)$ and $\partial^{\alpha-\beta-\nu}(I_{\rm m}''(v)) \in L^\infty(\Omega_{\rm i}^\varepsilon)$. Since $v \in H^k(\Omega_{\rm i}^\varepsilon)$, Sobolev injection $H^k(\Omega_{\rm i}^\varepsilon) \subset W^{k-1,4}(\Omega_{\rm i}^\varepsilon)$ yields $v \in W^{k-1,4}(\Omega_{\rm i}^\varepsilon)$. Hence $\partial^{\beta_1} v \in W^{k-2,4}(\Omega_{\rm i}^\varepsilon)$ and $\partial^{\beta_2} v \in W^{k-2,4}(\Omega_{\rm i}^\varepsilon)$, and therefore $\partial^{\beta_1} v \partial^{\beta_2} v \in W^{k-2,2}(\Omega_{\rm i}^\varepsilon)$. Since $|\nu| \leq |\alpha-\beta| \leq k-2$, it follows that $\partial^\nu \partial^{\beta_1} v \partial^{\beta_2} v \in L^2(\Omega_{\rm i}^\varepsilon)$.
On the other hand, by Sobolev injection $H^k(\Omega_{\rm i}^\varepsilon) \subset W^{k-2,\infty}(\Omega_{\rm i}^\varepsilon)$, we have $v \in W^{k-2,\infty}(\Omega_{\rm i}^\varepsilon)$, so all derivatives of v of order at most $k-2$ are bounded. If we develop the term $\partial^{\alpha-\beta-\nu}\left(I_{\rm m}''(v)\right)$, only derivatives of v of order at most $k-2$ appear. Since $I_{\rm m} \in \mathcal{C}^\infty(\mathbb{R})$, we conclude that $\partial^{\alpha-\beta-\nu}(I_{\rm m}''(v)) \in L^\infty(\Omega_{\rm i}^\varepsilon)$.
We now turn to the second term,

$$\partial^{\nu+\beta} v \partial^{\alpha-\beta-\nu}\left(I_{\rm m}'(v)\right).$$

Since $v \in H^k(\Omega_{\rm i}^\varepsilon)$ and $|\nu+\beta| \leq k$, we have $\partial^{\nu+\beta} v \in L^2(\Omega_{\rm i}^\varepsilon)$. Moreover, arguing as above and using again that $I_{\rm m} \in \mathcal{C}^\infty(\mathbb{R})$ and $v \in W^{k-2,\infty}(\Omega_{\rm i}^\varepsilon)$, we obtain $\partial^{\alpha-\beta-\nu}(I_{\rm m}'(v)) \in L^\infty(\Omega_{\rm i}^\varepsilon)$. Hence this term also belongs to $L^2(\Omega_{\rm i}^\varepsilon)$.

Therefore, $\partial^\alpha\left(I_{\rm m}(v)\right) \in L^2(\Omega_{\rm i}^\varepsilon)$ for every multi-index α with $|\alpha| = k$ so $\left(I_{\rm m}(v)\right) \in H^k(\Omega_{\rm i}^\varepsilon)$, which concludes the induction.
Third step: Prove that $u_{\rm i}^\varepsilon \in \mathcal{C}^\infty(\Omega_{\rm i}^\varepsilon)$ and $u_{\rm e}^\varepsilon \in \mathcal{C}^\infty(\Omega_{\rm e}^\varepsilon)$.
Since $u_{\rm i}^\varepsilon$ has regularity $H^k(\Omega_{\rm i}^\varepsilon)$ for all $k \in \mathbb{N}$ (by the second step), we conclude that $u_{\rm i}^\varepsilon \in \mathcal{C}^\infty(\Omega_{\rm i}^\varepsilon)$. Applying the same argument to $u_{\rm e}^\varepsilon$ yields $u_{\rm e}^\varepsilon \in \mathcal{C}^\infty(\Omega_{\rm e}^\varepsilon)$.
Energy estimates. To conclude the proof, it remains to establish the energy estimates. We recall that $v_{\rm m}^\varepsilon = u_{\rm i}^\varepsilon - u_{\rm e}^\varepsilon$. Setting $\phi_{\rm i} = u_{\rm i}^\varepsilon$ and $\phi_{\rm e} = u_{\rm e}^\varepsilon$ in the variational formulation (6) leads to

$$\begin{aligned}\sigma_{\rm i} \left\|\nabla u_{\rm i}^\varepsilon\right\|_{L^2(\Omega_{\rm i}^\varepsilon)}^2 + \sigma_{\rm e} \left\|\nabla u_{\rm e}^\varepsilon\right\|_{L^2(\Omega_{\rm e}^\varepsilon)}^2 + \varepsilon \int_{\Gamma_{\rm m}^\varepsilon} I_{\rm m}\left(\frac{v_{\rm m}^\varepsilon}{\varepsilon}\right) v_{\rm m}^\varepsilon \\ = (f, u_{\rm i}^\varepsilon)_{L^2(\Omega_{\rm i}^\varepsilon)} + (f, u_{\rm e}^\varepsilon)_{L^2(\Omega_{\rm e}^\varepsilon)}.\end{aligned}$$

This energy identity shows that $\|u_{\rm i}^\varepsilon\|_{H^1(\Omega_{\rm i}^\varepsilon)}^2 + \|u_{\rm e}^\varepsilon\|_{H^1(\Omega_{\rm e}^\varepsilon)}^2$ is bounded, and will thus be used to obtain the first two energy estimates.
First by using the norm equivalence given in Lemma A.2 (see Appendix A), there exists $C > 0$,

$$\begin{aligned}\|u_{\rm i}^\varepsilon\|_{H^1(\Omega_{\rm i}^\varepsilon)}^2 + \|u_{\rm e}^\varepsilon\|_{H^1(\Omega_{\rm e}^\varepsilon)}^2 \\ \leq C\left(\left\|\nabla u_{\rm i}^\varepsilon\right\|_{L^2(\Omega_{\rm i}^\varepsilon)}^2 + \left\|\nabla u_{\rm e}^\varepsilon\right\|_{L^2(\Omega_{\rm e}^\varepsilon)^2} + \varepsilon \left\|v_{\rm m}^\varepsilon\right\|_{L^2(\Gamma_{\rm m}^\varepsilon)}^2\right).\end{aligned}$$

Adding the strictly positive constants $\sigma_{\rm i}$, $\sigma_{\rm e}$, and $S_{\rm m}^0$, and noting that ε is assumed to be small (in particular, $\varepsilon < 1$), there exists a constant, still denoted by $C > 0$, such that

$$\begin{aligned}\|u_{\rm i}^\varepsilon\|_{H^1(\Omega_{\rm i}^\varepsilon)}^2 + \|u_{\rm e}^\varepsilon\|_{H^1(\Omega_{\rm e}^\varepsilon)}^2 \\ \leq C\left(\sigma_{\rm i} \left\|\nabla u_{\rm i}^\varepsilon\right\|_{L^2(\Omega_{\rm i}^\varepsilon)}^2 + \sigma_{\rm e} \left\|\nabla u_{\rm e}^\varepsilon\right\|_{L^2(\Omega_{\rm e}^\varepsilon)}^2 + S_{\rm m}^0 \left\|v_{\rm m}^\varepsilon\right\|_{L^2(\Gamma_{\rm m}^\varepsilon)}^2\right).\end{aligned}$$

Moreover,

$$S_{\mathrm{m}}^0 \left\| v_{\mathrm{m}}^\varepsilon \right\|_{L^2(\Gamma_{\mathrm{m}}^\varepsilon)}^2 \leq \int_{\Gamma_{\mathrm{m}}^\varepsilon} S_{\mathrm{m}} \left(\frac{v_{\mathrm{m}}^\varepsilon}{\varepsilon} \right) (v_{\mathrm{m}}^\varepsilon)^2 \left(= \varepsilon \int_{\Gamma_{\mathrm{m}}^\varepsilon} I_{\mathrm{m}} \left(\frac{v_{\mathrm{m}}^\varepsilon}{\varepsilon} \right) v_{\mathrm{m}}^\varepsilon \right)$$

and using the energy identity, one infers

$$\begin{aligned} &\left\| u_{\mathrm{i}}^\varepsilon \right\|_{H^1(\Omega_{\mathrm{i}}^\varepsilon)}^2 + \left\| u_{\mathrm{e}}^\varepsilon \right\|_{H^1(\Omega_{\mathrm{e}}^\varepsilon)}^2 \\ &\qquad \leq C \left| (f, u_{\mathrm{i}}^\varepsilon)_{L^2(\Omega_{\mathrm{i}}^\varepsilon)} + (f, u_{\mathrm{e}}^\varepsilon)_{L^2(\Omega_{\mathrm{e}}^\varepsilon)} \right|. \end{aligned}$$

Schwarz inequality implies then

$$\begin{aligned} &\left\| u_{\mathrm{i}}^\varepsilon \right\|_{H^1(\Omega_{\mathrm{i}}^\varepsilon)}^2 + \left\| u_{\mathrm{e}}^\varepsilon \right\|_{H^1(\Omega_{\mathrm{e}}^\varepsilon)}^2 \\ &\qquad \leq C \left(\left(\left\| u_{\mathrm{i}}^\varepsilon \right\|_{H^1(\Omega_{\mathrm{i}}^\varepsilon)} + \left\| u_{\mathrm{e}}^\varepsilon \right\|_{H^1(\Omega_{\mathrm{e}}^\varepsilon)} \right) \left\| f \right\|_{L^2(\Omega)} \right), \end{aligned}$$

thus $\left\| u_{\mathrm{i}}^\varepsilon \right\|_{H^1(\Omega_{\mathrm{i}}^\varepsilon)}$ and $\left\| u_{\mathrm{e}}^\varepsilon \right\|_{H^1(\Omega_{\mathrm{e}}^\varepsilon)}$ are bounded. To conclude, the last estimate is obtained once again using the energy identity. Exploiting the positivity of the first two terms, using once again Schwarz inequality and the fact that $\left\| u_{\mathrm{i}}^\varepsilon \right\|_{H^1(\Omega_{\mathrm{i}}^\varepsilon)}$ and $\left\| u_{\mathrm{e}}^\varepsilon \right\|_{H^1(\Omega_{\mathrm{e}}^\varepsilon)}$ are bounded, one get that there exists $C > 0$ such that

$$\begin{aligned} \varepsilon \int_{\Gamma_{\mathrm{m}}^\varepsilon} I_{\mathrm{m}} \left(\frac{v_{\mathrm{m}}^\varepsilon}{\varepsilon} \right) v_{\mathrm{m}}^\varepsilon &= \int_{\Gamma_{\mathrm{m}}^\varepsilon} S_{\mathrm{m}} \left(\frac{v_{\mathrm{m}}^\varepsilon}{\varepsilon} \right) (v_{\mathrm{m}}^\varepsilon)^2 \\ &\leq \left| (f, u_{\mathrm{i}}^\varepsilon)_{L^2(\Omega_{\mathrm{i}}^\varepsilon)} + (f, u_{\mathrm{e}}^\varepsilon)_{L^2(\Omega_{\mathrm{e}}^\varepsilon)} \right| \\ &\leq C \left\| f \right\|_{L^2(\Omega)}. \end{aligned}$$

As $S_{\mathrm{m}}(\lambda) \geq S_{\mathrm{m}}^0, \forall \lambda \in \mathbb{R}$, one get that there exists a constant still denoted by $C > 0$ such that $\left\| v_{\mathrm{m}}^\varepsilon \right\|_{L^2(\Gamma_{\mathrm{m}}^\varepsilon)}^2 \leq C \left\| f \right\|_{L^2(\Omega)}$. This concludes the proof. □

Remark 2.4. The first two estimates imply $\varepsilon \left\| v_{\mathrm{m}}^\varepsilon \right\|_{L^2(\Gamma_{\mathrm{m}}^\varepsilon)}^2 \leq C \left\| f \right\|_{L^2(\Omega)}$ (see Lemma A.2 in Appendix A) but we showed that, due to the structure of the equations, a stronger result holds, namely the third estimate $\left\| v_{\mathrm{m}}^\varepsilon \right\|_{L^2(\Gamma_{\mathrm{m}}^\varepsilon)}^2 \leq C \left\| f \right\|_{L^2(\Omega)}$.

3. Tissue scale model

After reviewing the context, the new proposed model – which forms the main contribution of this work – is introduced. It is derived from an asymptotic analysis of the microscopic system and consists of a limit problem (order 0) and a first-order correction. We also present numerical simulations to illustrate the behavior of the model solution. For the sake of readability, the rigorous justification of the asymptotic derivation of the model is deferred to the next section.

3.1. Context and related work

Regarding the asymptotic analysis, the nonlinearity of $\lambda \mapsto I_{\mathrm{m}}(\lambda)$ is the first main difficulty. Let us first consider a linear function, *i.e.* $I_{\mathrm{m}}(\lambda) = S^0_{\mathrm{m}}\lambda$. Under this assumption, the homogenization of System (4) falls into a broader class of problems where the interfacial flux takes the form $\varepsilon^\gamma \kappa v_{\mathrm{m}}$, with $\gamma \in \mathbb{R}$ and $\kappa > 0$. Such a setting arises in various contexts, including heat conduction in composite media with interfacial barriers [56], modeling of contact between two elastic bodies [57], electric conduction in biological tissues [58, 59, 60], and diffusion in fissured media [61]. A detailed discussion of the possible values of γ can be found in [62, 63], and further generalizations are presented in [64]. For the treatment of nonlinear interfacial resistance, we refer to [65].

However, all these works concentrate on the limit problem - i.e., the homogenized system obtained as $\varepsilon \to 0$ - which in our setting reads as will be shown later,

$$u^0_{\mathrm{i}} = u^0_{\mathrm{e}} =: u^0, \quad \text{in } \Omega, \quad -\nabla \cdot \Big((\Sigma_{\mathrm{i}} + \Sigma_{\mathrm{e}}) \nabla u^0 \Big) = f, \quad \text{in } \Omega, \ \int_\Omega u^0 = 0, \tag{8}$$

with periodic boundary conditions and effective tensors Σ_{i} and Σ_{e} to be defined later. System (8) corresponds to a monodomain model, in the sense that a single macroscopic potential u^0 characterizes the system at the limit. Notably, it does not retain any information about the flux transmission across the membrane.

To obtain a more precise approximation than the one given by the limit problem, we need to extend the asymptotic expansion to higher orders - this constitutes the second main difficulty of our work. We follow a procedure already explored in various contexts. In [32], the authors highlight the necessity of a second-order corrector in the homogenization of conductive-radiative heat transfer in perforated domains, particularly when the source term is a periodically oscillating function, in order to achieve an accurate temperature approximation. Similarly, in [34], the full two-scale expansion of the equation $-\nabla \cdot (A\,(x/\varepsilon)\,\nabla u^\varepsilon) = f$ is rigorously derived in the framework of elasticity, for a fixed domain with macroscopic periodic boundary conditions (see also [33] for the quasilinear case), leading to what is referred to as an "infinite-order" homogenized solution. More generally, these works propose a formal expansion, whose validity is ensured by proving that the difference between the exact solution and the expansion satisfies a well-posed PDE, which allows for quantitative error estimates. We adopt the same approach in our work - see the discussion in the beginning of Section 4. Such high-order development is also investigated in [66], where the authors compare classical asymptotic expansions with Bloch wave expansions for periodic homogenization, and advocate for higher-order corrections, notably suggesting that the error is better captured with a fourth-order term. In [30], the complete two-scale expansion of a perturbed convection equation is justified using two-scale convergence techniques (see also [29] for related results in the context of gyrokinetic approximations). In [31], effective models for linear elastic beams are obtained by retaining asymptotic terms up to order 2. To the best of our knowledge, the rigorous justification of a full two-scale expansion for System (4) together with the derivation of a non-linear physical model for PFA is original and constitutes the core contribution of the present article.

3.2. Limit problem

In the following, the α subscript designates either i or e, for the intra- and extracellular quantities, respectively.

We can gain a first insight into the behaviour of the microscopic system of equations in the asymptotic regime by studying the limit problem as $\varepsilon \to 0$. Using the estimates from Theorem 2.3, we apply in this section the theory of two-scale convergence (for an introduction, see [27], [67]) to derive the limit problem in Theorem 3.4. This problem is defined on the macroscopic domain Ω, yet it retains information about the microscopic structure through the solutions of the so-called cell problems introduced in the following proposition and defined on the single cell domain (see Section 2.1).

Proposition-Definition 3.1. *Let $F \in \mathcal{C}^\infty_{\mathrm{per}}(Y_\alpha)$ and $G \in \mathcal{C}^\infty_{\mathrm{per}}(\Gamma)$ such that $\int_{Y_\alpha} F = \int_\Gamma G$. We denote by*

$$\mathcal{P}_\alpha(F, G) := \chi,$$

the unique solution in $\mathcal{C}^\infty_{\mathrm{per}}(Y_\alpha)$ of

$$-\Delta\chi = F, \ \textit{in } Y_\alpha, \tag{9a}$$
$$-\nabla\chi \cdot n_\alpha = G, \ \textit{on } \Gamma, \tag{9b}$$
$$\int_{Y_\alpha} \chi = 0. \tag{9c}$$

It satisfies

$$\|\chi\|_{H^1(Y_\alpha)} \leq C \left(\|F\|_{L^2(Y_\alpha)} + \|G\|_{H^{-\frac{1}{2}}(\Gamma)} \right).$$

Proof. The proof is classic and the compatibility condition $\int_{Y_\alpha} F = \int_\Gamma G$ is used to show the equivalence between the variational formulation and System (9). By identifying Y to a torus and using Theorem 2.5.1.1 of [54], we conclude that $\chi \in \mathcal{C}^\infty_{\mathrm{per}}(Y_\alpha)$. □

Definition 3.2 (Cell problems)**.** For $1 \leq j \leq d$, we define

$$\left(\chi_{\mathrm{i}}^{1,0,1}\right)_j = \mathcal{P}_{\mathrm{i}}\left(0, e^j \cdot n_{\mathrm{i}}\right), \quad \left(\chi_{\mathrm{e}}^{1,0,1}\right)_j = \mathcal{P}_{\mathrm{e}}\left(0, e^j \cdot n_{\mathrm{e}}\right),$$
$$\chi_{\mathrm{i}}^{1,0,1} = \left(\left(\chi_{\mathrm{i}}^{1,0,1}\right)_1, \ldots, \left(\chi_{\mathrm{i}}^{1,0,1}\right)_d\right)^T, \quad \chi_{\mathrm{e}}^{1,0,1} = \left(\left(\chi_{\mathrm{e}}^{1,0,1}\right)_1, \ldots, \left(\chi_{\mathrm{e}}^{1,0,1}\right)_d\right)^T, \quad [\chi] = \chi_{\mathrm{i}}^{1,0,1} - \chi_{\mathrm{e}}^{1,0,1},$$

where e^j is the j-th vector of the canonical basis of $\mathbb{R}^d$. We also introduce the following definitions:

$$\chi_{\mathrm{i}}^{0,1,1} = \chi_{\mathrm{e}}^{0,1,1} = 1, \ \theta_{\mathrm{i}}^{0,0,1} = \theta_{\mathrm{e}}^{0,0,1} = 0.$$

Remark 3.3. One might be surprised by the use of triple indices in the corrector variables $\chi_{\mathrm{i}}^{1,0,1}$ and $\chi_{\mathrm{e}}^{1,0,1}$, as well as by the introduction of other variables that are not directly used at

this stage. This notation has been chosen for consistency with the general framework that will be developed at arbitrary order (see Definition 4.7).

Proposition 3.4 (Limit problem)**.** *Under Assumptions 1 and 2, the sequence* $(u_{\mathrm{i}}^{\varepsilon}, u_{\mathrm{e}}^{\varepsilon})$ *of solutions of System* (4) *in* $\mathcal{C}^{\infty}_{\mathrm{per}}(\Omega_{\mathrm{i}}^{\varepsilon}) \times \overline{\mathcal{C}^{\infty}_{\mathrm{per}}}(\Omega_{\mathrm{e}}^{\varepsilon})$ *satisfies, for all* $\phi \in \mathcal{D}(\Omega; \mathcal{C}^{\infty}_{\mathrm{per}}(Y))$*,*

$$\lim_{\varepsilon\to 0} \int_{\Omega_{\mathrm{i}}^{\varepsilon}} u_{\mathrm{i}}^{\varepsilon}(x)\phi\left(x, \frac{x}{\varepsilon}\right) = \int_{\Omega}\int_{Y_{\mathrm{i}}} u_{\mathrm{i}}^{0}(x)\phi(x,y),$$
$$\lim_{\varepsilon\to 0} \int_{\Omega_{\mathrm{e}}^{\varepsilon}} u_{\mathrm{e}}^{\varepsilon}(x)\phi\left(x, \frac{x}{\varepsilon}\right) = \int_{\Omega}\int_{Y_{\mathrm{e}}} u_{\mathrm{e}}^{0}(x)\phi(x,y),$$

where

$$u_{\mathrm{i}}^{0} = u_{\mathrm{e}}^{0} = u^{0}, \ \text{on } \Omega, \tag{10}$$

and u^0 *is the unique solution in* $\mathcal{C}^{\infty}_{\mathrm{per}}(\Omega)$ *of*

$$-\nabla\cdot\left(\left(\Sigma_{\mathrm{i}} + \Sigma_{\mathrm{e}}\right)\nabla u^{0}\right) = f, \ \text{on } \Omega, \tag{11a}$$
$$\int_{\Omega} u^{0} = 0, \tag{11b}$$

where

$$\Sigma_{\mathrm{i}} = \sigma_{\mathrm{i}}\left(|Y_{\mathrm{i}}|\,\mathrm{Id} + \int_{Y_{\mathrm{i}}}\nabla\chi_{\mathrm{i}}\right), \ \Sigma_{\mathrm{e}} = \sigma_{\mathrm{e}}\left(|Y_{\mathrm{e}}|\,\mathrm{Id} + \int_{Y_{\mathrm{e}}}\nabla\chi_{\mathrm{e}}\right). \tag{12}$$

Remark 3.5. The tensors Σ_{i} and Σ_{e} can be rewritten as follows:

$$(\Sigma_{\mathrm{i}})_{j,k} = \sigma_{\mathrm{i}}\int_{Y_{\mathrm{i}}}(e^{j} + \nabla\chi_{\mathrm{i}}^{j})\cdot(e^{k} + \nabla\chi_{\mathrm{i}}^{k}),$$
$$(\Sigma_{\mathrm{e}})_{j,k} = \sigma_{\mathrm{e}}\int_{Y_{\mathrm{e}}}(e^{j} + \nabla\chi_{\mathrm{e}}^{j})\cdot(e^{k} + \nabla\chi_{\mathrm{e}}^{k}),$$

or even

$$(\Sigma_{\mathrm{i}})_{j,k} = \sigma_{\mathrm{i}}\int_{\partial Y\cap\partial Y_{\mathrm{i}}} y_k\left(e^{j} + \nabla\chi_{\mathrm{i}}^{j}\right)\cdot n_{\mathrm{i}},$$
$$(\Sigma_{\mathrm{e}})_{j,k} = \sigma_{\mathrm{e}}\int_{\partial Y\cap\partial Y_{\mathrm{e}}} y_k\left(e^{j} + \nabla\chi_{\mathrm{e}}^{j}\right)\cdot n_{\mathrm{e}}.$$

The first expression shows that the tensors Σ_{i} and Σ_{e} are symmetric, while the second shows that if $\partial Y \cap \partial Y_{\mathrm{i}}$ (resp. $\partial Y \cap \partial Y_{\mathrm{e}}$) has zero measure, then Σ_{i} (resp. Σ_{e}) is null. In addition, for all $\xi \in \mathbb{R}^d \setminus \{0\}$, we have

$$\xi^{T}\cdot\Sigma_{\mathrm{i}}\cdot\xi = \sigma_i\int_{Y_{\mathrm{i}}}|\xi + \nabla\psi_{\xi}|^2 \geq 0,$$

where $\psi_\xi = \sum \xi_j \chi_{\mathrm{i}}^j$. If $\xi^T \cdot \Sigma_{\mathrm{i}} \cdot \xi = 0$, then

$$\nabla \psi_\xi = -\xi,$$

and therefore

$$\psi_\xi = -\xi \cdot y + C,$$

for some constant C, which is not possible if $\partial Y \cap \partial Y_{\mathrm{i}}$ has a nonzero measure, because then ψ_ξ has periodic constraints on the shared boundary. Therefore Σ_{i} (resp. Σ_{e}) is positive definite if and only if $\partial Y \cap \partial Y_{\mathrm{i}}$ (resp. $\partial Y \cap \partial Y_{\mathrm{e}}$) has a nonzero measure. In this work, we assumed that $\Omega_{\mathrm{e}}^\varepsilon$ are connected, so Σ_{e} is symmetric positive definite, ensuring that System (11) is elliptic.

Proof of Proposition 3.4. We first establish the well-posedness of System (11), and then apply classical two-scale convergence results to prove the convergence.
Existence of System (11). Thanks to the gauge condition, the regularity of f, the regularity of Σ_{i} and Σ_{e} (through the regularity of χ_{i} and χ_{e}) and the periodic boundary conditions, the well-posedness in $\mathcal{C}^\infty_{\mathrm{per}}(\Omega)$ follows directly by identifying Ω with a torus and using for instance Theorem 2.5.1.1 of [54].
Convergence. This proof presents no new difficulties and is a direct application of two-scale convergence. Using estimates of Theorem 2.3, we can apply a classical result of two-scale convergence: there exists

$$(u_{\mathrm{i}}^0, u_{\mathrm{e}}^0) \in \left(H^1(\Omega)\right)^2, \quad (u_{\mathrm{i}}^1, u_{\mathrm{e}}^1) \in L^2\left[\Omega; \overline{H^1_{\mathrm{per}}}(Y_{\mathrm{i}})\right] \times L^2\left[\Omega; \overline{H^1_{\mathrm{per}}}(Y_{\mathrm{e}})\right]$$

such that for all $\phi \in \mathcal{D}(\Omega; \mathcal{C}^\infty_{\mathrm{per}}(Y))$ and $\psi \in \left(\mathcal{D}(\Omega; \mathcal{C}^\infty_{\mathrm{per}}(Y))\right)^d$, the following convergences hold when $\varepsilon \to 0$ and up to a subsequence

$$\int_{\Omega_{\mathrm{i}}^\varepsilon} u_{\mathrm{i}}^\varepsilon(x) \phi\left(x, \frac{x}{\varepsilon}\right) \to \int_\Omega \int_{Y_{\mathrm{i}}} u_{\mathrm{i}}^0(x) \phi(x, y), \tag{13a}$$

$$\int_{\Omega_{\mathrm{e}}^\varepsilon} u_{\mathrm{e}}^\varepsilon(x) \phi\left(x, \frac{x}{\varepsilon}\right) \to \int_\Omega \int_{Y_{\mathrm{e}}} u_{\mathrm{e}}^0(x) \phi(x, y), \tag{13b}$$

$$\int_{\Omega_{\mathrm{i}}^\varepsilon} \nabla u_{\mathrm{i}}^\varepsilon(x) \cdot \psi\left(x, \frac{x}{\varepsilon}\right) \to \int_\Omega \int_{Y_{\mathrm{i}}} \left(\nabla u_{\mathrm{i}}^0(x) + \nabla_y u_{\mathrm{i}}^1(x, y)\right) \cdot \psi(x, y), \tag{13c}$$

$$\int_{\Omega_{\mathrm{e}}^\varepsilon} \nabla u_{\mathrm{e}}^\varepsilon(x) \cdot \psi\left(x, \frac{x}{\varepsilon}\right) \to \int_\Omega \int_{Y_{\mathrm{e}}} \left(\nabla u_{\mathrm{e}}^0(x) + \nabla_y u_{\mathrm{e}}^1(x, y)\right) \cdot \psi(x, y), \tag{13d}$$

$$\varepsilon \int_{\Gamma_{\mathrm{m}}^\varepsilon} u_{\mathrm{i}}^\varepsilon(x) \psi\left(x, \frac{x}{\varepsilon}\right) \to \int_\Omega \int_\Gamma u_{\mathrm{i}}^0(x) \psi(x, y), \tag{13e}$$

$$\varepsilon \int_{\Gamma_{\mathrm{m}}^\varepsilon} u_{\mathrm{e}}^\varepsilon(x) \psi\left(x, \frac{x}{\varepsilon}\right) \to \int_\Omega \int_\Gamma u_{\mathrm{e}}^0(x) \psi(x, y). \tag{13f}$$

Since $\varepsilon \int_{\Gamma_{\mathrm{m}}^\varepsilon} \left(u_{\mathrm{i}}^\varepsilon(x) - u_{\mathrm{e}}^\varepsilon(x)\right) \psi(x, \frac{x}{\varepsilon}) \to \int_\Omega \int_\Gamma \left(u_{\mathrm{i}}^0(x) - u_{\mathrm{e}}^0(x)\right) \psi(x, y)$, another classical result of

two-scale convergence (Proposition 2.5 in [67]) gives

$$\int_\Omega \int_\Gamma (u_{\rm i}^0(x) - u_{\rm e}^0(x))^2 \leq \lim_{\varepsilon\to 0} \varepsilon \int_{\Gamma_{\rm m}^\varepsilon} \left(u_{\rm i}^\varepsilon - u_{\rm e}^\varepsilon\right)^2.$$

We showed in Theorem 2.3 that $\|u_{\rm i}^\varepsilon - u_{\rm e}^\varepsilon\|_{L^2(\Gamma_{\rm m}^\varepsilon)} \leq C$, hence

$$u_{\rm i}^0 = u_{\rm e}^0.$$

To prove that (11) holds, we start from the variational formulation of System (4). We can show that, for all $(\phi_{\rm i}, \phi_{\rm e}) \in \left(\mathcal{D}(\Omega; \mathcal{C}^\infty_{\rm per}(Y)) \cap \mathcal{C}^\infty_{\rm per}(\Omega \times Y)\right)^2$, one has

$$\begin{aligned}
&\int_{\Omega_{\rm i}^\varepsilon} \sigma_{\rm i} \nabla u_{\rm i}^\varepsilon(x) \cdot \nabla \phi_{\rm i}\left(x, \frac{x}{\varepsilon}\right) {\rm d}x + \int_{\Omega_{\rm e}^\varepsilon} \sigma_{\rm e} \nabla u_{\rm e}^\varepsilon(x) \cdot \nabla \phi_{\rm e}\left(x, \frac{x}{\varepsilon}\right) {\rm d}x \\
&+\varepsilon \int_{\Gamma_{\rm m}^\varepsilon} I_{\rm m}\left(\frac{u_{\rm i}^\varepsilon(x) - u_{\rm e}^\varepsilon(x)}{\varepsilon}\right)\left(\phi_{\rm i}\left(x, \frac{x}{\varepsilon}\right) - \phi_{\rm e}\left(x, \frac{x}{\varepsilon}\right)\right) \\
&= \int_{\Omega_{\rm i}^\varepsilon} f(x) \phi_{\rm i}\left(x, \frac{x}{\varepsilon}\right) + \int_{\Omega_{\rm e}^\varepsilon} f(x) \phi_{\rm e}\left(x, \frac{x}{\varepsilon}\right),
\end{aligned} \tag{14}$$

where $\nabla \phi_{\rm i,e}\left(x, x/\varepsilon\right) = \nabla_x \phi_{\rm i,e}\left(x, x/\varepsilon\right) + \varepsilon^{-1} \nabla_y \phi_{\rm i,e}\left(x, x/\varepsilon\right)$. Let us multiply Eq. (14) by ε and make it tend towards 0. The surface term satisfies

$$\begin{aligned}
&\varepsilon^2 \int_{\Gamma_{\rm m}^\varepsilon} I_{\rm m}\left(\frac{u_{\rm i}^\varepsilon(x) - u_{\rm e}^\varepsilon(x)}{\varepsilon}\right)\left(\phi_{\rm i}\left(x, \frac{x}{\varepsilon}\right) - \phi_{\rm e}\left(x, \frac{x}{\varepsilon}\right)\right) \\
&\leq S_{\rm m}^1 \sqrt{\varepsilon} \left\|u_{\rm i}^\varepsilon - u_{\rm e}^\varepsilon\right\|_{L^2(\Gamma_{\rm m}^\varepsilon)} \sqrt{\varepsilon} \left\|\phi_{\rm i}\left(\cdot, \frac{\cdot}{\varepsilon}\right) - \phi_{\rm e}\left(\cdot, \frac{\cdot}{\varepsilon}\right)\right\|_{L^2(\Gamma_{\rm m}^\varepsilon)} \to 0
\end{aligned}$$

where $\sqrt{\varepsilon} \left\|\phi_{\rm i}\left(\cdot, \cdot/\varepsilon\right) - \phi_{\rm e}\left(\cdot, \cdot/\varepsilon\right)\right\|_{L^2(\Gamma_{\rm m}^\varepsilon)}$ is bounded because $\phi_{\rm i}$ and $\phi_{\rm e}$ are smooth enough (see for instance Lemma 2.4 in [67]) and $\sqrt{\varepsilon} \left\|u_{\rm i}^\varepsilon - u_{\rm e}^\varepsilon\right\|_{L^2(\Gamma_{\rm m}^\varepsilon)} \to 0$ because of the surface estimate in Theorem 2.3. Therefore, using Eq. (13), one has at the limit, by recalling that $u_{\rm i}^0 = u_{\rm e}^0$,

$$\int_\Omega \int_{Y_{\rm i}} \sigma_{\rm i} \left(\nabla u_{\rm e}^0 + \nabla_y u_{\rm i}^1\right) \cdot \nabla_y \phi_{\rm i} + \int_\Omega \int_{Y_{\rm e}} \sigma_{\rm e} \left(\nabla u_{\rm e}^0 + \nabla_y u_{\rm e}^1\right) \cdot \nabla_y \phi_{\rm e} = 0.$$

Note that $v_{\rm i}(x,y) := \sum_{j=1}^d \chi_{\rm i}^j(y) \frac{\partial u_{\rm e}^0}{\partial x_j}(x)$ and $v_{\rm e}(x,y) := \sum_{j=1}^d \chi_{\rm e}^j(y) \frac{\partial u_{\rm e}^0}{\partial x_j}(x)$ also satisfy

$$\int_\Omega \int_{Y_{\rm i}} \sigma_{\rm i} \left(\nabla u_{\rm e}^0 + \nabla_y v_{\rm i}\right) \cdot \nabla_y \phi_{\rm i} + \int_\Omega \int_{Y_{\rm e}} \sigma_{\rm e} \left(\nabla u_{\rm e}^0 + \nabla_y v_{\rm e}\right) \cdot \nabla_y \phi_{\rm e} = 0.$$

It implies that for all $(\phi_{\rm i}, \phi_{\rm e}) \in \left(\mathcal{D}(\Omega; \mathcal{C}^\infty_{\rm per}(Y)) \cap \mathcal{C}^\infty_{\rm per}(\Omega \times Y)\right)^2$,

$$\int_\Omega \int_{Y_{\rm i}} \sigma_{\rm i} \nabla_y (u_{\rm i}^1 - v_{\rm i}) \cdot \nabla_y \phi_{\rm i} + \int_\Omega \int_{Y_{\rm e}} \sigma_{\rm e} \nabla_y (u_{\rm e}^1 - v_{\rm e}) \cdot \nabla_y \phi_{\rm e} = 0. \tag{15}$$

Now, we use $\phi_{\rm i} = \phi_{\rm e} := \phi \in \mathcal{D}(\Omega) \cap \mathcal{C}^\infty_{\rm per}(\Omega)$ in (14) and make ε tend towards 0. Using (13),

one has

$$\int_\Omega \int_{Y_\mathrm{i}} \sigma_\mathrm{i} \left(\nabla u_\mathrm{e}^0 + \nabla_y u_\mathrm{i}^1 \right) \cdot \nabla \phi + \int_\Omega \int_{Y_\mathrm{e}} \sigma_\mathrm{e} \left(\nabla u_\mathrm{e}^0 + \nabla_y u_\mathrm{e}^1 \right) \cdot \nabla \phi = |Y| \int_\Omega f \phi.$$

Using (15) and $|Y| = 1$, one finally has

$$\int_\Omega \sum_{j=1}^{d} \left(\sigma_\mathrm{i} \left(|Y_\mathrm{i}|\, e^j + \int_{Y_\mathrm{i}} \nabla_y \chi_\mathrm{i}^j \right) + \sigma_\mathrm{e} \left(|Y_\mathrm{e}|\, e^j + \int_{Y_\mathrm{e}} \nabla_y \chi_\mathrm{e}^j \right) \right) \frac{\partial u_\mathrm{e}^0}{\partial x_j} \cdot \nabla \phi = \int_\Omega f \phi,$$

which rewrites into

$$\int_\Omega \left(\Sigma_\mathrm{i} + \Sigma_\mathrm{e} \right) \nabla u_\mathrm{e}^0 \cdot \nabla \phi = \int_\Omega f \phi.$$

Moreover, $\int_\Omega u_\mathrm{e}^0 = |Y_\mathrm{e}|^{-1} \lim_{\varepsilon \to 0} \int_{\Omega_\mathrm{e}^\varepsilon} u_\mathrm{e}^\varepsilon = 0$.

Therefore, since System (11) has a unique solution $u_\mathrm{e}^0 = u^0$ and the whole sequence $(u_\mathrm{i}^\varepsilon, u_\mathrm{e}^\varepsilon)$ converges. □

3.3. Ansatz and first order formal derivation

The leading-order (limit) problem (10)-(11) does not involve the membrane conductance S_m at all. This is a structural limitation of the order 0 model: the essential nonlinear effects due to electroporation are completely absent from the limit equations. As a result, describing the impact of S_m - and thus of electroporation - requires analyzing higher-order terms in the asymptotic expansion. This observation is consistent with both our numerical findings and with the fact that $\varepsilon = 10^{-2}$ is not particularly small. In contrast, in classical electrophysiology without PFA, ε is typically of the order 10^{-3}, and the order 0 model already provides a rich and accurate description of the dynamics.

We apply the method of two-scale asymptotic expansion to formally obtain the first-order expansion of the solution $(u_\mathrm{i}^\varepsilon, u_\mathrm{e}^\varepsilon)$ of System (4). This method consists in introducing a macroscopic variable x and a microscopic variable $y = x/\varepsilon$, thereby explicitly separating the scales involved in the model, and in assuming the following ansatz

$$u_\mathrm{i}^\varepsilon(x) = u_\mathrm{i}^0 \left(x, \frac{x}{\varepsilon} \right) + \sum_{n=1}^{\infty} \varepsilon^n u_\mathrm{i}^n \left(x, \frac{x}{\varepsilon} \right),$$
$$u_\mathrm{e}^\varepsilon(x) = u_\mathrm{e}^0 \left(x, \frac{x}{\varepsilon} \right) + \sum_{n=1}^{\infty} \varepsilon^n u_\mathrm{e}^n \left(x, \frac{x}{\varepsilon} \right),$$

where the functions $y \mapsto u_\mathrm{i}^n(x, y)$ and $y \mapsto u_\mathrm{e}^n(x, y)$ are Y-periodic for all $n \in \mathbb{N}$. This ansatz will be justified in Section 4.3 where we derive rigorous error estimates.

Plugging the ansatz into System (4) and identifying the powers of ε results in a cascade of equations that uniquely define all u_i^n and u_e^n. It involves the characterization of the

macroscopic parts (which only depend on x), denoted by a superscript $\sharp$:

$$u_{\mathrm{i}}^{n,\sharp}(x) := \frac{1}{|Y_{\mathrm{i}}|}\int_{Y_{\mathrm{i}}} u_{\mathrm{i}}^n(x,y),\ u_{\mathrm{e}}^{n,\sharp}(x) := \frac{1}{|Y_{\mathrm{e}}|}\int_{Y_{\mathrm{e}}} u_{\mathrm{e}}^n(x,y).$$

We then denote

$$v_{\mathrm{m}}^n := u_{\mathrm{i}}^n - u_{\mathrm{e}}^n, \quad v_{\mathrm{m}}^{n,\sharp} = u_{\mathrm{i}}^{n,\sharp} - u_{\mathrm{e}}^{n,\sharp}.$$

The first terms of each ansatz, u_{i}^0 and u_{e}^0, are the two-scale limits of $u_{\mathrm{i}}^\varepsilon$ and $u_{\mathrm{e}}^\varepsilon$. We showed in the previous section that they only depend on x and are equal to u^0 (as defined in Proposition 3.4).

To handle the nonlinearity, we remark that $v_{\mathrm{m}}^0 = 0$ and use Taylor expansion around $\varepsilon v_{\mathrm{m}}^1$: plugging the ansatz into I_{m} gives, at first order,

$$I_{\mathrm{m}}\left(\frac{v_{\mathrm{m}}^\varepsilon}{\varepsilon}\right) = I_{\mathrm{m}}(v_{\mathrm{m}}^1) + O(\varepsilon).$$

This expansion of the nonlinearity will be extended and proved later in Section 4.

Let us plug the ansatz into the microscopic equations and identify terms of different orders in ε. The first system of equations of the cascade is

$$-\nabla_y \cdot \left(\sigma_{\mathrm{i}}\left(\nabla_y u_{\mathrm{i}}^1 + \nabla_x u_{\mathrm{i}}^0\right)\right) = 0, \qquad \text{in } \Omega \times Y_{\mathrm{i}}, \tag{16a}$$

$$-\nabla_y \cdot \left(\sigma_{\mathrm{e}}\left(\nabla_y u_{\mathrm{e}}^1 + \nabla_x u_{\mathrm{e}}^0\right)\right) = 0, \qquad \text{in } \Omega \times Y_{\mathrm{e}}, \tag{16b}$$

$$\sigma_{\mathrm{i}}\left(\nabla_y u_{\mathrm{i}}^1 + \nabla_x u_{\mathrm{i}}^0\right) \cdot n_{\mathrm{i}} = \sigma_{\mathrm{e}}\left(\nabla_y u_{\mathrm{e}}^1 + \nabla_x u_{\mathrm{e}}^0\right) \cdot n_{\mathrm{i}}, \qquad \text{in } \Omega \times \Gamma, \tag{16c}$$

$$-\sigma_{\mathrm{i}}\left(\nabla_y u_{\mathrm{i}}^1 + \nabla_x u_{\mathrm{i}}^0\right) \cdot n_{\mathrm{i}} = 0, \qquad \text{in } \Omega \times \Gamma, \tag{16d}$$

$$+\ x \text{ and } y \text{ periodic conditions.} \tag{16e}$$

Considering x as a parameter and $(y \mapsto u_{\mathrm{i}}^1(x,y), y \mapsto u_{\mathrm{e}}^1(x,y))$ as the unknown, this system has a unique solution, up to a constant which depends on x. Note, as in the proof of Theorem 3.4, that $(\chi_{\mathrm{i}} \cdot \nabla u^0, \chi_{\mathrm{e}} \cdot \nabla u^0)$ is a solution. Therefore, we can write

$$u_{\mathrm{i}}^1(x,y) = \chi_{\mathrm{i}}(y) \cdot \nabla u^0(x) + u_{\mathrm{i}}^{1,\sharp}(x), \tag{17a}$$

$$u_{\mathrm{e}}^1(x,y) = \chi_{\mathrm{e}}(y) \cdot \nabla u^0(x) + u_{\mathrm{e}}^{1,\sharp}(x), \tag{17b}$$

where $u_{\rm i}^{1,\sharp}, u_{\rm e}^{1,\sharp}$ are periodic functions depending only on x. The next system reads

$$-\nabla_y \cdot \left(\sigma_{\rm i}\left(\nabla_y u_{\rm i}^2 + \nabla_x u_{\rm i}^1\right)\right) = \nabla_x \cdot \left(\sigma_{\rm i}\left(\nabla_y u_{\rm i}^1 + \nabla_x u_{\rm i}^0\right)\right) + f, \qquad \text{in } \Omega \times Y_{\rm i}, \tag{18a}$$

$$-\nabla_y \cdot \left(\sigma_{\rm e}\left(\nabla_y u_{\rm e}^2 + \nabla_x u_{\rm e}^1\right)\right) = \nabla_x \cdot \left(\sigma_{\rm e}\left(\nabla_y u_{\rm e}^1 + \nabla_x u_{\rm e}^0\right)\right) + f, \qquad \text{in } \Omega \times Y_{\rm e}, \tag{18b}$$

$$\sigma_{\rm i}\left(\nabla_y u_{\rm i}^2 + \nabla_x u_{\rm i}^1\right) \cdot n_{\rm i} = \sigma_{\rm e}\left(\nabla_y u_{\rm e}^2 + \nabla_x u_{\rm e}^1\right) \cdot n_{\rm i}, \qquad \text{in } \Omega \times \Gamma, \tag{18c}$$

$$-\sigma_{\rm i}\left(\nabla_y u_{\rm i}^2 + \nabla_x u_{\rm i}^1\right) \cdot n_{\rm i} = I_{\rm m}(v_{\rm m}^1), \qquad \text{in } \Omega \times \Gamma, \tag{18d}$$

$$+ \ x \text{ and } y \text{ periodic conditions.} \tag{18e}$$

Again, considering x as a parameter and $(y \mapsto u_{\rm i}^2(x,y), y \mapsto u_{\rm e}^2(x,y))$ as the unknown, this system has a unique solution, up to a constant which depends on x, if and only if the following compatibility condition is satisfied, for all $x \in \Omega$,

$$\int_{Y_{\rm i}} \nabla_x \cdot \left(\sigma_{\rm i}\left(\nabla_y u_{\rm i}^1 + \nabla_x u_{\rm i}^0\right)\right) + |Y_{\rm i}|\, f = \int_\Gamma I_{\rm m}(v_{\rm m}^1),$$
$$\int_{Y_{\rm e}} \nabla_x \cdot \left(\sigma_{\rm e}\left(\nabla_y u_{\rm e}^1 + \nabla_x u_{\rm e}^0\right)\right) + |Y_{\rm e}|\, f = -\int_\Gamma I_{\rm m}(v_{\rm m}^1).$$

By using (17) and recalling that

$$\Sigma_{\rm i} = \sigma_{\rm i}\left(|Y_{\rm i}|\,{\rm Id} + \int_{Y_{\rm i}} \nabla\chi_{\rm i}\right), \ \Sigma_{\rm e} = \sigma_{\rm e}\left(|Y_{\rm e}|\,{\rm Id} + \int_{Y_{\rm e}} \nabla\chi_{\rm e}\right),$$

it rewrites

$$\nabla \cdot \left(\Sigma_{\rm i} \nabla u^0\right) + |Y_{\rm i}|\, f = \int_\Gamma I_{\rm m}((\chi_{\rm i} - \chi_{\rm e}) \cdot \nabla u^0 + u_{\rm i}^{1,\sharp} - u_{\rm e}^{1,\sharp}),$$
$$\nabla \cdot \left(\Sigma_{\rm e} \nabla u^0\right) + |Y_{\rm e}|\, f = -\int_\Gamma I_{\rm m}((\chi_{\rm i} - \chi_{\rm e}) \cdot \nabla u^0 + u_{\rm i}^{1,\sharp} - u_{\rm e}^{1,\sharp}).$$

Summing both equations, we get back to the limit problem 11,

$$-\nabla \cdot \left(\left(\Sigma_{\rm i} + \Sigma_{\rm e}\right) \nabla u^0\right) = f, \ \text{in } \Omega, \tag{19}$$

and it remains the equation satisfied by $v_{\rm m}^{1,\sharp}$,

$$\nabla \cdot \left(\Sigma_{\rm i} \nabla u^0\right) + |Y_{\rm i}|\, f = \int_\Gamma I_{\rm m}((\chi_{\rm i} - \chi_{\rm e}) \cdot \nabla u^0 + v_{\rm m}^{1,\sharp}), \ \text{in } \Omega, \tag{20}$$

which uniquely defines $v_{\rm m}^{1,\sharp}$ as it will be shown later in Proposition 4.1 applied to $B(x,y) = [\chi]\,(y) \cdot \nabla u^0(x)$ and $F(x) = \nabla \cdot \Sigma_{\rm i} \nabla u^0(x) + |Y_{\rm i}|\, f(x)$. These two equations allow to entirely define u^0 and $v_{\rm m}^1$ (defined as the difference between the 2 equations of (17)) such that the compatibility condition of System (18) is satisfied. We can then express the solutions of this system thanks to new cell problems.

We recall that in Definition 3.2, we denote $\mathcal{P}_\alpha(F,G)$ as the unique solution in $\mathcal{C}^\infty_{\rm per}(Y_\alpha)$ of System (9) with source terms F and G.

Definition 3.6. We define for $1 \leq j \leq d$ and $1 \leq k \leq d$,

$$\begin{aligned}
\left(\chi_{\mathrm{i}}^{1,0,2}\right)_j &= \mathcal{P}_{\mathrm{i}}\left(\frac{1}{|Y_{\mathrm{i}}|}\int_\Gamma S_{\mathrm{m}}(v_{\mathrm{m}}^1)\chi_{\mathrm{i}}^j,\ S_{\mathrm{m}}(v_{\mathrm{m}}^1)\chi_{\mathrm{i}}^j\right),\\
\left(\theta_{\mathrm{i}}^{1,0,2}\right)_j &= \mathcal{P}_{\mathrm{i}}\left(\frac{1}{|Y_{\mathrm{i}}|}\int_\Gamma S_{\mathrm{m}}(v_{\mathrm{m}}^1)\chi_{\mathrm{e}}^j,\ S_{\mathrm{m}}(v_{\mathrm{m}}^1)\chi_{\mathrm{e}}^j\right),\\
\chi_{\mathrm{i}}^{0,1,2} &= \mathcal{P}_{\mathrm{i}}\left(\frac{1}{|Y_{\mathrm{i}}|}\int_\Gamma S_{\mathrm{m}}(v_{\mathrm{m}}^1),\ S_{\mathrm{m}}(v_{\mathrm{m}}^1)\right),\\
\left(\chi_{\mathrm{i}}^{2,0,2}\right)_{j,k} &= \mathcal{P}_{\mathrm{i}}\left(2\frac{\partial\chi_{\mathrm{i}}^j}{\partial y_k} - \frac{1}{|Y_{\mathrm{i}}|}\int_{Y_{\mathrm{i}}}\frac{\partial\chi_{\mathrm{i}}^j}{\partial y_k},\ \chi_{\mathrm{i}}^j n_{i,k}\right),
\end{aligned}$$

and

$$\begin{aligned}
\left(\chi_{\mathrm{e}}^{1,0,2}\right)_j &= \mathcal{P}_{\mathrm{e}}\left(-\frac{1}{|Y_{\mathrm{e}}|}\int_\Gamma S_{\mathrm{m}}(v_{\mathrm{m}}^1)\chi_{\mathrm{e}}^j,\ -S_{\mathrm{m}}(v_{\mathrm{m}}^1)\chi_{\mathrm{e}}^j\right),\\
\left(\theta_{\mathrm{e}}^{1,0,2}\right)_j &= \mathcal{P}_{\mathrm{e}}\left(-\frac{1}{|Y_{\mathrm{e}}|}\int_\Gamma S_{\mathrm{m}}(v_{\mathrm{m}}^1)\chi_{\mathrm{i}}^j,\ -S_{\mathrm{m}}(v_{\mathrm{m}}^1)\chi_{\mathrm{i}}^j\right),\\
\chi_{\mathrm{e}}^{0,1,2} &= \mathcal{P}_{\mathrm{e}}\left(-\frac{1}{|Y_{\mathrm{e}}|}\int_\Gamma S_{\mathrm{m}}(v_{\mathrm{m}}^1),\ -S_{\mathrm{m}}(v_{\mathrm{m}}^1)\right),\\
\left(\chi_{\mathrm{e}}^{2,0,2}\right)_{j,k} &= \mathcal{P}_{\mathrm{e}}\left(2\frac{\partial\chi_{\mathrm{e}}^j}{\partial y_k} - \frac{1}{|Y_{\mathrm{e}}|}\int_{Y_{\mathrm{e}}}\frac{\partial\chi_{\mathrm{e}}^j}{\partial y_k},\ \chi_{\mathrm{e}}^j n_{e,k}\right).
\end{aligned}$$

For consistency with the generalization at any order, we also introduce

$$\theta_{\mathrm{i}}^{0,1,2} = \chi_{\mathrm{i}}^{0,1,2},\ \theta_{\mathrm{e}}^{0,1,2} = \chi_{\mathrm{e}}^{0,1,2}.$$

Thanks to these new correctors, we can explicitly write the solutions of System (18) up to constants $u_{\mathrm{i}}^{2,\sharp}(x)$ and $u_{\mathrm{e}}^{2,\sharp}(x)$,

$$u_{\mathrm{i}}^2(x,y) = \chi_{\mathrm{i}}(y)\cdot\nabla u_{\mathrm{i}}^{1,\sharp}(x) + \chi_{\mathrm{i}}^{2,0,2}(y)\cdot\nabla^2 u^0(x) + \frac{1}{\sigma_{\mathrm{i}}}\chi_{\mathrm{i}}^{0,1,2}(x,y)v_{\mathrm{m}}^{1,\sharp}(x) \tag{21a}$$

$$+\frac{1}{\sigma_{\mathrm{i}}}\left(\chi_{\mathrm{i}}^{1,0,2}(x,y) - \theta_{\mathrm{i}}^{1,0,2}(x,y)\right)\cdot\nabla u^0(x) + u_{\mathrm{i}}^{2,\sharp}(x), \tag{21b}$$

$$u_{\mathrm{e}}^2(x,y) = \chi_{\mathrm{e}}(y)\cdot\nabla u_{\mathrm{e}}^{1,\sharp}(x) + \chi_{\mathrm{e}}^{2,0,2}(y)\cdot\nabla^2 u^0(x) + \frac{1}{\sigma_{\mathrm{e}}}\chi_{\mathrm{e}}^{0,1,2}(x,y)v_{\mathrm{m}}^{1,\sharp}(x) \tag{21c}$$

$$+\frac{1}{\sigma_{\mathrm{e}}}\left(-\chi_{\mathrm{e}}^{1,0,2}(x,y) + \theta_{\mathrm{e}}^{1,0,2}(x,y)\right)\cdot\nabla u^0(x) + u_{\mathrm{e}}^{2,\sharp}(x). \tag{21d}$$

Similarly as before, we can show that the next system in the cascade has solutions if and

only if some compatibility conditions are satisfied. The first one is

$$-\int_{Y_\mathrm{i}} \nabla_x \cdot \left(\sigma_\mathrm{i}\left(\nabla_y u_\mathrm{i}^2 + \nabla_x u_\mathrm{i}^1\right)\right) - \int_{Y_\mathrm{e}} \nabla_x \cdot \left(\sigma_\mathrm{e}\left(\nabla_y u_\mathrm{e}^2 + \nabla_x u_\mathrm{e}^1\right)\right) = 0. \tag{22}$$

Combining it with Eq. (21), we deduce an equation on $u_\mathrm{e}^{1,\sharp}$ which can be rewritten using the following lemma.

Lemma 3.7. *Let $\chi \in \mathcal{C}^\infty_{\mathrm{per}}(Y_\alpha)$ and let $1 \leq j \leq d$, we have*

$$\int_{Y_\alpha} \frac{\partial \chi}{\partial y_j} = \int_{Y_\alpha} \Delta\chi \chi_\alpha^j - \int_\Gamma \nabla\chi \cdot n_\alpha \chi_\alpha^j.$$

Proof.

$$\begin{aligned}\int_{Y_\alpha} \frac{\partial \chi}{\partial y_j} &= \int_\Gamma \chi n_{\alpha,j} = -\int_\Gamma \chi \nabla\chi_\alpha^j \cdot n_\alpha = -\int_{Y_\alpha} \nabla\chi \cdot \nabla\chi_\alpha^j \\ &= \int_{Y_\alpha} \Delta\chi\chi_\alpha^j - \int_\Gamma \nabla\chi \cdot n_\alpha \chi_\alpha^j.\end{aligned}$$

□

After some computation, Eq. (22) can be rewritten as:

$$-\nabla \cdot \left(\Sigma_\mathrm{i} \nabla u_\mathrm{i}^{1,\sharp}\right) - \nabla \cdot \left(\Sigma_\mathrm{e} \nabla u_\mathrm{e}^{1,\sharp}\right) = \nabla \cdot \left(\int_\Gamma I_\mathrm{m}(v_\mathrm{m}^1)\,[\chi]\right).$$

Replacing $u_\mathrm{i}^{1,\sharp}$ by $u_\mathrm{e}^{1,\sharp} + v_\mathrm{m}^{1,\sharp}$, we get an equation for $u_\mathrm{e}^{1,\sharp}$

$$-\nabla \cdot \left(\left(\Sigma_\mathrm{i} + \Sigma_\mathrm{e}\right) \nabla u_\mathrm{e}^{1,\sharp}\right) = \nabla \cdot \left(\Sigma_\mathrm{i} \nabla v_\mathrm{m}^{1,\sharp}\right) + \nabla \cdot \left(\int_\Gamma I_\mathrm{m}(v_\mathrm{m}^1)\,[\chi]\right), \text{ in } \Omega, \tag{23}$$

that we complement with the gauge condition

$$\int_\Omega u_\mathrm{e}^{1,\sharp} = 0.$$

Remark that $f_1 := \nabla \cdot \left(\Sigma_\mathrm{i} \nabla v_\mathrm{m}^{1,\sharp}\right) + \nabla \cdot \left(\int_\Gamma I_\mathrm{m}(v_\mathrm{m}^1)\,[\chi]\right) \in \mathcal{C}^\infty_{\mathrm{per}}(\Omega)$ satisfies $\int_\Omega f_1 = 0$, as the divergence of periodic quantities. Therefore this system has a unique solution, as it will be shown in the next section in Theorem 4.2.

In order to progress in the expansion, the remaining steps of the expansion proceed similarly. The second compatibility condition defines $v_\mathrm{m}^{2,\sharp} := u_\mathrm{i}^{2,\sharp} - u_\mathrm{e}^{2,\sharp}$, so that u_i^d and u_e^d can be expressed with new cell correctors and injected in the next compatibility condition which defines $v_\mathrm{m}^{3,\sharp} := u_\mathrm{i}^{3,\sharp} - u_\mathrm{e}^{3,\sharp}$ and $u_\mathrm{e}^{2,\sharp}$, and so forth. The reasoning by induction is summed up in Section 4, along with the rigorous justification of the full asymptotic expansion.

3.4. Effective model

The first-order model is composed of equations (11), (20), and (23) and can be rewritten as

$$u_{\mathrm{e}}^0 - u_{\mathrm{i}}^0 = 0, \text{ in } \Omega, \tag{24a}$$

$$-\nabla \cdot \Big(\big(\Sigma_{\mathrm{i}} \nabla u_{\mathrm{i}}^0 + \Sigma_{\mathrm{e}} \nabla u_{\mathrm{e}}^0 \big) \Big) = f, \text{ in } \Omega, \tag{24b}$$

$$\begin{aligned} 2 \int_\Gamma I_{\mathrm{m}} (u_{\mathrm{i}}^{1,\sharp} - u_{\mathrm{e}}^{1,\sharp} + (\chi_{\mathrm{i}} - \chi_{\mathrm{e}}) \cdot \nabla \frac{u_{\mathrm{e}}^0 + u_{\mathrm{i}}^0}{2}) &= \nabla \cdot \big(\Sigma_{\mathrm{i}} \nabla u_{\mathrm{i}}^0 - \Sigma_{\mathrm{e}} \nabla u_{\mathrm{e}}^0 \big), \text{ in } \Omega, \\ &\quad + (|Y_{\mathrm{i}}| - |Y_{\mathrm{e}}|) f \end{aligned} \tag{24c}$$

$$\begin{aligned} -\nabla \cdot \Big(\big(\Sigma_{\mathrm{i}} \nabla u_{\mathrm{i}}^{1,\sharp} + \Sigma_{\mathrm{e}} \nabla u_{\mathrm{e}}^{1,\sharp} \big) \Big) = \nabla \cdot \Big(\int_\Gamma I_{\mathrm{m}} \big(u_{\mathrm{i}}^{1,\sharp} - u_{\mathrm{e}}^{1,\sharp} \\ + (\chi_{\mathrm{i}} - \chi_{\mathrm{e}}) \cdot \nabla \frac{u_{\mathrm{e}}^0 + u_{\mathrm{i}}^0}{2} \big) [\chi] \Big) \end{aligned}, \text{ in } \Omega, \tag{24d}$$

$$\int_\Omega u_{\mathrm{e}}^0 = \int_\Omega u_{\mathrm{e}}^{1,\sharp} = 0, \tag{24e}$$

along with periodic boundary conditions. It is interesting to derive from these first two orders an effective model at the order 1, that can be compared for instance to the classical bidomain model for cardiac electrophysiology [28].

Introducing the variables $(U_{\mathrm{i}}^\varepsilon, U_{\mathrm{e}}^\varepsilon)$ solution to the following problem

$$-\nabla \cdot (\Sigma_{\mathrm{i}} \nabla U_{\mathrm{i}}^\varepsilon + \Sigma_{\mathrm{e}} \nabla U_{\mathrm{e}}^\varepsilon) = f + \varepsilon \nabla \cdot \Big(\int_\Gamma I_{\mathrm{m}} \big(\frac{U_{\mathrm{i}}^\varepsilon - U_{\mathrm{e}}^\varepsilon}{\varepsilon} + (\chi_{\mathrm{i}} - \chi_{\mathrm{e}}) \cdot \nabla \frac{U_{\mathrm{i}}^\varepsilon + U_{\mathrm{e}}^\varepsilon}{2} \big) [\chi] \Big) \tag{25a}$$

$$2\varepsilon \int_\Gamma I_{\mathrm{m}} \big(\frac{U_{\mathrm{i}}^\varepsilon - U_{\mathrm{e}}^\varepsilon}{\varepsilon} + (\chi_{\mathrm{i}} - \chi_{\mathrm{e}}) \cdot \nabla \frac{U_{\mathrm{i}}^\varepsilon + U_{\mathrm{e}}^\varepsilon}{2} \big) dy = \varepsilon \left(\nabla \cdot (\Sigma_{\mathrm{i}} \nabla U_{\mathrm{i}}^\varepsilon - \Sigma_{\mathrm{e}} \nabla U_{\mathrm{e}}^\varepsilon) + (|Y_{\mathrm{i}}| - |Y_{\mathrm{e}}|) f \right). \tag{25b}$$

One can show that if the solution $(U_{\mathrm{i}}^\varepsilon, U_{\mathrm{e}}^\varepsilon)$ of the above system exists, then thanks to an expansion in powers of ε of the solution, tedious yet straightforward calculations show that, at least formally, the first two orders of the expansion of $(U_{\mathrm{i}}^\varepsilon, U_{\mathrm{e}}^\varepsilon)$ satisfy the same problem as $(u_{\mathrm{e}}^0, u_{\mathrm{i}}^0)$ and $(u_{\mathrm{i}}^{1,\sharp}, u_{\mathrm{e}}^{1,\sharp})$.

This effective model is presented here for informational purposes only and is not used in the following numerical simulations, which deal separately with the first two orders. More precisely, the first-order model used in the subsequent numerical simulations and recommended for practical computations reads as follows:

$$-\nabla \cdot \Big((\Sigma_{\mathrm{i}} + \Sigma_{\mathrm{e}}) \nabla u^0 \Big) = f, \text{ in } \Omega, \tag{26a}$$

$$\nabla \cdot \Big(\Sigma_{\mathrm{i}} \nabla u^0 \Big) + |Y_{\mathrm{i}}| f = \int_\Gamma I_{\mathrm{m}} ((\chi_{\mathrm{i}} - \chi_{\mathrm{e}}) \cdot \nabla u^0 + v_{\mathrm{m}}^{1,\sharp}), \text{ in } \Omega, \tag{26b}$$

$$-\nabla \cdot \Big((\Sigma_{\mathrm{i}} + \Sigma_{\mathrm{e}}) \nabla u_{\mathrm{e}}^{1,\sharp} \Big) = \nabla \cdot \Big(\Sigma_{\mathrm{i}} \nabla v_{\mathrm{m}}^{1,\sharp} \Big) + \nabla \cdot \Big(\int_\Gamma I_{\mathrm{m}} (v_{\mathrm{m}}^1) [\chi] \Big), \text{ in } \Omega, \tag{26c}$$

$$\int_\Omega u^0 = \int_\Omega u_{\mathrm{e}}^{1,\sharp} = 0, \tag{26d}$$

along with periodic boundary conditions. This model enables the computation of approximations of the electric field, as detailed in the next section (see Eq. (27)), as well as other quantities of interest, as discussed in Section 3.5.3.

3.5. Numerical simulations

Once the paper accepted, the code will be publicly available online.

3.5.1. Implementation

In this section, we detail our strategy and our choices concerning the numerical illustrations.

Algorithm. Numerical simulations are performed using the *FreeFem++* software [68]. The spatial discretization and fixed-point convergence criteria have been selected finely enough to ensure that numerical errors remain negligible and do not interfere with the observed convergence or the validity of the results. The steps are the following:

- compute the order 1 cell correctors χ_α by solving the cell problems (3.2), with P^2 Lagrangian finite elements and a Lagrange multiplier to force the gauge condition,
- compute u^0 by solving the limit problem (11) with P^2 Lagrangian finite elements,
- compute $v_{\mathrm{m}}^{1,\sharp}$ by solving the non-linear algebraic equation (20), using a fixed-point method on each point of the mesh,
- compute $u_{\mathrm{e}}^{1,\sharp}$ by solving the problem (23), using P^2 Lagrangian finite elements,
- compute the order 2 cell correctors $\chi_\alpha^{2,0,2}$, $\chi_\alpha^{0,1,2}$, $\chi_\alpha^{1,0,2}$, $\theta_\alpha^{1,0,2}$ by solving the cell problems given in Theorem 3.6, with P^2 Lagrangian finite elements and a Lagrange multiplier to force the gauge condition.

Then, for a given ε, the approximations of the potentials $u_\alpha^{1,\varepsilon}\left(x, \frac{x}{\varepsilon}\right)$, and the electric fields $\boldsymbol{E}_\alpha^0\left(x, \frac{x}{\varepsilon}\right)$ and $\boldsymbol{E}_\alpha^{1,\varepsilon}\left(x, \frac{x}{\varepsilon}\right)$ are given by

$$u_\alpha^{1,\varepsilon}(x,y) := u^0(x) + \varepsilon u_\alpha^1(x,y), \tag{27a}$$

$$\boldsymbol{E}_\alpha^0(x,y) := -\left(\nabla u^0(x) + \nabla_y u_\alpha^1(x,y)\right), \tag{27b}$$

$$\boldsymbol{E}_\alpha^{1,\varepsilon}(x,y) := \boldsymbol{E}_\alpha^0(x,y) - \varepsilon\left(\nabla_x u_\alpha^1(x,y) + \nabla_y u_\alpha^2(x,y)\right). \tag{27c}$$

As a consequence of the problem being non-linear, the cell problems for $\chi_\alpha^{0,1,2}$, $\chi_\alpha^{1,0,2}$ and $\theta_\alpha^{1,0,2}$ cannot be computed once and for all. Indeed, their source term depends on

$$I_{\mathrm{m}}\left((\chi_{\mathrm{i}}(y) - \chi_{\mathrm{e}}(y)) \cdot \nabla u^0(x) + v_{\mathrm{m}}^{1,\sharp}(x)\right)$$

and therefore on the macroscopic variable x. Consequently, it must be solved on each point of the macroscopic domain. We loop over every point $x_j \in \mathbb{R}^2$ of the macroscopic mesh and

(a) Isotropic cell

(b) Ellipsoid cell

Figure 2: Different types of cells Y

compute $\chi_\alpha^{0,1,2}(x_j,\cdot)$, $\chi_\alpha^{1,0,2}(x_j,\cdot)$ and $\theta_\alpha^{1,0,2}(x_j,\cdot)$. In practice, for a given ε, we only store $\chi_\alpha^{0,1,2}(x_j,\frac{x_j}{\varepsilon})$, $\chi_\alpha^{1,0,2}(x_j,\frac{x_j}{\varepsilon})$ and $\theta_\alpha^{1,0,2}(x_j,\frac{x_j}{\varepsilon})$ and not the whole functions.

Although solving these corrector problems at each macroscopic point is computationally demanding, it still requires a much coarser mesh than what would be needed to solve the full multiscale problem. In practice, depending on the quantity of interest, it may not even be necessary to compute all these correctors, which further reduces the computational cost.

Membrane conductivity. As often in electroporation modeling, either at tissue [69] or cell scale [47], S_m is modeled as a sigmoid function. We choose the following profile:

$$S_\mathrm{m}(\lambda) = S_\mathrm{m}^0 + \frac{S_\mathrm{m}^1 - S_\mathrm{m}^0}{1+\exp\left(-k\left(\frac{\lambda^2}{V_\mathrm{ep}^2}-1\right)\right)},$$

with the following physical parameters:

$$\sigma_\mathrm{i} = 2,\ \sigma_\mathrm{e} = 1,\ S_\mathrm{m}^0 = 0.01,\ S_\mathrm{m}^1 = 0.5,\ k = 5,\ V_\mathrm{ep} = 0.1.$$

Geometry. The domain is $\Omega = [0,1]^2$, and, as explained in Section 2.1, is the juxtaposition of $N \in \mathbb{N}$ square cell domains Y in each direction, meaning that ε takes values $1/N$. We considered two types of cells to study the effect of the cell shape on the convergence and the solution itself, since cardiac muscle cells are very elongated. We considered isotropic cells (Fig. 2a) and ellipses oriented towards the x-axis (Fig. 2b).

Source term. The source term f is modeled as

$$\begin{aligned} f(x_1,x_2) = A\Big(&\exp\left(-\nu((x_1-0.5)^2+(x_2-0.35)^2)\right) \\ &+ \exp\left(-\nu((x_1-0.5)^2+(x_2-0.65)^2)\right)\Big), \end{aligned} \tag{28}$$

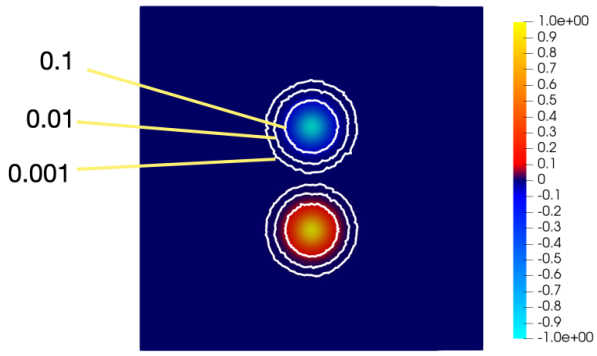

Figure 3: Profile of the normalized source term f/A. Contour lines are those of $|f/A|$.

where $\nu = 100$ and $A = 10$, which corresponds to the amplitude of a typical electroporation current $\sim 1\,\mathrm{A}$, after nondimensionalization. This source term aims to mimic the insertion of two electrodes, the first one centered at point $(0.5, 0.35)$ and the second one at point $(0.5, 0.65)$, see Fig. 3.

3.5.2. Convergence study

We conduct a numerical convergence study with respect to ε. For a range of decreasing values of ε, we compute the non-linear microscopic problem (1) using a fixed point method and P^2 Lagrangian finite elements, and compare its solutions to the homogenized approximations. More precisely, we study the order 0 and order 1 approximations of $(u_{\mathrm{i}}^\varepsilon, u_{\mathrm{e}}^\varepsilon)$, $v_{\mathrm{m}}^\varepsilon$ and $(\boldsymbol{E}_{\mathrm{i}}^\varepsilon, \boldsymbol{E}_{\mathrm{e}}^\varepsilon) := (-\nabla u_{\mathrm{i}}^\varepsilon, -\nabla u_{\mathrm{e}}^\varepsilon)$ given by Equation (27).

Consequently, the following errors will be numerically approximated and monitored:

$$e_{\mathrm{L}_2}^{\alpha,0} := \frac{\|u_\alpha^\varepsilon(x) - u^0(x)\|_{L^2(\Omega_\alpha^\varepsilon)}}{\sqrt{|Y_\alpha|}\,\|u^0(x)\|_{L^2(\Omega)}}, \tag{29a}$$

$$e_{\mathrm{L}_2}^{\alpha,1} := \frac{\left\|u_\alpha^\varepsilon(x) - u^0(x) - \varepsilon u_\alpha^1\left(x, \frac{x}{\varepsilon}\right)\right\|_{L^2(\Omega_\alpha^\varepsilon)}}{\sqrt{|Y_\alpha|}\,\|u^0(x)\|_{L^2(\Omega)}}, \tag{29b}$$

$$e_{\mathrm{H}^1}^{\alpha,0} := \frac{\left\|\boldsymbol{E}_\alpha^\varepsilon(x) - \boldsymbol{E}_\alpha^0\left(x, \frac{x}{\varepsilon}\right)\right\|_{L^2(\Omega_\alpha^\varepsilon)}}{\sqrt{|Y_\alpha|}\,\|\nabla u^0(x)\|_{L^2(\Omega)}}, \tag{29c}$$

$$e_{\mathrm{H}^1}^{\alpha,1} := \frac{\left\|\boldsymbol{E}_\alpha^\varepsilon(x) - \boldsymbol{E}_\alpha^{1,\varepsilon}\left(x, \frac{x}{\varepsilon}\right)\right\|_{L^2(\Omega_\alpha^\varepsilon)}}{\sqrt{|Y_\alpha|}\,\|\nabla u^0(x)\|_{L^2(\Omega)}}, \tag{29d}$$

$$e_{\mathrm{L}_2}^{v_{\mathrm{m}}} := \left\|(u_{\mathrm{i}}^\varepsilon - u_{\mathrm{e}}^\varepsilon) - \varepsilon(u_{\mathrm{i}}^1 - u_{\mathrm{e}}^1)\left(x, \frac{x}{\varepsilon}\right)\right\|_{L^2(\Gamma_{\mathrm{m}}^\varepsilon)}. \tag{29e}$$

Convergence rates. Numerical convergence rates are shown in Fig. 4. The numerical values are also given in Table B.1 in Appendix B. For each cell type, the errors defined in Eq. (29) are

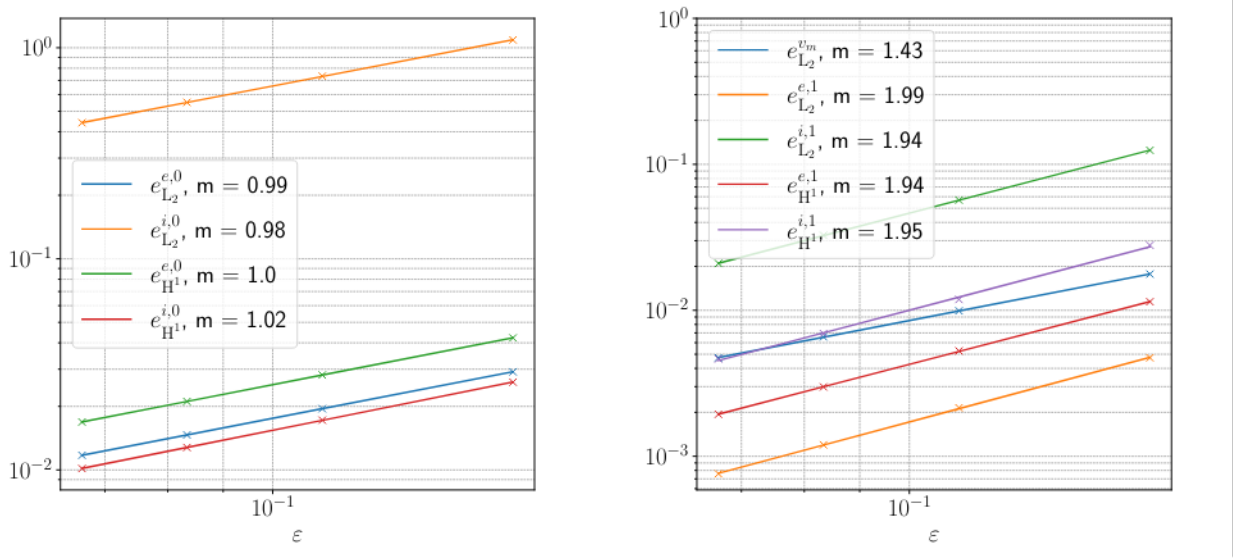

(a) Isotropic cell

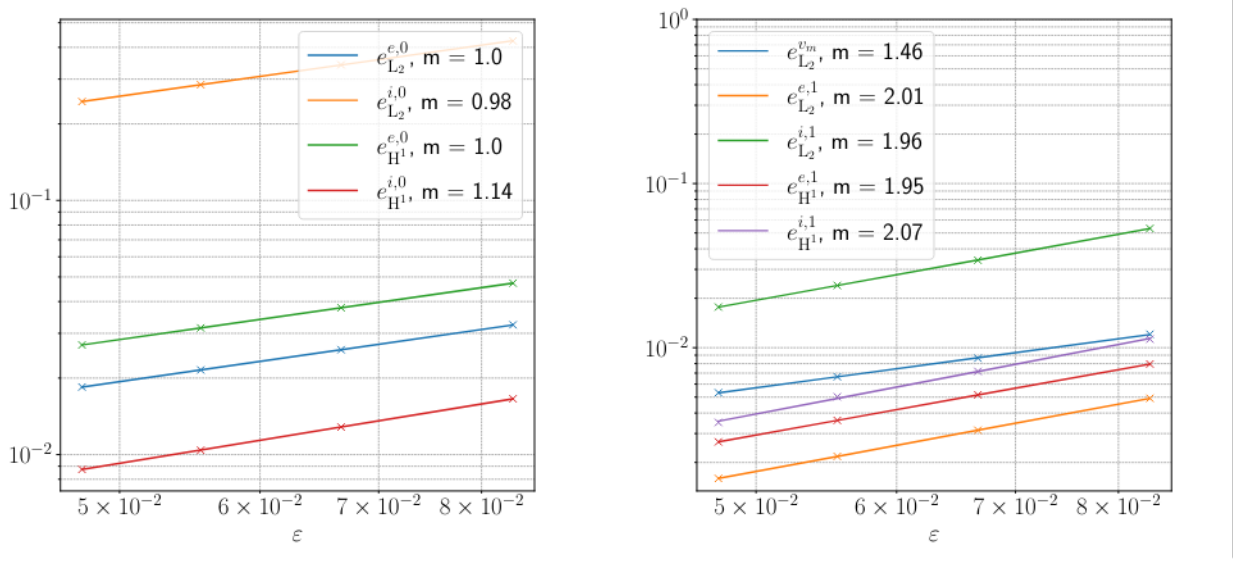

(b) Anisotropic cell (oriented towards x)

Figure 4: Errors defined in Eq. (29), for the order 0 (left) and order 1 (right) homogenized models as a function of ε in a log-log scale. m is the slope of the linear regression. The values of ε are $(1/6, 1/9, 1/12, 1/15)$ for the isotropic cell and $(1/12, 1/15, 1/18, 1/21)$ for the anisotropic cell. The numerical values of the errors are also given in Table B.1 (see Appendix B).

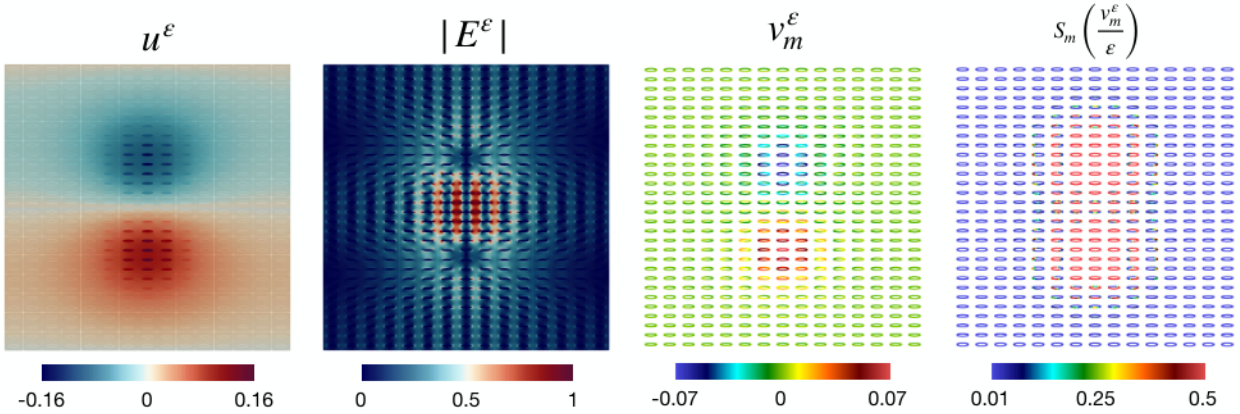

Figure 5: Solution of the microscopic problem with $\varepsilon = 1/15$ and an anisotropic cell oriented towards the x-axis. From left to right, the electric potential $u^\varepsilon = u_{\mathrm{i}}^\varepsilon 1_{\Omega_{\mathrm{i}}^\varepsilon} + u_{\mathrm{e}}^\varepsilon 1_{\Omega_{\mathrm{e}}^\varepsilon}$, the amplitude of the electric field $|\boldsymbol{E}^\varepsilon| = |\boldsymbol{E}_{\mathrm{i}}^\varepsilon| 1_{\Omega_{\mathrm{i}}^\varepsilon} + |\boldsymbol{E}_{\mathrm{e}}^\varepsilon| 1_{\Omega_{\mathrm{e}}^\varepsilon}$, the transmembrane potential $v_{\mathrm{m}}^\varepsilon$ and the membrane conductance $S_{\mathrm{m}}\,(v_{\mathrm{m}}^\varepsilon/\varepsilon)$. All the quantities are unitless.

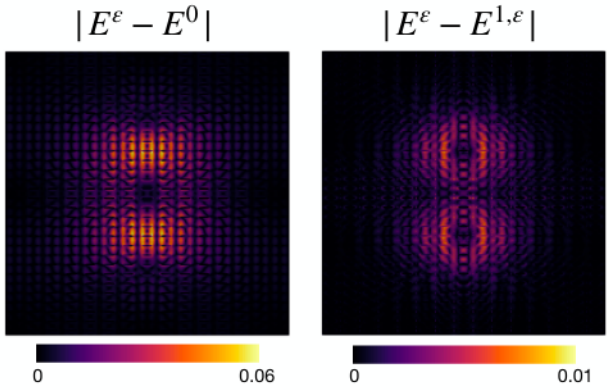

Figure 6: Spatial distribution of the difference between the electric fields computed with the microscopic model ($\boldsymbol{E}^\varepsilon$) and the homogenized models at order 0 ($\boldsymbol{E}^0$) and order 1 ($\boldsymbol{E}^1$) for $\varepsilon = 1/15$ and the anisotropic cell. This difference is used to compute the normalized errors $e_{\mathrm{H}^1}^{\alpha,0}$ and $e_{\mathrm{H}^1}^{\alpha,1}$ that are plotted on Fig. 4 and given in Table B.1. Note the 6-fold difference between the errors at order 0 and order 1.

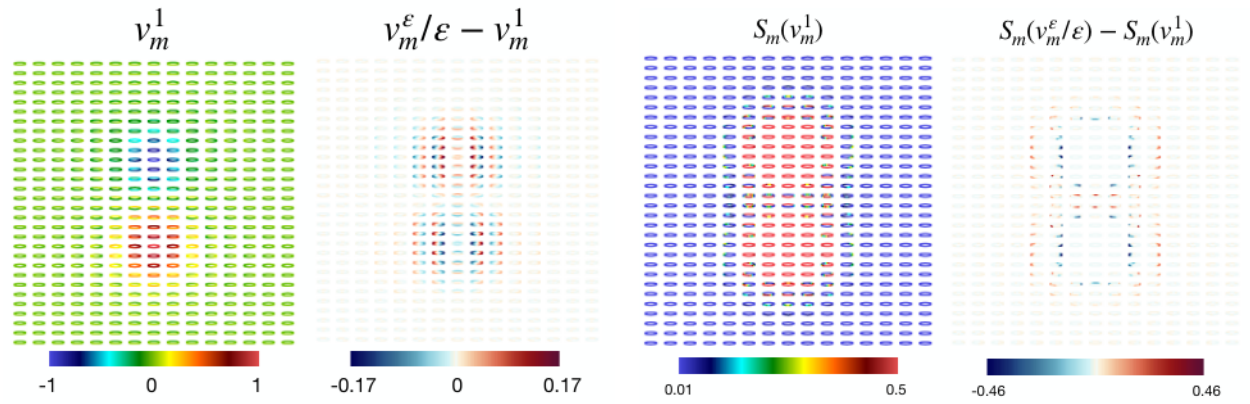

(a) Transmembrane potential

(b) Cell membrane conductance

Figure 7: Approximation of the transmembrane potential and the resulting cell membrane conductance for $\varepsilon = 1/15$. The difference $v_{\mathrm{m}}^\varepsilon/\varepsilon - v_{\mathrm{m}}^1$ is used to computed the error $e_{\mathrm{L}^2}^{v_{\mathrm{m}}}$ that is reported on Fig. 4 and in Table B.1. All quantities are unitless. Recall that S_m ranges from $S_{\mathrm{m}}^0 = 0.01$ to $S_{\mathrm{m}}^1 = 0.5$.

computed for four different values of ε, and a linear regression is performed to estimate the convergence rate. The computational cost of these evaluations grows significantly as ε goes to smaller values, since each cell of size ε must be sufficiently meshed to capture the shape of the membrane. We chose values for ε from $1/12$ down to $1/21$. In all cases, the mesh consists of approximately 10^6 nodes, with computations taking around half an hour on 32 cores. This highlights the advantage of a homogenized model, which reduces the need for fine meshing, especially in 3D. As a result of using not small enough values of ε, some errors are quite large, but we can already observe that we have reached the asymptotic regime and evaluate safely the convergence rates. The measured rates are as follows: order ε for the zeroth-order approximations of $(u_{\mathrm{i}}^\varepsilon, u_{\mathrm{e}}^\varepsilon)$ and $(\boldsymbol{E}_{\mathrm{i}}^\varepsilon, \boldsymbol{E}_{\mathrm{e}}^\varepsilon)$, order $\varepsilon^{\frac{3}{2}}$ for the first-order approximation of $v_{\mathrm{m}}^\varepsilon$ and order ε^2 for the first-order approximations of $(u_{\mathrm{i}}^\varepsilon, u_{\mathrm{e}}^\varepsilon)$ and $(\boldsymbol{E}_{\mathrm{i}}^\varepsilon, \boldsymbol{E}_{\mathrm{e}}^\varepsilon)$. These encouraging results suggest that theoretical convergence estimates can indeed be established. This will be the focus of the next section.

Comparison between microscopic and homogenized models. Numerical illustrations of the approximate quantities of interest obtained from the microscopic and homogenized models — when the anisotropic cell is aligned with the x-axis and $\varepsilon = 1/15$ — are displayed in Fig. 5. On Figs. 6 and 7, we show how the difference with the first orders, used to compute the errors $e_{\mathrm{H}^1}^{\alpha,0}$, $e_{\mathrm{H}^1}^{\alpha,1}$ and $e_{\mathrm{L}^2}^{v_{\mathrm{m}}}$ from Fig. 4, is distributed, for this single value of ε.

3.5.3. Characterization of the ablated zone

To conclude this numerical study and as a first step towards potential biological applications, we illustrate the average membrane conductance over the unit cell membrane, defined by

$$S_{\mathrm{m}}^{\mathrm{eff},0}(x) = \frac{1}{|\Gamma|}\int_\Gamma S_{\mathrm{m}}(v_{\mathrm{m}}^1(x,y))dy.$$

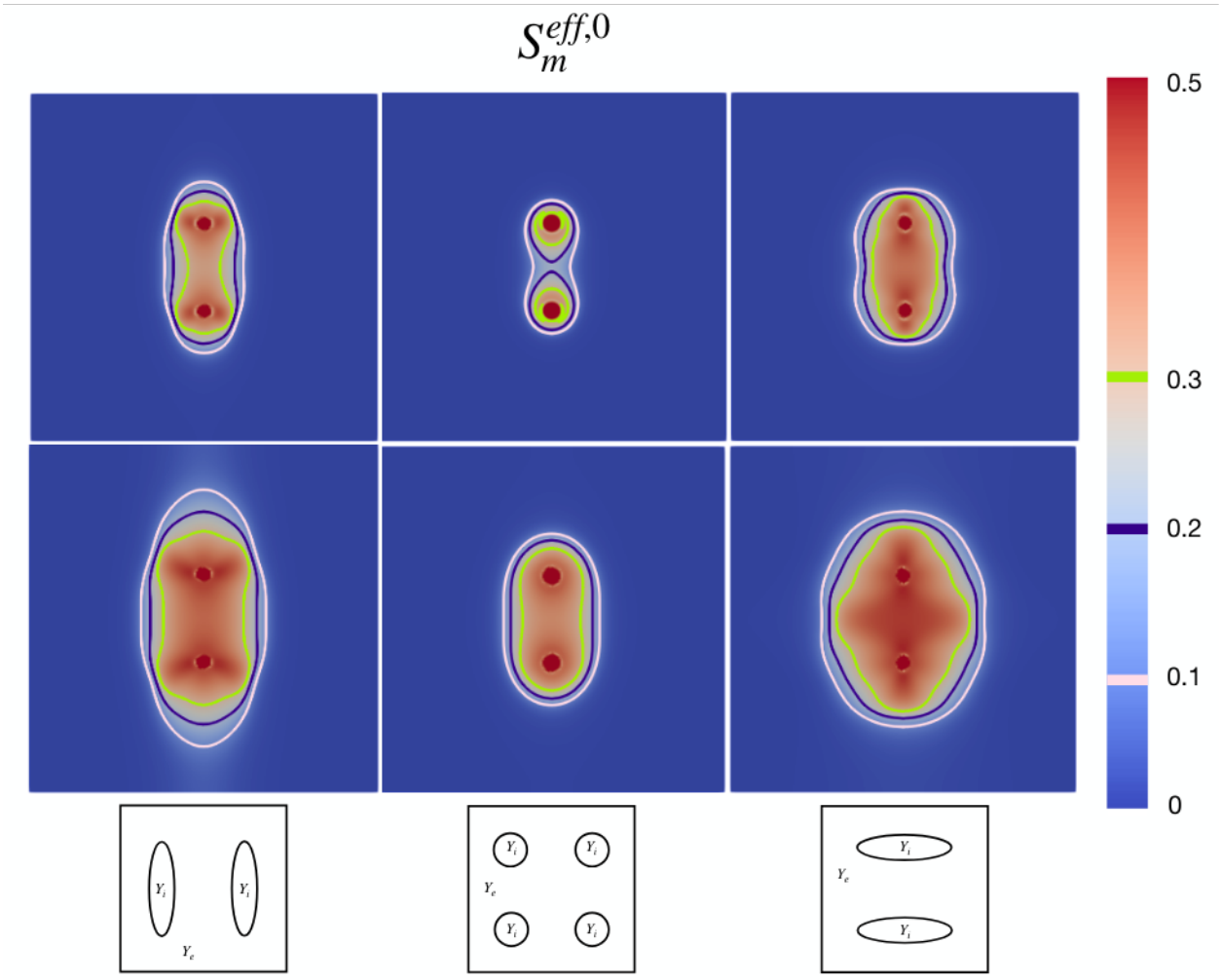

Figure 8: Average membrane conductance over the unit cell membrane ranging from $S_{\mathrm{m}}^0 = 0.01$ (no cell membrane electroporated) to $S_{\mathrm{m}}^1 = 0.5$ (all the cell membrane is electroporated). Recall that all quantities are unitless. Delivered current is $I = 0.5$A (top), $I = 1$A (bottom). Three cell types are considered, displayed below the results, representing fibers oriented towards x (left), towards y (right) and no privileged direction (middle). Isolines are 0.1 (light pink), 0.2 (blue), 0.3 (light green).

This quantity may serve as a preliminary marker for characterizing the effectively ablated zone in PFA.

Remark 3.8. In standard electroporation modeling, lesions are delineated using isolines of $|\nabla u^0|$. Since in those models, the tissue conductivity has a direct dependence on $|\nabla u^0|$, using either levels of S_{m} or $|\nabla u^0|$ is equivalent. In our case, it is necessary to use $S_{\mathrm{m}}^{\mathrm{eff},0}$ as it also depends on the transmembrane voltage defined on Γ.

The numerical setup is qualitatively the same as before. The nonlinearity profile and the physical parameters σ_{i}, σ_{e}, S_{m}^0, S_{m}^1, k and V_{ep} remain unchanged. The size of the domain and the distance between the electrodes are inspired from [69] to be closer to a realistic experimental setup. Instead of setting A the amplitude of the source term, we set I the total current injected into the domain and choose A accordingly ($\nu = 100$ is set in Eq. (28)). We compare specific isolines of $S_{\mathrm{m}}^{\mathrm{eff},0}$ for different current values ($I = 0.5\,\mathrm{A}$ and $I = 1\,\mathrm{A}$) and for cells with varying privileged directions: aligned along the x-axis, aligned along the y-axis, and isotropic (no privileged direction). The size of the cells was set to have similar intra/extra volume ratios, and similar membrane length. This is why the number of connected components, which actually represent the cells, may vary within the cellular domain. Figure 8 presents these unit cells along with the results of the comparison.

The orientation of the fibers, as determined by the cell geometry, has a significant impact on both the shape and the area of the ablated zone. In both anisotropic configurations, the area of the ablated region is relatively similar, albeit for different reasons. When the cells are aligned along the x-axis, a large portion of the cell membrane exhibits conductance values above S_{m}^0. In contrast, when the cells are aligned along the y-axis, only a small portion of the membrane reaches that threshold, but the conductance values are significantly higher, resulting in a similar average $S_{\mathrm{m}}^{\mathrm{eff},0}$. This suggests that additional quantities may need to be considered - such as the variance of the membrane conductance across the membrane, or the root mean square of the membrane conductance - in order to better understand and characterize the ablation behavior.

4. Rigorous justification of the full asymptotic expansion

The goal of this section is to provide a rigorous mathematical justification of the asymptotic model introduced earlier. While the derivation was formal, the numerical results presented in the previous section strongly support the validity of the expansion: the observed convergence rates align well with the expected orders in ε. This motivates a detailed analysis to establish precise error bounds and confirm that the homogenized system, together with its higher-order corrections, accurately approximates the microscopic model in the asymptotic limit.

We now discuss the strategy adopted in this section. In the variational formulation (14), we formally have

$$\varepsilon \int_{\Gamma_{\mathrm{m}}^{\varepsilon}} I_{\mathrm{m}} \left(\frac{u_{\mathrm{i}}^{\varepsilon} - u_{\mathrm{e}}^{\varepsilon}}{\varepsilon} \right) (\phi_{\mathrm{i}} - \phi_{\mathrm{e}}) \to \int_{\Omega} \int_{\Gamma} I_{\mathrm{m}} (u_{\mathrm{i}}^1 - u_{\mathrm{e}}^1)(\phi_{\mathrm{i}} - \phi_{\mathrm{e}}).$$

Using $\phi_{\rm i} = \phi_{\rm i}(x)$ and $\phi_{\rm e} = \phi_{\rm e}(x)$, and making $\varepsilon \to 0$ in Eq. (14), we find

$$\nabla \cdot \left(\Sigma_{\rm i} \nabla u^0\right) + |Y_{\rm i}|\, f = \int_\Gamma I_{\rm m}(u_{\rm i}^1 - u_{\rm e}^1), \text{ in } \Omega$$
$$\nabla \cdot \left(\Sigma_{\rm e} \nabla u^0\right) + |Y_{\rm e}|\, f = -\int_\Gamma I_{\rm m}(u_{\rm i}^1 - u_{\rm e}^1), \text{ in } \Omega.$$

These equations are consistent with the limit problem (11) (already rigorously justified) and the first correction equation (20). However, rigorously justifying the above convergence would require proving that $u_{\rm i}^\varepsilon - u_{\rm e}^\varepsilon = O(\varepsilon)$ (in a suitable norm), which is stronger than what we already have *i.e.* $u_{\rm i}^\varepsilon - u_{\rm e}^\varepsilon = o(1)$ in H^1 norm. It usually requires that $u_{\rm i}^1 - u_{\rm e}^1$ is already defined. In fact, the process of proving these improved estimates, via the construction of $u_{\rm i}^1$ and $u_{\rm e}^1$ and the study of the error, already gives the wanted result, *i.e.* the justification of the first-order term in the ansatz, making it unnecessary to rely on two-scale convergence arguments.

For these reasons, we adopt a constructive approach: we explicitly define the higher-order correctors via the formal multi-scale expansion and then derive quantitative error estimates to rigorously justify the asymptotic approximation. Importantly, we extend this justification to the full asymptotic expansion at all orders, since the process of constructing correctors and proving error bounds is analogous at each step.

We recall the ansatz

$$u_{\rm i}^\varepsilon(x) = u_{\rm i}^0(x) + \sum_{n=1}^{\infty} \varepsilon^n u_{\rm i}^n\left(x, \frac{x}{\varepsilon}\right),$$
$$u_{\rm e}^\varepsilon(x) = u_{\rm e}^0(x) + \sum_{n=1}^{\infty} \varepsilon^n u_{\rm e}^n\left(x, \frac{x}{\varepsilon}\right),$$

and before pursuing the formal multi-scale development initiated in Section 3.3, we give in the following sub-section several mathematical tools that will be required. In the final sub-section, we prove rigorous estimates at any order by studying the system satisfied by the error.

4.1. Mathematical tools

In this subsection, we introduce two types of mathematical tools required for our asymptotic analysis: (1) existence and uniqueness results for PDE systems arising in the formal derivation, and (2) the expansion of the nonlinear term.

Existence and uniqueness. We present existence and uniqueness results for two prototype systems that arise in our asymptotic analysis. The first system appears in the determination of the transmembrane voltage at order one, using the voltage at the order zero.

Proposition 4.1. *Let $B \in \mathcal{C}^\infty_{\rm per}(\Omega \times \Gamma)$ and $F \in \mathcal{C}^\infty_{\rm per}(\Omega)$, there exists a unique $w \in \mathcal{C}^\infty_{\rm per}(\Omega)$ such that*

$$\int_\Gamma I_{\rm m}(B(x,y) + w(x)) = F(x), \ \Omega,$$

where $I_{\mathrm{m}} : \lambda \mapsto S_{\mathrm{m}}(\lambda)\lambda$ satisfies Assumption 2.

Proof. We identify Ω to a torus. Let $G : (x, \lambda) \in \mathcal{C}^\infty(\Omega \times \mathbb{R})$ such that

$$G(x, \lambda) = \int_\Gamma I_{\mathrm{m}} \left(B(x, y) + \lambda \right) - F(x).$$

Let $x_0 \in \Omega$, the function $\lambda \in \mathbb{R} \mapsto G(x_0, \lambda)$ is in $\mathcal{C}^\infty(\mathbb{R})$, is strictly increasing (see Assumption 2 and Theorem 2.2) and tends towards $\pm\infty$ as $\lambda \to \pm\infty$. Therefore, there exists a unique λ, denoted by $w(x_0)$ such that $G(x_0, \lambda) = 0$. Moreover,

$$\partial_\lambda G(x_0, w(x_0)) \neq 0.$$

So, by the implicit function theorem, there exists a neighborhood U of $(x_0, w(x_0))$, a neighborhood V of x_0 and a function $\psi \in \mathcal{C}^\infty(V, \Omega)$ such that for all $(x, y) \in \Omega \times \mathbb{R}$,

$$((x, y) \in U \text{ and } G(x, y) = 0) \iff (x \in V \text{ and } y = \psi(x)).$$

Therefore, for any $x \in V$, $G(x, \psi(x)) = 0$ and thus, by uniqueness, $\psi(x) = w(x)$. It is true in the neighborhood of any point $x_0 \in \Omega$, hence $w \in \mathcal{C}^\infty(\Omega)$. □

The approximation at order n of $u_{\mathrm{e}}^\varepsilon$ includes the solution of a partial differential equation that has the same structure as the limit problem (11), as described in the following proposition.

Proposition 4.2. *Let $n \in \mathbb{N}$, let $f_n \in \mathcal{C}^\infty_{\mathrm{per}}(\Omega)$ such that $\int_\Omega f_n = 0$. There exists a unique $u_{\mathrm{e}}^{n,\sharp} \in \mathcal{C}^\infty_{\mathrm{per}}(\Omega)$ such that*

$$-\nabla \cdot \left(\left(\Sigma_{\mathrm{i}} + \Sigma_{\mathrm{e}} \right) \nabla u_{\mathrm{e}}^{n,\sharp} \right) = f_n, \ \Omega, \tag{30a}$$

$$\int_\Omega u_{\mathrm{e}}^{n,\sharp} = 0, \tag{30b}$$

where Σ_{i} and Σ_{e} are given by (12)*. It satisfies*

$$\left\| u_{\mathrm{e}}^{n,\sharp} \right\|_{H^1(\Omega)} \leq C \left\| f_n \right\|_{L^2(\Omega)}.$$

Proof. Existence and uniqueness of a solution in $H^1(\Omega)$, along with the continuity relatively to the source term, are obtained by classic arguments. To get more smoothness, we identify Ω to a torus. As $f_n \in \mathcal{C}^\infty(\Omega)$, we get $u_{\mathrm{e}}^{n,\sharp} \in \mathcal{C}^\infty(\Omega)$, using for instance Theorem 2.5.1.1 of [54]. □

Expansion of the non-linear term. Because $v_m^0 = 0$, we expand the non-linear term around εv_m^1,

Lemma-Definition 4.3. *Let $N \in \mathbb{N}$, let $v_{\mathrm{m}}^{\varepsilon,N} = \sum_{k=1}^{N} \varepsilon^k v_{\mathrm{m}}^k \in \mathbb{R}$, the following series expansion holds*

$$I_{\mathrm{m}}\left(\frac{v_{\mathrm{m}}^{\varepsilon,N}}{\varepsilon}\right) = I_{\mathrm{m}}(v_{\mathrm{m}}^1) + \sum_{p=2}^{N}\left(\varepsilon^{p-1} I_{\mathrm{m}}^{(1)}(v_{\mathrm{m}}^1) v_{\mathrm{m}}^p + F_p\left(\left(v_{\mathrm{m}}^i\right)_{1\le i\le p-1}\right)\right) + O(\varepsilon^N),$$

where

$$F_p\left(\left(v_{\mathrm{m}}^i\right)_{1\le i\le p-1}\right) = \sum_{\vec{k}\ s.t.\ \sum ik_i = p-1,\ |\vec{k}|>1} \frac{1}{|\vec{k}|}\binom{|\vec{k}|}{\vec{k}} I_{\mathrm{m}}^{(|\vec{k}|)}(v_{\mathrm{m}}^1) \prod_{i=1}^{+\infty}\left(v_{\mathrm{m}}^{i+1}\right)^{k_i}.$$

Proof. It involves a sequence of computations derived from the Taylor–Lagrange expansion. A similar case is developed in [70]. □

Remark 4.4. Note that $F_0 = F_1 = F_2 = 0$.

The term $F_n\left(\left(v_{\mathrm{m}}^k\right)_{1\le k\le n-1}\right)$ appears in the two-scale expansion at order n. Handling it explicitly, as a combination of v_{m}^k, adds a lot of complexity in the notations and computations as the n-th term of the expansion, defined in Equation (38), would contain combinations of products of derivatives of lower order terms. Instead, we treat it as a source term accounting for the non-linear behaviour of I_{m}. The cumulative effect of these "source terms" F_n appears in the expression of $(u_{\mathrm{i}}^n, u_{\mathrm{e}}^n)$ as a term $(G_{\mathrm{i}}^n, G_{\mathrm{e}}^n)$ (null if $n \le 2$) that is defined by induction in Theorem 4.5 and could be made explicit with the same reasoning developed in this section.

4.2. Development at any order

The cascade of equations writes, for $n \ge 2$,

$$-\nabla_y \cdot \left(\sigma_{\mathrm{i}}\left(\nabla_y u_{\mathrm{i}}^{n+1} + \nabla_x u_{\mathrm{i}}^n\right)\right) = \nabla_x \cdot \left(\sigma_{\mathrm{i}}\left(\nabla_y u_{\mathrm{i}}^n + \nabla_x u_{\mathrm{i}}^{n-1}\right)\right), \qquad \text{in } \Omega\times Y_{\mathrm{i}}, \tag{31a}$$

$$-\nabla_y \cdot \left(\sigma_{\mathrm{e}}\left(\nabla_y u_{\mathrm{e}}^{n+1} + \nabla_x u_{\mathrm{e}}^n\right)\right) = \nabla_x \cdot \left(\sigma_{\mathrm{e}}\left(\nabla_y u_{\mathrm{e}}^n + \nabla_x u_{\mathrm{e}}^{n-1}\right)\right), \qquad \text{in } \Omega\times Y_{\mathrm{e}}, \tag{31b}$$

$$\sigma_{\mathrm{i}}\left(\nabla_y u_{\mathrm{i}}^{n+1} + \nabla_x u_{\mathrm{i}}^n\right)\cdot n_{\mathrm{i}} = \sigma_{\mathrm{e}}\left(\nabla_y u_{\mathrm{e}}^{n+1} + \nabla_x u_{\mathrm{e}}^n\right)\cdot n_{\mathrm{i}}, \qquad \text{in } \Omega\times\Gamma, \tag{31c}$$

$$-\sigma_{\mathrm{i}}\left(\nabla_y u_{\mathrm{i}}^{n+1} + \nabla_x u_{\mathrm{i}}^n\right)\cdot n_{\mathrm{i}} = I_{\mathrm{m}}'(v_{\mathrm{m}}^1)\left(u_{\mathrm{i}}^n - u_{\mathrm{e}}^n\right) + F_n, \qquad \text{in } \Omega\times\Gamma, \tag{31d}$$

$$+\ x \text{ and } y \text{ periodic conditions}, \tag{31e}$$

where, for readability, we write F_n instead of $F_n\left(\left(v_{\mathrm{m}}^k\right)_{1\le k\le n-1}\right)$. Once again, seeing it as a system satisfied by $y \mapsto u_{\mathrm{i}}^{n+1}(x,y)$ and $y \mapsto u_{\mathrm{e}}^{n+1}(x,y)$ for all $x \in \Omega$, it has a unique solution (up to a constant depending on x) if and only if the following compatibility conditions are satisfied

$$\int_{Y_{\mathrm{i}}} \nabla_x \cdot \sigma_{\mathrm{i}}\left(\nabla_y u_{\mathrm{i}}^n + \nabla_x u_{\mathrm{i}}^{n-1}\right) = \int_{\Gamma}\left(I_{\mathrm{m}}'(v_{\mathrm{m}}^1)\left(u_{\mathrm{i}}^n - u_{\mathrm{e}}^n\right) + F_n\right), \qquad \text{in } \Omega, \tag{32a}$$

$$\int_{Y_{\mathrm{e}}} \nabla_x \cdot \sigma_{\mathrm{e}}\left(\nabla_y u_{\mathrm{e}}^n + \nabla_x u_{\mathrm{e}}^{n-1}\right) = -\int_{\Gamma}\left(I_{\mathrm{m}}'(v_{\mathrm{m}}^1)\left(u_{\mathrm{i}}^n - u_{\mathrm{e}}^n\right) + F_n\right), \qquad \text{in } \Omega. \tag{32b}$$

As explained before, for the sake of simplicity and readability, the non-linear term is not handled explicitly. Instead, we prove that we can define $((G_{\mathrm{i}}^n, G_{\mathrm{e}}^n))_{n\in\mathbb{N}}$ as in the following proposition.

Proposition-Definition 4.5. *Given* $\left(v_{\mathrm{m}}^k\right)_{n\in\mathbb{N}} \in \mathcal{C}^\infty_{\mathrm{per}}\left(\Omega; \mathcal{C}^\infty_{\mathrm{per}}(\Gamma)\right)^{\mathbb{N}}$*, there exists for all* $n \in \mathbb{N}$*,* $(G_{\mathrm{i}}^n, G_{\mathrm{e}}^n) \in \mathcal{C}^\infty_{\mathrm{per}}\left(\Omega; \mathcal{C}^\infty_{\mathrm{per}}(Y_{\mathrm{i}})\right) \times \overline{\mathcal{C}^\infty_{\mathrm{per}}}(\Omega; \mathcal{C}^\infty_{\mathrm{per}}(Y_{\mathrm{e}}))$ *such that*

$$-\nabla_y \cdot \left(\sigma_{\mathrm{i}}\left(\nabla_y G_{\mathrm{i}}^{n+1} + \nabla_x G_{\mathrm{i}}^n\right)\right) = \nabla_x \cdot \left(\sigma_{\mathrm{i}}\left(\nabla_y G_{\mathrm{i}}^n + \nabla_x G_{\mathrm{i}}^{n-1}\right)\right) \qquad \text{in } \Omega \times Y_{\mathrm{i}} \tag{33a}$$

$$-\nabla_y \cdot \left(\sigma_{\mathrm{e}}\left(\nabla_y G_{\mathrm{e}}^{n+1} + \nabla_x G_{\mathrm{e}}^n\right)\right) = \nabla_x \cdot \left(\sigma_{\mathrm{e}}\left(\nabla_y G_{\mathrm{e}}^n + \nabla_x G_{\mathrm{e}}^{n-1}\right)\right) \qquad \text{in } \Omega \times Y_{\mathrm{e}} \tag{33b}$$

$$\sigma_{\mathrm{i}}\left(\nabla_y G_{\mathrm{i}}^{n+1} + \nabla_x G_{\mathrm{i}}^n\right) \cdot n_{\mathrm{i}} = \sigma_{\mathrm{e}}\left(\nabla_y G_{\mathrm{e}}^{n+1} + \nabla_x G_{\mathrm{e}}^n\right) \cdot n_{\mathrm{i}} \qquad \text{in } \Omega \times \Gamma \tag{33c}$$

$$-\sigma_{\mathrm{i}}\left(\nabla_y G_{\mathrm{i}}^{n+1} + \nabla_x G_{\mathrm{i}}^n\right) \cdot n_{\mathrm{i}} = I'_{\mathrm{m}}(v_m^1)(G_{\mathrm{i}}^n - G_{\mathrm{e}}^n) + F_n \qquad \text{in } \Omega \times \Gamma, \tag{33d}$$

and

$$\int_{Y_{\mathrm{i}}} \nabla_x \cdot \left(\sigma_{\mathrm{i}}\left(\nabla_y G_{\mathrm{i}}^n + \nabla_x G_{\mathrm{i}}^{n-1}\right)\right) = \int_\Gamma I'_{\mathrm{m}}(v_{\mathrm{m}}^1)(G_{\mathrm{i}}^n - G_{\mathrm{e}}^n) + F_n, \qquad \text{in } \Omega, \tag{34}$$

$$\int_{Y_{\mathrm{i}}} \nabla_x \cdot \left(\sigma_{\mathrm{i}}\left(\nabla_y G_{\mathrm{i}}^n + \nabla_x G_{\mathrm{i}}^{n-1}\right)\right) \tag{35a}$$

$$+ \int_{Y_{\mathrm{e}}} \nabla_x \cdot \left(\sigma_{\mathrm{e}}\left(\nabla_y G_{\mathrm{e}}^n + \nabla_x G_{\mathrm{e}}^{n-1}\right)\right) = 0, \text{ in } \Omega, \tag{35b}$$

where $G_{\mathrm{i}}^n = G_{\mathrm{e}}^n = 0$ *for* $n \leq 2$.

Remark 4.6. Let $N \in \mathbb{N}$, note that we only need the knowledge of $\left(v_{\mathrm{m}}^k\right)_{1\leq k\leq N-1}$ to define uniquely G_α^n for all $0 \leq n \leq N$ and G_α^{N+1} up to a constant depending on x.

Proof. We show by induction, for $N \geq 2$, that:

- for all $0 \leq n \leq N-1$, there exist $G_{\mathrm{i}}^n \in \mathcal{C}^\infty_{\mathrm{per}}\left(\Omega; \mathcal{C}^\infty_{\mathrm{per}}(Y_{\mathrm{i}})\right)$ and $G_{\mathrm{e}}^n \in \overline{\mathcal{C}^\infty_{\mathrm{per}}}(\Omega; \mathcal{C}^\infty_{\mathrm{per}}(Y_{\mathrm{e}}))$ satisfying Equations (33), (34) and (35),
- there exist $\tilde{G_{\mathrm{i}}}^N \in \mathcal{C}^\infty_{\mathrm{per}}\left(\Omega; \mathcal{C}^\infty_{\mathrm{per}}(Y_{\mathrm{i}})\right)$ and $\tilde{G_{\mathrm{e}}}^N \in \overline{\mathcal{C}^\infty_{\mathrm{per}}}(\Omega; \mathcal{C}^\infty_{\mathrm{per}}(Y_{\mathrm{e}}))$ such that $\int_{Y_{\mathrm{i}}} \tilde{G_{\mathrm{i}}}^N = \int_{Y_{\mathrm{e}}} \tilde{G_{\mathrm{e}}}^N = 0$ and Equation (33) holds with $n = N-1$ and G_α^{n+1} replaced by $\tilde{G_\alpha}^N$. (Conceptually, $\tilde{G_\alpha}^N$ is the part of G_α^N with null average over the y variable.)

The induction is initialized with $G_\alpha^0 = G_\alpha^1 = G_\alpha^2 = 0$ because $F_0 = F_1 = F_2 = 0$. We now describe how to go from rank N to rank $N+1$. Let

$$v_G^N := \frac{1}{\int_\Gamma I'_{\mathrm{m}}(v_{\mathrm{m}}^1)} \left(\int_{Y_{\mathrm{i}}} \nabla_x \cdot \left(\sigma_{\mathrm{i}}\left(\nabla_y \tilde{G_{\mathrm{i}}}^N + \nabla_x G_{\mathrm{i}}^{N-1}\right)\right) - F_{N-1} \right.$$
$$\left. - \int_\Gamma I'_{\mathrm{m}}(v_{\mathrm{m}}^1)\left(\tilde{G_{\mathrm{i}}}^N - \tilde{G_{\mathrm{e}}}^N\right)\right).$$

Conceptually, $\left(G_{\mathrm{i}}^N - G_{\mathrm{e}}^N\right)(x,y) = \left(\tilde{G_{\mathrm{i}}}^N - \tilde{G_{\mathrm{e}}}^N\right)(x,y) + v_G^N(x)$. Let $(v_{\mathrm{i}}, v_{\mathrm{e}})$ the solution in $\mathcal{C}^\infty_{\mathrm{per}}\left(\Omega; \overline{\mathcal{C}^\infty_{\mathrm{per}}}(Y_{\mathrm{i}})\right) \times \mathcal{C}^\infty_{\mathrm{per}}\left(\Omega; \overline{\mathcal{C}^\infty_{\mathrm{per}}}(Y_{\mathrm{e}})\right)$ of

$$\begin{aligned}
-\nabla_y \cdot \left(\sigma_{\mathrm{i}}\left(\nabla_y v_{\mathrm{i}} + \nabla_x \tilde{G_{\mathrm{i}}}^N\right)\right) &= \nabla_x \cdot \left(\sigma_{\mathrm{i}}\left(\nabla_y \tilde{G_{\mathrm{i}}}^N + \nabla_x G_{\mathrm{i}}^{N-1}\right)\right) && \text{in } \Omega \times Y_{\mathrm{i}} \\
-\nabla_y \cdot \left(\sigma_{\mathrm{e}}\left(\nabla_y v_{\mathrm{e}} + \nabla_x \tilde{G_{\mathrm{e}}}^N\right)\right) &= \nabla_x \cdot \left(\sigma_{\mathrm{e}}\left(\nabla_y \tilde{G_{\mathrm{e}}}^N + \nabla_x G_{\mathrm{e}}^{N-1}\right)\right) && \text{in } \Omega \times Y_{\mathrm{e}} \\
\sigma_{\mathrm{i}}\left(\nabla_y v_{\mathrm{i}} + \nabla_x \tilde{G_{\mathrm{i}}}^N\right) \cdot n_{\mathrm{i}} &= \sigma_{\mathrm{e}}\left(\nabla_y v_{\mathrm{e}} + \nabla_x \tilde{G_{\mathrm{e}}}^N\right) \cdot n_{\mathrm{i}} && \text{in } \Omega \times \Gamma \\
-\sigma_{\mathrm{i}}\left(\nabla_y v_{\mathrm{i}} + \nabla_x \tilde{G_{\mathrm{i}}}^N\right) \cdot n_{\mathrm{i}} &= I'_{\mathrm{m}}(v_m^1)(\tilde{G_{\mathrm{i}}}^N - \tilde{G_{\mathrm{e}}}^N + v_G^N) + F_n && \text{in } \Omega \times \Gamma,
\end{aligned}$$

where the variable x is seen as a parameter. Conceptually, $v_\alpha = \tilde{G}_\alpha^{N+1} - \chi_\alpha \cdot \nabla \overline{G_\alpha}^N$. This system has a solution because its compatibility condition is satisfied using the definitions of $\tilde{G_\alpha}^N$ and v_G^N. The regularity of $(v_{\mathrm{i}}, v_{\mathrm{e}})$ in the x-variable comes from the x-regularity of the source terms and the use of error estimates. Let us define $\overline{G_{\mathrm{e}}}^N$, and thus $\overline{G_i}^N := \overline{G_{\mathrm{e}}}^N + v_G^N$, as the solution in $\overline{\mathcal{C}^\infty_{\mathrm{per}}}(\Omega)$ of

$$-\nabla \cdot \left((\Sigma_{\mathrm{i}} + \Sigma_{\mathrm{e}}) \cdot \nabla \overline{G_{\mathrm{e}}}^N\right) - \nabla \cdot \left(\Sigma_{\mathrm{i}} \cdot \nabla v_G^N\right) = f_N, \text{ in } \Omega,$$

where

$$f_N = \int_{Y_{\mathrm{i}}} \nabla_x \cdot \left(\sigma_{\mathrm{i}}\left(\nabla_y v_{\mathrm{i}} + \nabla_x \tilde{G_{\mathrm{i}}}^n\right)\right) + \int_{Y_{\mathrm{e}}} \nabla_x \cdot \left(\sigma_{\mathrm{e}}\left(\nabla_y v_{\mathrm{e}} + \nabla_x \tilde{G_{\mathrm{e}}}^n\right)\right).$$

The existence of a solution is ensured by f_N and $\nabla \cdot \left(\Sigma_{\mathrm{i}} \cdot \nabla v_G^N\right)$ having a null average over Ω as divergences of Ω-periodic functions. To conclude the induction, let us define

$$\begin{aligned}
G_\alpha^N &= \tilde{G_\alpha}^N + \overline{G_\alpha}^N, \\
\tilde{G_\alpha}^{N+1} &= \chi_\alpha \cdot \nabla \overline{G_\alpha}^N + v_\alpha.
\end{aligned}$$

Computations show that indeed these quantities satisfy the rank $N+1$ induction step. □

We previously defined the first and second order cell problems. In the same spirit, we define the cell problems at order $n \geq 3$.

Definition 4.7 (Cell problems at order n)**.** Let us denote $\mathcal{P}_\alpha(F, G)$ the unique solution in $\mathcal{C}^\infty_{\mathrm{per}}(Y_\alpha)$ of System (9) with source terms F and G. The subscript β is e, resp. i, if α is i, resp. e. Let $n \geq 3$, let $p \in \mathbb{N}$ and $k \in \mathbb{N}$. If $p + k > n$, then $\chi_\alpha^{p,k,n} = 0$. Otherwise, for

$(l_1, \dots, l_p) \in [1; d]^p$,

$$\begin{aligned}\left(\chi_\alpha^{p,k,n}\right)_{(l_1,\dots,l_p)} &= \delta_{p\geq 1}\mathcal{P}_\alpha\left(2\frac{\partial\chi_1}{\partial y_{l_p}} - \frac{1}{|Y_\alpha|}\int_{Y_\alpha}\frac{\partial\chi_1}{\partial y_{l_p}},\ \chi_1\left(n_\alpha\right)_{l_p}\right)\\ &+ \delta_{p\geq 2}\mathcal{P}_\alpha\left(\chi_2 - \frac{1}{|Y_\alpha|}\int_{Y_\alpha}\chi_2,\ 0\right)\delta_{l_{p-1}=l_p}\\ &+ \frac{1}{\sigma_\alpha}\mathcal{P}_\alpha\left(\frac{1}{|Y_\alpha|}\int_\Gamma I'_{\mathrm{m}}(v_m^1)\chi_3,\ I'_{\mathrm{m}}(v_m^1)\chi_3\right) + \delta_{p=0,k=n},\end{aligned}$$

where

$$\begin{aligned}\chi_1 &= \left(\chi_\alpha^{p-1,k,n-1}\right)_{(l_1,\dots,l_{p-1})},\\ \chi_2 &= \left(\chi_\alpha^{p-2,k,n-2}\right)_{(l_1,\dots,l_{p-2})},\\ \chi_3 &= \left(\chi_\alpha^{p,k,n-1} - \theta_\beta^{p,k,n-1}\right)_{(l_1,\dots,l_p)}.\end{aligned}$$

If $p + k \geq n$, then $\theta_\alpha^{p,k,n} = 0$. Otherwise, for $(l_1, \dots, l_p) \in [1; d]^p$,

$$\begin{aligned}\left(\theta_\alpha^{p,k,n}\right)_{(l_1,\dots,l_p)} &= \delta_{p\geq 1}\mathcal{P}_\alpha\left(2\frac{\partial\theta_1}{\partial y_{l_p}} - \frac{1}{|Y_\alpha|}\int_{Y_\alpha}\frac{\partial\theta_1}{\partial y_{l_p}},\ \theta_1\left(n_\alpha\right)_{l_p}\right)\\ &+ \delta_{p\geq 2}\mathcal{P}_\alpha\left(\theta_2 - \frac{1}{|Y_\alpha|}\int_{Y_\alpha}\theta_2,\ 0\right)\delta_{l_{p-1}=l_p}\\ &+ \frac{1}{\sigma_\alpha}\mathcal{P}_\alpha\left(\frac{1}{|Y_\alpha|}\int_\Gamma I'_{\mathrm{m}}(v_m^1)\theta_3,\ I'_{\mathrm{m}}(v_m^1)\theta_3\right),\end{aligned}$$

where

$$\begin{aligned}\theta_1 &= \left(\theta_\alpha^{p-1,k,n-1}\right)_{(l_1,\dots,l_{p-1})},\\ \theta_2 &= \left(\theta_\alpha^{p-2,k,n-2}\right)_{(l_1,\dots,l_{p-2})},\\ \theta_3 &= \left(\theta_\alpha^{p,k,n-1} - \chi_\beta^{p,k,n-1}\right)_{(l_1,\dots,l_p)}.\end{aligned}$$

Remark 4.8. By construction,

$$\int_{Y_\alpha}\chi_\alpha^{p,k,n} = \int_{Y_\alpha}\theta_\alpha^{p,k,n} = 0,$$

except for $p = 0$ and $k = n$, where

$$\int_{Y_\alpha}\chi_\alpha^{0,n,n} = |Y_\alpha|.$$

We can now define by induction the terms $(u_{\mathrm{i}}^n, u_{\mathrm{e}}^n)$. At each step, the macroscopic

quantities $u_{\mathrm{i}}^{n,\sharp} - u_{\mathrm{e}}^{n,\sharp}$ and $u_{\mathrm{e}}^{n,\sharp}$ are defined such that the compatibility conditions (32) are satisfied, then the solution of System (31) is written as a linear combination of derivatives of the non-oscillating terms $\left(u_{\mathrm{i}}^{k,\sharp}, u_{\mathrm{e}}^{k,\sharp}\right)$ weighted by the correctors that we previously defined. The first terms $(u_{\mathrm{i}}^0, u_{\mathrm{e}}^0)$ and $(u_{\mathrm{i}}^1, u_{\mathrm{e}}^1)$ were defined previously, we deal with the terms $n \geq 2$ by induction in the following Proposition-Definition:

Proposition-Definition 4.9. *Let $n \geq 2$. Assume that for all $0 \leq k \leq n-1$, $u_{\mathrm{i}}^k \in \mathcal{C}_{\mathrm{per}}^\infty(\Omega \times Y_{\mathrm{i}})$ and $u_{\mathrm{e}}^k \in \mathcal{C}_{\mathrm{per}}^\infty(\Omega \times Y_{\mathrm{e}})$ are defined. We proceed in four steps:*

1. With $\left(v^k\right)_{0\leq k\leq n-1} = \left(v_{\mathrm{m}}^k\right)_{0\leq k\leq n-1}$, we can define uniquely $G_{\mathrm{i,e}}^k$ for $0 \leq k \leq n$ and $G_{\mathrm{i,e}}^{n+1}$ up to a constant, depending on x, thanks to Theorem 4.5.
2. We define $v_{\mathrm{m}}^{n,\sharp} \in \mathcal{C}_{\mathrm{per}}^\infty(\Omega)$ such that

$$\left(\int_\Gamma I'_{\mathrm{m}}(v_{\mathrm{m}}^1)\right) v_{\mathrm{m}}^{n,\sharp} = g_n, \tag{36}$$

where

$$\begin{aligned} g_n = \int_{Y_{\mathrm{i}}} \nabla_x \cdot \sigma_{\mathrm{i}} \nabla_x u_{\mathrm{i}}^{n-1} - \int_\Gamma F_n - \int_\Gamma I'_{\mathrm{m}}(v_m^1)\left(G_{\mathrm{i}}^n - G_{\mathrm{e}}^n\right) \\ + \sum_{k=0}^{n-1}\sum_{p=0}^{n-k} \int_{Y_{\mathrm{i}}} \nabla_x \cdot \sigma_{\mathrm{i}} \nabla_y \left(\chi_{\mathrm{i}}^{p,k,n} \nabla^p u_{\mathrm{i}}^{k,\sharp} + \theta_{\mathrm{i}}^{p,k,n} \nabla^p u_{\mathrm{e}}^{k,\sharp}\right) + \int_{Y_{\mathrm{i}}} \nabla_x \cdot \sigma_{\mathrm{i}} \nabla_y G_i^n \\ - \sum_{k=0}^{n-1}\sum_{p=0}^{n-k} \int_\Gamma I'_{\mathrm{m}}(v_{\mathrm{m}}^1)\left(\chi_{\mathrm{i}}^{p,k,n} \nabla^p u_{\mathrm{i}}^{k,\sharp} + \theta_{\mathrm{i}}^{p,k,n} \nabla^p u_{\mathrm{e}}^{k,\sharp} - \chi_{\mathrm{e}}^{p,k,n} \nabla^p u_{\mathrm{e}}^{k,\sharp} - \theta_{\mathrm{e}}^{p,k,n} \nabla^p u_{\mathrm{i}}^{k,\sharp}\right). \end{aligned}$$

It is well defined because $I'_{\mathrm{m}}(v_{\mathrm{m}}^1) > 0$ (see Theorem 2.2) and because $g_n \in \mathcal{C}_{\mathrm{per}}^\infty(\Omega)$, as a sum of terms belonging to $\mathcal{C}_{\mathrm{per}}^\infty(\Omega)$.
3. We then define $u_{\mathrm{e}}^{n,\sharp} \in \mathcal{C}_{\mathrm{per}}^\infty(\Omega)$ such that

$$-\nabla \cdot \left(\left(\Sigma_{\mathrm{i}} + \Sigma_{\mathrm{e}}\right) \nabla u_{\mathrm{e}}^{n,\sharp}\right) = f_n - \frac{1}{|\Omega|}\int_\Omega f_n, \ \Omega, \tag{37a}$$

$$\int_\Omega u_{\mathrm{e}}^{n,\sharp} = 0, \tag{37b}$$

where

$$
\begin{aligned}
f_n = \nabla_x \cdot \left(\int_\Gamma I'_{\mathrm{m}}(v^1_{\mathrm{m}}) \left(\chi_{\mathrm{i}} - \chi_{\mathrm{e}}\right) \right) v^{n,\sharp}_{\mathrm{m}} + \nabla_x \cdot \Sigma_{\mathrm{i}} \nabla_x v^{n,\sharp}_{\mathrm{m}} + \delta_{n=0} \left|Y_{\mathrm{e}}\right| f \\
+ \sum_{k=0}^{n-1} \sum_{p=0}^{n-k+1} \int_{Y_{\mathrm{i}}} \nabla_x \cdot \sigma_{\mathrm{i}} \nabla_y \left(\chi^{p,k,n+1}_{\mathrm{i}} \nabla^p u^{k,\sharp}_{\mathrm{i}} + \theta^{p,k,n+1}_{\mathrm{i}} \nabla^p u^{k,\sharp}_{\mathrm{e}} \right) + \int_{Y_{\mathrm{i}}} \nabla_x \cdot \sigma_{\mathrm{i}} \nabla_y G^{n+1}_{\mathrm{i}} \\
+ \sum_{k=0}^{n-1} \sum_{p=0}^{n-k} \int_{Y_{\mathrm{i}}} \nabla_x \cdot \sigma_{\mathrm{i}} \nabla_x \left(\chi^{p,k,n}_{\mathrm{i}} \nabla^p u^{k,\sharp}_{\mathrm{i}} + \theta^{p,k,n}_{\mathrm{i}} \nabla^p u^{k,\sharp}_{\mathrm{e}} \right) + \int_{Y_{\mathrm{i}}} \nabla_x \cdot \sigma_{\mathrm{i}} \nabla_x G^{n}_{\mathrm{i}} \\
+ \sum_{k=0}^{n-1} \sum_{p=0}^{n-k+1} \int_{Y_{\mathrm{e}}} \nabla_x \cdot \sigma_{\mathrm{e}} \nabla_y \left(\chi^{p,k,n+1}_{\mathrm{e}} \nabla^p u^{k,\sharp}_{\mathrm{e}} + \theta^{p,k,n+1}_{\mathrm{e}} \nabla^p u^{k,\sharp}_{\mathrm{i}} \right) + \int_{Y_{\mathrm{e}}} \nabla_x \cdot \sigma_{\mathrm{e}} \nabla_y G^{n+1}_{\mathrm{e}} \\
+ \sum_{k=0}^{n-1} \sum_{p=0}^{n-k} \int_{Y_{\mathrm{e}}} \nabla_x \cdot \sigma_{\mathrm{e}} \nabla_x \left(\chi^{p,k,n}_{\mathrm{e}} \nabla^p u^{k,\sharp}_{\mathrm{e}} + \theta^{p,k,n}_{\mathrm{e}} \nabla^p u^{k,\sharp}_{\mathrm{i}} \right) + \int_{Y_{\mathrm{e}}} \nabla_x \cdot \sigma_{\mathrm{e}} \nabla_y G^{n}_{\mathrm{e}}.
\end{aligned}
$$

It is well defined by use of Theorem 4.2, and noting that $f_n \in \mathcal{C}^\infty_{\mathrm{per}}$ *and* $\int_\Omega f_n = 0$ *(f_n is a periodic divergence).*

4. Finally, we define

$$
\begin{aligned}
u^n_{\mathrm{i}}(x,y) &= \sum_{k=0}^{n-1} \sum_{p=0}^{n-k} \left(\chi^{p,k,n}_{\mathrm{i}}(x,y) \nabla^p u^{k,\sharp}_{\mathrm{i}}(x) + \theta^{p,k,n}_{\mathrm{i}}(x,y) \nabla^p u^{k,\sharp}_{\mathrm{e}}(x) \right) \\
&\quad + G^n_{\mathrm{i}}(x,y) + u^{n,\sharp}_{\mathrm{i}}(x), \qquad (38) \\
u^n_{\mathrm{e}}(x,y) &= \sum_{k=0}^{n-1} \sum_{p=0}^{n-k} \left(\chi^{p,k,n}_{\mathrm{e}}(x,y) \nabla^p u^{k,\sharp}_{\mathrm{e}}(x) + \theta^{p,k,n}_{\mathrm{e}}(x,y) \nabla^p u^{k,\sharp}_{\mathrm{i}}(x) \right) \\
&\quad + G^n_{\mathrm{e}}(x,y) + u^{n,\sharp}_{\mathrm{e}}(x). \qquad (39)
\end{aligned}
$$

Remark 4.10. The definition of $v^{n,\sharp}_{\mathrm{m}}$ (36) reads

$$
\int_{Y_{\mathrm{i}}} \nabla_x \cdot \sigma_{\mathrm{i}} \left(\nabla_y u^n_{\mathrm{i}} + \nabla_x u^{n-1}_{\mathrm{i}} \right) = \int_\Gamma \left(I'_{\mathrm{m}} \left(u^n_{\mathrm{i}} - u^n_{\mathrm{e}} \right) + F_n \right),
$$

and the definition of $u^{n,\sharp}_{\mathrm{e}}$ (37) reads

$$
\int_{Y_{\mathrm{i}}} \nabla_x \cdot \sigma_{\mathrm{i}} \left(\nabla_y u^{n+1}_{\mathrm{i}} + \nabla_x u^n_{\mathrm{i}} \right) + \int_{Y_{\mathrm{e}}} \nabla_x \cdot \sigma_{\mathrm{e}} \left(\nabla_y u^{n+1}_{\mathrm{e}} + \nabla_x u^n_{\mathrm{e}} \right) = 0,
$$

which are the compatibility conditions (32).

The cell correctors are defined such that the following proposition holds. We do not give the proof which consists of heavy computations.

Proposition 4.11. *For all* $n \geq 2$, u^n_{i} *and* u^n_{e}, *as defined in Definition 4.9, are solutions of System* (31).

4.3. Error estimates

The formal two-scale asymptotic expansion led us towards a definition of u_{i}^n, u_{e}^n. Now comes the time to rigorously prove that this definition is the right one, in the sense that it is consistent with the ansatz. We therefore prove that the finite development $\sum_{k=0}^n \varepsilon^k u_\alpha^k$ is an approximation of u_α^ε at order ε^{n+1}.

Note that in the previous sub-section, we approximated the gauge condition $\int_{\Omega_{\mathrm{e}}^\varepsilon} u_{\mathrm{e}}^\varepsilon = 0$ by $\int_\Omega \int_{Y_{\mathrm{e}}} u_{\mathrm{e}}^n = 0$ for all $n \in \mathbb{N}$. Theorem C.3, given with its proof in Appendix C confirms that it is accurate enough, as it shows that the difference between these two terms can be controlled by $C(n,f)\varepsilon^n$ for all $n \in \mathbb{N}$ where $C(n,f)$ is a constant dependent only on f and n.

Proposition 4.12 (Error estimates)**.** *Under Assumptions 1 and 2, let* $(u_{\mathrm{i}}^\varepsilon, u_{\mathrm{e}}^\varepsilon) \in \mathcal{C}^\infty_{\mathrm{per}}(\Omega_{\mathrm{i}}^\varepsilon) \times \overline{\mathcal{C}^\infty_{\mathrm{per}}}(\Omega_{\mathrm{e}}^\varepsilon)$ *the sequence of solutions of System* (1) *and let* $(u_{\mathrm{i}}^k, u_{\mathrm{e}}^k)$ *defined as in Theorem 4.9. For all* $n \in \mathbb{N}$ *and* $\varepsilon > 0$ *small enough, there exists* C *independent of* ε*, but depending on* n*, such that the quantities*

$$z_{\mathrm{i}}^{\varepsilon,n}(x) = u_{\mathrm{i}}^\varepsilon(x) - \left(u_{\mathrm{i}}^0(x) + \sum_{k=1}^n \varepsilon^k u_{\mathrm{i}}^k(x, \frac{x}{\varepsilon}) \right),$$
$$z_{\mathrm{e}}^{\varepsilon,n}(x) = u_{\mathrm{e}}^\varepsilon(x) - \left(u_{\mathrm{e}}^0(x) + \sum_{k=1}^n \varepsilon^k u_{\mathrm{e}}^k(x, \frac{x}{\varepsilon}) \right),$$

satisfy

$$\|z_{\mathrm{i}}^{\varepsilon,n}\|_{H^1(\Omega_{\mathrm{i}}^\varepsilon)} + \|z_{\mathrm{e}}^{\varepsilon,n}\|_{H^1(\Omega_{\mathrm{e}}^\varepsilon)} \leq C\varepsilon^n,$$
$$\|z_{\mathrm{i}}^{\varepsilon,n} - z_{\mathrm{e}}^{\varepsilon,n}\|_{L^2(\Gamma_{\mathrm{m}}^\varepsilon)} \leq C\varepsilon^{n+\frac{1}{2}}.$$

Proof. This proof uses Lemmas A.2 and C.3 given with their proofs in Appendix A and Appendix C, respectively.

It relies on firstly finding the system satisfied by the errors $z_{\mathrm{i}}^{\varepsilon,n}$ and $z_{\mathrm{e}}^{\varepsilon,n}$, which has the same structure as the original system, and then deriving estimates to get a bound on the error in some energy norms. The computation of the error system is straightforward and relies on the fact that the correctors u_{i}^n and u_{e}^n are defined to satisfy the cascade of equations

found previously. We find

$$
\begin{aligned}
-\nabla\cdot\sigma_{\mathrm{i}}\nabla z_{\mathrm{i}}^{\varepsilon,n} &= -\varepsilon^{n-1}\nabla_y\cdot\sigma_{\mathrm{i}}\nabla_y u_{\mathrm{i}}^{n+1}+\varepsilon^n\nabla_x\cdot\sigma_{\mathrm{i}}\nabla_x u_{\mathrm{i}}^n, && \text{in } \Omega_{\mathrm{i}}^\varepsilon,\\
-\nabla\cdot\sigma_{\mathrm{e}}\nabla z_{\mathrm{e}}^{\varepsilon,n} &= -\varepsilon^{n-1}\nabla_y\cdot\sigma_{\mathrm{e}}\nabla_y u_{\mathrm{e}}^{n+1}+\varepsilon^n\nabla_x\cdot\sigma_{\mathrm{e}}\nabla_x u_{\mathrm{e}}^n, && \text{in } \Omega_{\mathrm{e}}^\varepsilon,\\
-\sigma_{\mathrm{i}}\nabla z_{\mathrm{i}}^{\varepsilon,n}\cdot n_{\mathrm{i}} &= \varepsilon I_{\mathrm{m}}\left(\frac{u_{\mathrm{i}}^\varepsilon-u_{\mathrm{e}}^\varepsilon}{\varepsilon}\right)-\varepsilon I_{\mathrm{m}}(v_{\mathrm{m}}^1)\\
&\quad-\sum_{k=2}^n\varepsilon^k\left(I_{\mathrm{m}}'(v_{\mathrm{m}}^1)\left(u_{\mathrm{i}}^k-u_{\mathrm{e}}^k\right)+F_k\right)-\varepsilon^n\sigma_{\mathrm{i}}\nabla_y u_{\mathrm{i}}^{n+1}\cdot n_{\mathrm{i}}, && \text{on } \Gamma_{\mathrm{m}}^\varepsilon,\\
-\sigma_{\mathrm{e}}\nabla z_{\mathrm{e}}^{\varepsilon,n}\cdot n_{\mathrm{e}} &= -\varepsilon I_{\mathrm{m}}\left(\frac{u_{\mathrm{i}}^\varepsilon-u_{\mathrm{e}}^\varepsilon}{\varepsilon}\right)+\varepsilon I_{\mathrm{m}}(v_{\mathrm{m}}^1)\\
&\quad+\sum_{k=2}^n\varepsilon^k\left(I_{\mathrm{m}}'(v_{\mathrm{m}}^1)\left(u_{\mathrm{i}}^k-u_{\mathrm{e}}^k\right)+F_k\right)-\varepsilon^n\sigma_{\mathrm{e}}\nabla_y u_{\mathrm{e}}^{n+1}\cdot n_{\mathrm{e}}, && \text{on } \Gamma_{\mathrm{m}}^\varepsilon.
\end{aligned}
$$

In order to find estimates, we multiply the volume equations by $z_{\mathrm{i}}^{\varepsilon,n}$ and $z_{\mathrm{e}}^{\varepsilon,n}$, integrate over $\Omega_{\mathrm{i}}^\varepsilon$ and $\Omega_{\mathrm{e}}^\varepsilon$ and sum. We use the fact that if $(x,y)\mapsto\psi(x,y)$ is y-periodic and smooth enough then $\int_{\Omega_\alpha^\varepsilon}\psi(x,\frac{x}{\varepsilon})^2$ is uniformly bounded because it converges to $\int_\Omega\int_{Y_\alpha}\psi(x,y)^2$. Together with the series development given in Theorem 4.3, we can show that the right hand side is bounded by

$$
C\varepsilon^n\left(\|z_{\mathrm{i}}^{\varepsilon,n}\|_{H^1(\Omega_{\mathrm{i}}^\varepsilon)}+\|z_{\mathrm{e}}^{\varepsilon,n}\|_{H^1(\Omega_{\mathrm{e}}^\varepsilon)}\right).
$$

Therefore, using Assumption 2, the estimate becomes

$$
\begin{aligned}
\int_{\Omega_{\mathrm{i}}^\varepsilon}\sigma_{\mathrm{i}}\left|\nabla z_{\mathrm{i}}^{\varepsilon,n}\right|^2+\int_{\Omega_{\mathrm{e}}^\varepsilon}\sigma_{\mathrm{e}}\left|\nabla z_{\mathrm{e}}^{\varepsilon,n}\right|^2+\int_{\Gamma_{\mathrm{m}}^\varepsilon}S_{\mathrm{m}}^0\left|z_{\mathrm{i}}^{\varepsilon,n}-z_{\mathrm{e}}^{\varepsilon,n}\right|^2\\
\le C\varepsilon^n\left(\|z_{\mathrm{i}}^{\varepsilon,n}\|_{H^1(\Omega_{\mathrm{i}}^\varepsilon)}+\|z_{\mathrm{e}}^{\varepsilon,n}\|_{H^1(\Omega_{\mathrm{e}}^\varepsilon)}\right).
\end{aligned}
$$

Then, using the norm equivalence given in Lemma A.2 (Appendix A) on $\left(z_{\mathrm{i}}^{\varepsilon,n}-\frac{1}{|\Omega_{\mathrm{e}}^\varepsilon|}\int_{\Omega_{\mathrm{e}}^\varepsilon}z_{\mathrm{e}}^{\varepsilon,n},z_{\mathrm{e}}^{\varepsilon,n}-\frac{1}{|\Omega_{\mathrm{e}}^\varepsilon|}\int_{\Omega_{\mathrm{e}}^\varepsilon}z_{\mathrm{e}}^{\varepsilon,n}\right)$, we get for ε small enough,

$$
\begin{aligned}
&\|z_{\mathrm{i}}^{\varepsilon,n}\|_{H^1(\Omega_{\mathrm{i}}^\varepsilon)}^2+\|z_{\mathrm{e}}^{\varepsilon,n}\|_{H^1(\Omega_{\mathrm{e}}^\varepsilon)}^2\\
&\qquad\le C\left(\varepsilon^n\left(\|z_{\mathrm{i}}^{\varepsilon,n}\|_{H^1(\Omega_{\mathrm{i}}^\varepsilon)}+\|z_{\mathrm{e}}^{\varepsilon,n}\|_{H^1(\Omega_{\mathrm{e}}^\varepsilon)}\right)+\frac{|\Omega|}{|\Omega_{\mathrm{e}}^\varepsilon|^2}\left(\int_{\Omega_e^\varepsilon}z_{\mathrm{e}}^{\varepsilon,n}\right)^2\right).
\end{aligned}
$$

Now remark that $\int_{\Omega_{\mathrm{e}}^\varepsilon}z_{\mathrm{e}}^{\varepsilon,n}=-\sum_{k=0}^n\int_{\Omega_{\mathrm{e}}^\varepsilon}\varepsilon^k u_{\mathrm{e}}^k\left(x,\frac{x}{\varepsilon}\right)\le C\varepsilon^{n+1}$ by using Lemma C.3 (Appendix C), where C depends on n. We obtain finally

$$
\begin{aligned}
\|z_{\mathrm{i}}^{\varepsilon,n}\|_{H^1(\Omega_{\mathrm{i}}^\varepsilon)}+\|z_{\mathrm{e}}^{\varepsilon,n}\|_{H^1(\Omega_{\mathrm{e}}^\varepsilon)}&\le C\varepsilon^n,\\
\|z_{\mathrm{i}}^{\varepsilon,n}-z_{\mathrm{e}}^{\varepsilon,n}\|_{L^2(\Gamma_{\mathrm{m}}^\varepsilon)}&\le C\varepsilon^n.
\end{aligned}
$$

To improve the last result, note that

$$\begin{aligned}\|z_{\mathrm{i}}^{\varepsilon,n} - z_{\mathrm{e}}^{\varepsilon,n}\|_{L^2(\Gamma_{\mathrm{m}}^\varepsilon)} &\leq \left\|z_{\mathrm{i}}^{\varepsilon,n+1} - z_{\mathrm{e}}^{\varepsilon,n+1}\right\|_{L^2(\Gamma_{\mathrm{m}}^\varepsilon)} \\ &\quad + \varepsilon^{n+1}\left\|u_{\mathrm{i}}^{n+1}\left(x, \frac{x}{\varepsilon}\right) - u_{\mathrm{e}}^{n+1}\left(x, \frac{x}{\varepsilon}\right)\right\|_{L^2(\Gamma_{\mathrm{m}}^\varepsilon)} \\ &\leq C\varepsilon^{n+\frac{1}{2}},\end{aligned}$$

because $\sqrt{\varepsilon}\left\|u_{\mathrm{i}}^{n+1}\left(x, \frac{x}{\varepsilon}\right) - u_{\mathrm{e}}^{n+1}\left(x, \frac{x}{\varepsilon}\right)\right\|_{L^2(\Gamma_{\mathrm{m}}^\varepsilon)}$ is bounded. □

Remark 4.13. We have

$$\|z_\alpha^{\varepsilon,n}\|_{L^2(\Omega_\alpha^\varepsilon)} \leq \left\|z_\alpha^{\varepsilon,n+1}\right\|_{L^2(\Omega_\alpha^\varepsilon)} + \varepsilon^{n+1}\left\|u_\alpha^{n+1}\right\|_{L^2(\Omega_\alpha^\varepsilon)} \leq C\varepsilon^{n+1}$$

and

$$\begin{aligned}\left\|\nabla z_\alpha^{\varepsilon,n} + \varepsilon^n \nabla_y u_\alpha^{n+1}\right\|_{L^2(\Omega_\alpha^\varepsilon)} &\leq \left\|\nabla z_\alpha^{\varepsilon,n+1}\right\|_{L^2(\Omega_\alpha^\varepsilon)} + \varepsilon^{n+1}\left\|\nabla_x u_\alpha^{n+1}\right\|_{L^2(\Omega_\alpha^\varepsilon)} \\ &\leq C\varepsilon^{n+1}.\end{aligned}$$

The last inequality is useful in practice because it allows us to gain one order of convergence without having to solve a new macroscopic problem, indeed $\nabla_y u_\alpha^{n+1}(x,y)$ does not contain the term $u_\alpha^{n+1,\sharp}(x)$, it is a combination of cell problems solutions and of the previous macroscopic quantities $u_{\mathrm{i}}^{k,\sharp}$ and $u_{\mathrm{e}}^{k,\sharp}$ for $k \leq n$.

Remark 4.14 (On the regularity). We assumed that f, S_{m} and Γ are infinitely smooth, so that the expansion can be done at any order n. These assumptions on regularity can obviously be weakened if the expansion is stopped at a fixed order n_0. We would then work in Hilbert spaces of order depending on n_0.

5. Conclusion

In this work, we have developed and rigorously justified a multiscale model for pulsed field ablation in cardiac tissue, based on high-order two-scale asymptotic expansions. The resulting homogenized bidomain system captures key nonlinear effects of electroporation at the macroscopic level. An interesting feature of our model lies in the fact that the gradient of the potential, thus the electric field plays a role in the nonlinearity. This is the main difference with the usual bidomain model used in electrocardiology, in which the nonlinearity involves only the transmembrane voltage. It is also important to note that the electric field magnitude and the macroscopic transmembrane voltage appear in the nonlinearity of the macroscopic effective model, while the nonlinearity of the microscopic model involved only the microscopic transmembrane voltage. From the modeling viewpoint, our result clarifies and quantifies the fact that at the cell scale, electroporation is driven by the increase of the transmembrane voltage while at the tissue scale, the magnitude of the electric field is the key variable. Our analysis ensures the convergence of the expansion at arbitrary order, providing a solid

mathematical foundation for the model. Thanks to this high-order asymptotic approach, we now have a reliable and well-structured framework ready to be confronted with biological data, which constitutes the natural next step in this study.

Acknowledgements

This work was partly funded by the French Federation of Cardiology through the Dielectric project. It also received support from the French National Research Agency through several grants (Liryc ANR-10-IAHU-04, MIRE4VTACH ANR-22-CE45-0014, IMITATE ANR-22-CE51-0043), and from Inserm Plan Cancer MECI project (21CM119_00). Simulations were carried out on the computing facilities of the MCIA (Mésocentre de Calcul Intensif Aquitain).

We thank kindly the reviewers of this paper for their useful comments and constructive criticism.

Appendix A. Spaces that depend on ε

Lemma A.1 (Usual inequalities - dependence on ε)**.** *There exists a constant C independent of ε such that for all $v_{\mathrm{e}} \in H^1(\Omega_{\mathrm{e}}^\varepsilon)$ and $v_{\mathrm{i}} \in H^1(\Omega_{\mathrm{i}}^\varepsilon)$, we have*

$$\left\| v_{\mathrm{e}} - \frac{1}{|\Omega_{\mathrm{e}}^\varepsilon|} \int_{\Omega_{\mathrm{e}}^\varepsilon} v_{\mathrm{e}} \right\|_{L^2(\Omega_{\mathrm{e}}^\varepsilon)} \leq C \left\| \nabla v_{\mathrm{e}} \right\|_{L^2(\Omega_{\mathrm{e}}^\varepsilon)}, \ \textit{(Poincaré-Wirtinger ineq.)},$$
$$\left\| v_\alpha \right\|^2_{L^2(\Gamma_{\mathrm{m}}^\varepsilon)} \leq C\varepsilon^{-1} \left\| v_\alpha \right\|^2_{L^2(\Omega_\alpha^\varepsilon)} + C\varepsilon \left\| \nabla v_\alpha \right\|^2_{L^2(\Omega_\alpha^\varepsilon)}, \ \textit{(Trace ineq.)}.$$

Proof. See appendices of [52]. □

Lemma A.2 (Norm equivalence)**.** *There exist $c > 0$ and $C > 0$ independent of ε such that for all $(v_{\mathrm{i}}, v_{\mathrm{e}}) \in H^1(\Omega_{\mathrm{i}}^\varepsilon) \times \overline{H^1}(\Omega_{\mathrm{e}}^\varepsilon)$,*

$$\begin{aligned} c \left\| (v_{\mathrm{i}}, v_{\mathrm{e}}) \right\|_{H^1(\Omega_{\mathrm{i}}^\varepsilon) \times H^1(\Omega_{\mathrm{e}}^\varepsilon)} &\leq \left(\left\| \nabla v_{\mathrm{i}} \right\|^2_{L^2(\Omega_{\mathrm{i}}^\varepsilon)} + \left\| \nabla v_{\mathrm{e}} \right\|^2_{L^2(\Omega_{\mathrm{e}}^\varepsilon)} + \varepsilon \left\| v_{\mathrm{i}} - v_{\mathrm{e}} \right\|^2_{L^2(\Gamma_{\mathrm{m}}^\varepsilon)} \right)^{\frac{1}{2}} \\ &\leq C \left\| (v_{\mathrm{i}}, v_{\mathrm{e}}) \right\|_{H^1(\Omega_{\mathrm{i}}^\varepsilon) \times H^1(\Omega_{\mathrm{e}}^\varepsilon)}. \end{aligned}$$

Proof. First of all, throughout this proof, we repeatedly use the following inequality for $a, b \geq 0$ without explicitly mentioning it: for $a, b \geq 0$, $a^2 + b^2 \leq (a+b)^2 \leq 2(a^2+b^2)$. The second inequality directly comes from the triangle inequality, the definition of the norm on $H^1(\Omega_{\mathrm{i}}^\varepsilon)$ and $\overline{H^1}(\Omega_{\mathrm{e}}^\varepsilon)$ and the trace theorem. The first inequality follows from Lemma C.2 in the Appendix of [52]. Specifically, the lemma states that there exists a constant $C > 0$ independent of ε such that $\forall v_{\mathrm{i}} \in H^1(\Omega_{\mathrm{i}}^\varepsilon)$,

$$\|v_{\mathrm{i}}\|_{L^2(\Omega_{\mathrm{i}}^\varepsilon)} \leq C(\sqrt{\varepsilon}\|v_{\mathrm{i}}\|_{L^2(\Gamma_{\mathrm{m}}^\varepsilon)} + \varepsilon\|\nabla v_{\mathrm{i}}\|_{L^2(\Omega_{\mathrm{i}}^\varepsilon)}).$$

Then applying the triangle inequality on $v_\mathrm{i} = v_\mathrm{i} - v_\mathrm{e} + v_\mathrm{e}$, considering H^1-norm for v_i and the smallness of ε, there exists a constant still denoted by $C > 0$ such that

$$\|v_\mathrm{i}\|_{H^1(\Omega_\mathrm{i}^\varepsilon)} \leq C(\sqrt{\varepsilon}\|v_\mathrm{i} - v_\mathrm{e}\|_{L^2(\Gamma_\mathrm{m}^\varepsilon)} + \sqrt{\varepsilon}\|v_\mathrm{e}\|_{L^2(\Gamma_\mathrm{m}^\varepsilon)} + \|\nabla v_\mathrm{i}\|_{L^2(\Omega_\mathrm{i}^\varepsilon)}).$$

Then applying the Poincaré-Wirtinger inequality to v_e on both sides of the inequality along with the trace theorem and the smallness of ε, we get that there exists a constant still denoted by $C > 0$,

$$\|(v_\mathrm{i}, v_\mathrm{e})\|_{H^1(\Omega_\mathrm{i}^\varepsilon)\times\overline{H^1}(\Omega_\mathrm{e}^\varepsilon)} \leq C(\sqrt{\varepsilon}\|v_\mathrm{i} - v_\mathrm{e}\|_{L^2(\Gamma_\mathrm{m}^\varepsilon)} + \|\nabla v_\mathrm{i}\|_{L^2(\Omega_\mathrm{i}^\varepsilon)} + \|\nabla v_\mathrm{e}\|_{L^2(\Omega_\mathrm{e}^\varepsilon)}).$$

This allows to conclude the proof. □

Appendix B. Numerical errors

Table B.1 summarizes the numerical values shown in Fig. 4, corresponding to ε-orders 0 and 1 of the errors defined in (29).

Appendix C. Approximation of the gauge condition

In Section 4.2, the quantities $u_\mathrm{e}^{k,\sharp}$ (and thus u_e^k) can be defined up to a constant. For $\sum_{k=0}^n \varepsilon^k u_\mathrm{e}^k$ to be a good approximation of u_e^ε, the average $\sum_{k=0}^n \varepsilon^k \int_{\Omega_\mathrm{e}^\varepsilon} u_\mathrm{e}^k(x, x/\varepsilon)$ has to be close to $\int_{\Omega_\mathrm{e}^\varepsilon} u_\mathrm{e}^\varepsilon = 0$, as seen in the proof of Theorem 4.12.

A classic result tells us that

$$\int_{\Omega_\mathrm{e}^\varepsilon} u_\mathrm{e}^k\left(x, \frac{x}{\varepsilon}\right) = \int_\Omega \int_{Y_\mathrm{e}} u_\mathrm{e}^k(x, y) + O(\varepsilon). \tag{C.1}$$

So, for an approximation at order ε, it suffices to set

$$\int_\Omega u_\mathrm{e}^{k,\sharp}(x) = \int_\Omega \int_{Y_\mathrm{e}} u_\mathrm{e}^k(x, y) = 0.$$

But for approximation at order ε^{n+1}, we need to develop the remainder $O(\varepsilon)$ in (C.1). This is done in Theorem C.1. The new terms still depend on x/ε, therefore, in Theorem C.2, we recursively apply Theorem C.1 to approximate them. Finally, in Theorem C.3, we get the final approximation result, that is, in fact

$$\int_{\Omega_\mathrm{e}^\varepsilon} u_\mathrm{e}^k\left(x, \frac{x}{\varepsilon}\right) = \int_\Omega \int_{Y_\mathrm{e}} u_\mathrm{e}^k(x, y) + O(\varepsilon^{n+1}).$$

This result is a generalization of Lemma 1 in [33] and a variant of Lemma 3.1 in [32] for higher order approximation. It is also close to the Theorem in Appendix C of [34].

Lemma C.1. *Let $(D, E) = (Y, \Omega)$ or $(Y_\mathrm{e}, \Omega_\mathrm{e}^\varepsilon)$. Let $f : \Omega \times D \to \mathbb{R}$ such that for all $y \in D$, $x \mapsto f(x, y) \in \mathcal{C}^\infty_\mathrm{per}(\Omega)$ and for all $x \in \Omega$, $y \mapsto f(x, y) \in L^1(D)$ and is Y-periodic.*

Table B.1: Errors defined in Eq. (29), for the isotropic and anisotropic cells.

ε	$e^{\mathrm{e},0}_{\mathrm{L}^2}$	$e^{\mathrm{i},0}_{\mathrm{L}^2}$	$e^{\mathrm{e},0}_{\mathrm{H}^1}$	$e^{\mathrm{i},0}_{\mathrm{H}^1}$
Isotropic cell				
1/12	2.91×10^{-2}	1.08×10^{0}	4.22×10^{-2}	2.60×10^{-2}
1/15	1.94×10^{-2}	7.32×10^{-1}	2.81×10^{-2}	1.72×10^{-2}
1/18	1.46×10^{-2}	5.51×10^{-1}	2.11×10^{-2}	1.27×10^{-2}
1/21	1.17×10^{-2}	44.1×10^{-1}	1.69×10^{-2}	1.02×10^{-2}
Regression slope	0.99	0.98	1.00	1.02
Anisotropic cell				
1/12	3.24×10^{-2}	4.24×10^{-1}	4.72×10^{-2}	1.65×10^{-2}
1/15	2.56×10^{-2}	3.41×10^{-1}	3.79×10^{-2}	1.28×10^{-2}
1/18	2.15×10^{-2}	2.85×10^{-1}	3.15×10^{-2}	1.04×10^{-2}
1/21	1.84×10^{-2}	2.44×10^{-1}	2.69×10^{-2}	8.74×10^{-3}
Regression slope	1.00	0.98	1.00	1.14

ε	$e^{v_{\mathrm{m}}}_{\mathrm{L}^2}$	$e^{\mathrm{e},1}_{\mathrm{L}^2}$	$e^{\mathrm{i},1}_{\mathrm{L}^2}$	$e^{\mathrm{e},1}_{\mathrm{H}^1}$	$e^{\mathrm{i},1}_{\mathrm{H}^1}$
Isotropic cell					
1/12	1.77×10^{-2}	4.72×10^{-3}	1.25×10^{-1}	1.15×10^{-2}	2.79×10^{-2}
1/15	9.91×10^{-3}	2.15×10^{-3}	5.69×10^{-2}	5.27×10^{-3}	1.19×10^{-2}
1/18	6.57×10^{-3}	1.20×10^{-3}	3.27×10^{-2}	2.98×10^{-3}	6.92×10^{-3}
1/21	4.72×10^{-3}	7.59×10^{-4}	2.09×10^{-2}	1.94×10^{-3}	4.64×10^{-3}
Regression slope	1.43	1.99	1.94	1.94	1.95
Anisotropic cell					
1/12	1.20×10^{-2}	4.92×10^{-3}	5.32×10^{-2}	7.95×10^{-3}	1.12×10^{-2}
1/15	8.63×10^{-3}	3.14×10^{-3}	3.41×10^{-2}	5.16×10^{-3}	7.17×10^{-3}
1/18	6.65×10^{-3}	2.17×10^{-3}	2.39×10^{-2}	3.60×10^{-3}	5.02×10^{-3}
1/21	5.31×10^{-3}	1.60×10^{-3}	1.76×10^{-2}	2.66×10^{-3}	3.50×10^{-3}
Regression slope	1.46	2.01	1.96	1.95	2.07

For all $n \in \mathbb{N}$, we have

$$\int_E f\left(x, \frac{x}{\varepsilon}\right) = \int_\Omega \int_D f(x,y) + \sum_{k=1}^{n} \varepsilon^k \int_\Omega \mathcal{S}_k^D(f)\left(x, \frac{x}{\varepsilon}\right) + \varepsilon^{n+1} R_n^{\varepsilon,D}(f),$$

where

$$\mathcal{S}_k^D(f)(x,y) = \sum_{|\alpha|=k} \frac{1}{\alpha!} \int_D (z - \{y\})^\alpha \partial_x^\alpha f(x,z) dz, \tag{C.2}$$

where $\{y\}$ is the fractional part of y defined component-wise by

$$\{y\}_i = y_i - \lfloor y_i \rfloor, \quad i = 1, \dots, d,$$

with $\lfloor \cdot \rfloor$ the floor function, and

$$R_n^{\varepsilon,D}(f) = \tag{C.3}$$
$$\sum_{|\alpha|=n+1} \frac{n+1}{\alpha!} \int_{\Omega \times D} \left(y - \left\{\frac{x}{\varepsilon}\right\}\right)^\alpha \int_0^1 (1-t)^n (\partial_x^\alpha f)\left(x + \varepsilon t \left(y - \left\{\frac{x}{\varepsilon}\right\}\right), y\right) \mathrm{d}^3 t y x.$$

Proof. Let $\varepsilon > 0$, let $m \in N_\varepsilon$. Let $y \in D$ and $z \in Y$, the Taylor development of $f(\cdot, y)$ gives for $n \in \mathbb{N}$,

$$\begin{aligned} f(\varepsilon(y+m), y) = f(\varepsilon(z+m), y) &+ \sum_{k=1}^{n} \varepsilon^k \sum_{|\alpha|=k} \frac{1}{\alpha!} (y-z)^\alpha \partial_x^\alpha f(\varepsilon(z+m), y) \\ &+ \varepsilon^{n+1} \sum_{|\alpha|=n+1} \frac{n+1}{\alpha!} (y-z)^\alpha \int_0^1 (1-t)^n \partial_x^\alpha f\left(\varepsilon(z+m+t(y-z)), y\right). \end{aligned}$$

Integrate this equation over Y and D, and by change of variable, one gets

$$\begin{aligned} |Y| \int_{\varepsilon(D+m)} f\left(x, \frac{x}{\varepsilon}\right) &= \int_{\varepsilon(Y+m)} \int_D f(x,y) \\ &+ \sum_{k=1}^{n} \varepsilon^k \sum_{|\alpha|=k} \frac{1}{\alpha!} \int_{\varepsilon(Y+m)} \int_D (y - \left\{\frac{x}{\varepsilon}\right\})^\alpha \partial_x^\alpha f(x,y) \\ + \varepsilon^{n+1} \sum_{|\alpha|=n+1} \frac{n+1}{\alpha!} \int_{\varepsilon(Y+m)} \int_D (y - \left\{\frac{x}{\varepsilon}\right\})^\alpha \int_0^1 (1-t)^n \partial_x^\alpha f\left(x + \varepsilon t (y - \left\{\frac{x}{\varepsilon}\right\}), y\right). \end{aligned}$$

Sum over all $m \in N_\varepsilon$ and the proof is over. □

The correction $\int_\Omega \mathcal{S}_k^D(f)\,(x, x/\varepsilon)$ depends on ε, therefore it also needs to be approximated.

Lemma C.2. *Under the same hypothesis as Theorem C.1, for all $n \in \mathbb{N}$, we have*

$$\begin{aligned}\int_E f\left(x, \frac{x}{\varepsilon}\right) = \frac{1}{|Y|}\int_\Omega \int_D f(x,y) \\ + \frac{1}{|Y|}\sum_{k=1}^{n} \varepsilon^k \int_\Omega \int_Y \sum_{\substack{(\beta_j)\in(\mathbb{N}^*)^J \\ |\beta|=k}} \left(\mathcal{S}^Y_{\beta_1} \circ \cdots \circ \mathcal{S}^Y_{\beta_{J-1}} \circ \mathcal{S}^D_{\beta_J} \circ f\right)(x,y) \\ + \varepsilon^{n+1}\left(\sum_{l=0}^{n-1} \sum_{\substack{(\beta_j)\in(\mathbb{N}^*)^J \\ |\beta|=n-l}} R_l^{\varepsilon,Y}(\mathcal{S}^Y_{\beta_1} \circ \cdots \circ \mathcal{S}^Y_{\beta_{J-1}} \circ \mathcal{S}^D_{\beta_J} \circ f) + R_n^{\varepsilon,D}(f)\right),\end{aligned}$$

where $\mathcal{S}^D_k$ and $R^{\varepsilon,D}_k$ are defined in (C.2) *and* (C.3)*.*

Proof. The proof is done by induction. The case $n = 0$ is true because

$$\int_E f\left(x, \frac{x}{\varepsilon}\right) = \frac{1}{|Y|}\int_\Omega \int_D f(x,y) + \varepsilon R_0^{\varepsilon,D}(f).$$

To go from rank n to rank $n+1$, remark the induction relation (using Theorem C.1 at rank n and $n+1$)

$$R_n^{\varepsilon,D}(f) = \int_\Omega \mathcal{S}^D_{n+1}(f)\left(x, \frac{x}{\varepsilon}\right) + \varepsilon R^{\varepsilon,D}_{n+1}(f).$$

Using Theorem C.1 on $\mathcal{S}^D_{n+1}(f)$, we get

$$R_n^{\varepsilon,D}(f) = \frac{1}{|Y|}\int_\Omega \int_Y \mathcal{S}^D_{n+1}(f)(x,y) + \varepsilon(R_0^{\varepsilon,Y}(\mathcal{S}_{n+1}(f)) + R^{\varepsilon,D}_{n+1}(f)).$$

Therefore

$$\begin{aligned}R_l^{\varepsilon,Y}(\mathcal{S}^Y_{\beta_1} \circ \cdots \circ \mathcal{S}^Y_{\beta_{J-1}} \circ \mathcal{S}^D_{\beta_J} \circ f) \\ = \frac{1}{|Y|}\int_\Omega \int_Y (\mathcal{S}^Y_{l+1} \circ \mathcal{S}^Y_{\beta_1} \circ \cdots \circ \mathcal{S}^Y_{\beta_{J-1}} \circ \mathcal{S}^D_{\beta_J} \circ f)(x,y) \\ + \varepsilon(R_0^{\varepsilon,Y}(\mathcal{S}^Y_{l+1} \circ \mathcal{S}^Y_{\beta_1} \circ \cdots \circ \mathcal{S}^Y_{\beta_{J-1}} \circ \mathcal{S}^D_{\beta_J} \circ f) \\ + R^{\varepsilon,Y}_{l+1}(\mathcal{S}^Y_{\beta_1} \circ \cdots \circ \mathcal{S}^Y_{\beta_{J-1}} \circ \mathcal{S}^D_{\beta_J} \circ f)),\end{aligned}$$

and by change of indexes, the proof is over. □

Lemma C.3. *Under the same hypothesis as Theorem C.1, for all $n \in \mathbb{N}$, we have*

$$\left|\int_E f\left(x, \frac{x}{\varepsilon}\right) - \frac{1}{|Y|}\int_\Omega \int_D f(x,y)\right| \leq C(n,f)\varepsilon^{n+1},$$

where $C(n, f) > 0$ is a constant depending on n and f.

Proof. Starting from the result of Theorem C.2, we first show that for any $g : \Omega \times D \to \mathbb{R}$ such that for all $y \in D,\ x \mapsto g(x, y) \in \mathcal{C}^\infty_{\text{per}}(\Omega)$ and for all $x \in \Omega,\ y \mapsto g(x, y)$ is Y-periodic, for any $k \geq 1$,

$$\int_\Omega \int_Y \mathcal{S}_k^D(g)(x, y) = 0.$$

It suffices to perform an integration by parts relatively to the x-variable and recall that g and all its derivatives are x-periodic. Finally we bound the remainder, using the fact that for the same kind of g as before, for $l \in \mathbb{N}$,

$$|R_l^{\varepsilon,D}(g)| \leq \frac{d^{\frac{3(l+1)}{2}}}{(l+1)!}|\Omega||D| \sup_{(x,y)\in\Omega\times D,\ |\alpha|=l+1} |\partial_x^\alpha g(x, y)|$$

and

$$|\mathcal{S}_l^D(g)(x, y)| \leq \frac{d^{\frac{3l}{2}}}{l!}|D| \sup_{(x',y')\in\Omega\times D,\ |\alpha|=l} |\partial^\alpha g(x', y')|.$$

□

References

[1] S. Nath, J. P. DiMarco, D. E. Haines, Basic aspects of radiofrequency catheter ablation, Journal of Cardiovascular Electrophysiology 5 (10) (1994) 863–876. doi:10.1111/j.1540-8167.1994.tb01125.x.

[2] J. G. Andrade, Cryoablation for atrial fibrillation, Heart Rhythm O2 1 (1) (2020) 44–58. doi:10.1016/j.hroo.2020.02.004.

[3] J. Koruth, K. Kuroki, J. Iwasawa, Y. Enomoto, R. Viswanathan, R. Brose, E. D. Buck, M. Speltz, S. R. Dukkipati, V. Y. Reddy, Preclinical evaluation of pulsed field ablation: electrophysiological and histological assessment of thoracic vein isolation, Circulation: Arrhythmia and Electrophysiology 12 (12) (2019) e007781. doi:10.1161/CIRCEP.119.007781.

[4] G. Caluori, E. Odehnalova, T. Jadczyk, M. Pesl, I. Pavlova, L. Valikova, S. Holzinger, V. Novotna, V. Rotrekl, A. Hampl, et al., Ac pulsed field ablation is feasible and safe in atrial and ventricular settings: a proof-of-concept chronic animal study, Frontiers in Bioengineering and Biotechnology 8 (2020) 552357. doi:10.3389/fbioe.2020.552357.

[5] V. Y. Reddy, S. R. Dukkipati, P. Neuzil, A. Anic, J. Petru, M. Funasako, H. Cochet, K. Minami, T. Breskovic, I. Sikiric, et al., Pulsed field ablation of paroxysmal atrial fibrillation: 1-year outcomes of impulse, pefcat, and pefcat ii, Clinical Electrophysiology 7 (5) (2021) 614–627. doi:10.1016/j.jacep.2021.02.014.

[6] F. H. Wittkampf, H. Nakagawa, RF catheter ablation: lessons on lesions, Pacing and Clinical Electrophysiology 29 (11) (2006) 1285–1297. doi:10.1111/j.1540-8159.2006.00533.x.

[7] C. Tabaja, A. Younis, A. A. Hussein, T. L. Taigen, H. Nakagawa, W. I. Saliba, J. Sroubek, P. Santangeli, O. M. Wazni, Catheter-based electroporation: A novel technique for catheter ablation of cardiac arrhythmias, JACC: Clinical Electrophysiology 9 (9) (2023) 2008–2023. doi:10.1016/j.jacep.2023.03.014.

[8] D. Miklavcic, L. Towhidi, Numerical study of the electroporation pulse shape effect on molecular uptake of biological cells, Radiology and Oncology 44 (1) (2010) 34–41. doi:10.2478/v10019-010-0002-3.

[9] A. Ivorra, J. Villemejane, L. Mir, Electrical modeling of the influence of medium conductivity on electroporation, Physical Chemistry Chemical Physics 12 (34) (2010). doi:10.1039/C004419A.

[10] G. Jankowiak, C. Taing, C. Poignard, A. Collin, Comparison and calibration of different electroporation models - Application to rabbit livers experiments, ESAIM: Proceedings and Surveys 67 (Jun. 2020). doi:10.1051/proc/202067014.

[11] D. Voyer, A. Silve, L. M. Mir, R. Scorretti, C. Poignard, Dynamical modeling of tissue electroporation, Bioelectrochemistry 119 (2018) 98–110. doi:10.1016/j.bioelechem.2017.08.007.

[12] P. Agnass, E. van Veldhuisen, M. J. C. van Gemert, C. W. M. van der Geld, K. P. van Lienden, T. M. van Gulik, M. R. Meijerink, M. G. Besselink, H. P. Kok, J. Crezee, Mathematical modeling of the thermal effects of irreversible electroporation for in vitro, in vivo, and clinical use: a systematic review, International Journal of Hyperthermia 37 (1) (2020) 486–505, pMID: 32423258. doi:10.1080/02656736.2020.1753828.

[13] E. J. Jacobs, P. P. Santos, R. V. Davalos, Comprehensive characterization of waveform-dependent cardiac tissue electroporation for pulsed field ablation, Biosensors and Bioelectronics 289 (2025) 117890. doi:10.1016/j.bios.2025.117890.

[14] D. Meckes, M. Emami, I. Fong, D. H. Lau, P. Sanders, Pulsed-field ablation: Computational modeling of electric fields for lesion depth analysis, Heart Rhythm O2 3 (4) (2022) 433–440. doi:10.1016/j.hroo.2022.05.009.

[15] A. Petras, G. Amoros Figueras, Z. Moreno Weidmann, T. García-Sánchez, D. Viladés Medel, A. Ivorra, J. M. Guerra, L. Gerardo-Giorda, Is a single lethal electric field threshold sufficient to characterize the lesion size in computational modeling of cardiac pulsed-field ablation?, Heart Rhythm O2 6 (5) (2025) 671–677. doi:10.1016/j.hroo.2025.02.014.

[16] Q. Castellvi, A. Ivorra, Computational multiscale modeling of pulsed field ablation considering conductivity and damage anisotropy reveals deep lesion morphologies, International Journal for Numerical Methods in Biomedical Engineering 41 (8) (2025) e70077, e70077 CNM-Feb-25-0196.R1. doi:10.1002/cnm.70077.

[17] N. Labarbera, C. Drapaca, Anistropically varying conductivity in irreversible electroporation simulations, Theoretical Biology and Medical Modelling 14 (1) (nov 1 2017). doi:10.1186/s12976-017-0065-6.

[18] F. Aguel, K. A. Debrutn, W. Krassowska, N. A. Trayanova, Effects of electroporation on the transmembrane potential distribution in a two-dimensional bidomain model of cardiac tissue, Journal of Cardiovascular Electrophysiology 10 (5) (1999) 701–714. doi:10.1111/j.1540-8167.1999.tb00247.x.

[19] M. Deville, Mathematical Modeling of enhanced drug delivery by mean of Electroporation or Enzymatic treatment, Theses, Université de Bordeaux ; Università degli studi di Roma "Tor Vergata" (1972-....) (Nov. 2017).
URL https://theses.hal.science/tel-01699066

[20] O. Kavian, M. Leguèbe, C. Poignard, L. Weynans, "classical" electropermeabilization modeling at the cell scale, Journal of Mathematical Biology 68 (1–2) (2014) 235–265. doi:10.1007/s00285-012-0629-3.
URL http://dx.doi.org/10.1007/s00285-012-0629-3

[21] T. Kotnik, G. Pucihar, D. Miklavčič, Induced transmembrane voltage and its correlation with electroporation-mediated molecular transport, The Journal of Membrane Biology 236 (1) (2010) 3–13. doi:10.1007/s00232-010-9279-9.
URL http://dx.doi.org/10.1007/s00232-010-9279-9

[22] M. Leguèbe, A. Silve, L. Mir, C. Poignard, Conducting and permeable states of cell membrane submitted to high voltage pulses: Mathematical and numerical studies validated by the experiments, Journal of Theoretical Biology 360 (2014) 83–94. doi:10.1016/j.jtbi.2014.06.027.

[23] F. Chegini, A. Froehly, N. M. M. Huynh, L. F. Pavarino, M. Potse, S. Scacchi, M. Weiser, Efficient numerical methods for simulating cardiac electrophysiology with cellular resolution, in: COUPLED 2023 - 10th International Conference on Computational Methods for Coupled Problems in Science and Engineering, Chania, Greece, 2023.
URL https://inria.hal.science/hal-04407791

[24] M. Bendahmane, F. Mroue, M. Saad, R. Talhouk, Unfolding homogenization method applied to physiological and phenomenological bidomain models in electrocardiology, Nonlinear Analysis: Real World Applications 50 (2019) 413–447. doi:10.1016/j.nonrwa.2019.05.006.

[25] M. Pennacchio, G. Savaré, P. Colli Franzone, Multiscale modeling for the bioelectric activity of the heart, SIAM Journal on Mathematical Analysis 37 (2005) 1333–1370. doi:10.1137/040615249.

[26] G. Nguetseng, A general convergence result for a functional related to the theory of homogenization, SIAM Journal on Mathematical Analysis 20 (3) (1989) 608–623. doi:10.1137/0520043.

[27] G. Allaire, Homogenization and two-scale convergence, SIAM Journal on Mathematical Analysis 23 (6) (1992) 1482–1518. doi:10.1137/0523084.

[28] A. Collin, S. Imperiale, Mathematical analysis and 2-scale convergence of a heterogeneous microscopic bidomain model, Mathematical Models and Methods in Applied Sciences 28 (2018) 1–57. doi:10.1142/S0218202518500264.

[29] E. Frénod, Application of the averaging method to the gyrokinetic plasma, Asymptotic Analysis 46 (03 2007). doi:10.3233/ASY-2006-722.

[30] E. Frénod, P.-A. Raviart, E. Sonnendrücker, Two-scale expansion of a singularly perturbed convection equation, Journal de Mathématiques Pures et Appliquées 80 (8) (2001) 815–843. doi:10.1016/S0021-7824(01)01215-6.

[31] L. Trabucho, J. M. Viaño, Existence and characterization of higher-order terms in an asymptotic expansion method for linearized elastic beams, Asymptotic Analysis 2 (3) (1989) 223–255. doi:10.3233/ASY-1989-2303.

[32] G. Allaire, Z. Habibi, Second order corrector in the homogenization of a conductive-radiative heat transfer problem, Discrete and Continuous Dynamical Systems - B 18 (1) (2013) 1–36. doi:10.3934/dcdsb.2013.18.1.

[33] K. D. Cherednichenko, V. P. Smyshlyaev, On full two-scale expansion of the solutions of nonlinear periodic rapidly oscillating problems and higher-order homogenised variational problems, Archive for Rational Mechanics and Analysis 174 (2004) 385–442. doi:10.1007/s00205-004-0335-4.

[34] V. P. Smyshlyaev, K. D. Cherednichenko, On rigorous derivation of strain gradient effects in the overall behaviour of periodic heterogeneous media, Journal of the Mechanics and Physics of Solids 48 (6) (2000) 1325–1357. doi:10.1016/S0022-5096(99)00090-3.

[35] P. C. Franzone, G. Savaré, Degenerate evolution systems modeling the cardiac electric field at micro-and macroscopic level, in: Evolution Equations, Semigroups and Functional Analysis: in memory of Brunello Terreni, Springer, 2002, pp. 49–78.

[36] S. Sanfelici, Convergence of the Galerkin approximation of a degenerate evolution problem in electrocardiology, Numerical Methods for Partial Differential Equations: An International Journal 18 (2) (2002) 218–240.

[37] M. Bendahmane, K. H. Karlsen, Analysis of a class of degenerate reaction-diffusion systems and the bidomain model of cardiac tissue, Networks Heterog. Media 1 (1) (2006) 185–218.

[38] M. Boulakia, M. A. Fernández, J.-F. Gerbeau, N. Zemzemi, A coupled system of PDEs and ODEs arising in electrocardiograms modeling, Applied Mathematics Research eXpress 2008 (2008) abn002.

[39] M. Veneroni, Reaction–diffusion systems for the macroscopic bidomain model of the cardiac electric field, Nonlinear Analysis: Real World Applications 10 (2) (2009) 849–868.

[40] Y. Bourgault, Y. Coudière, C. Pierre, Existence and uniqueness of the solution for the bidomain model used in cardiac electrophysiology, Nonlinear Analysis: Real World Applications 10 (1) (2009) 458–482. doi:https://doi.org/10.1016/j.nonrwa.2007.10.007.
URL https://www.sciencedirect.com/science/article/pii/S146812180700199X

[41] F. Bader, M. Bendahmane, M. Saad, R. Talhouk, Microscopic tridomain model of electrical activity in the heart with dynamical gap junctions. part 1 – modeling and well-posedness, Acta Applicandae Mathematicae 179 (1) (May 2022). doi:10.1007/s10440-022-00498-7.
URL http://dx.doi.org/10.1007/s10440-022-00498-7

[42] A. Hodgkin, A. F. Huxley, A quantitative description of membrane current and its application to conduction and excitation in nerve, Journal of Physiology 117 (4) (1952) 500–544.

[43] K. ten Tusscher, A. Panfilov, Alternans and spiral breakup in a human ventricular tissue model, American Journal of Physiology-Heart and Circulatory Physiology 291 (3) (2006). doi:10.1152/ajpheart.00109.2006.

[44] R. Aliev, A. Panfilov, A simple two-variable model of cardiac excitation, Chaos, Solitons and Fractals 7 (3) (1996) 293–301. doi:10.1016/0960-0779(95)00089-5.

[45] C. C. Mitchell, D. G. Schaeffer, A two-current model for the dynamics of cardiac membrane, Bulletin of mathematical biology 65 (5) (2003) 767–793. doi:10.1016/S0092-8240(03)00041-7.

[46] K. DeBruin, W. Krassowska, Modelling electroporation in a single cell. I. Effects of field strength and rest potential., Biophysical Journal 77 (3) (1999) 1213–1224. doi:10.1016/S0006-3495(99)76973-0.

[47] O. Kavian, M. Leguèbe, C. Poignard, L. Weynans, "Classical" Electropermeabilization Modeling at the Cell Scale, Journal of Mathematical Biology 68 (1-2) (2014) 30. doi:10.1007/s00285-012-0629-3.

[48] A. Petras, G. Amoros Figueras, Z. Moreno Weidmann, T. García-Sánchez, D. Viladés Medel, A. Ivorra, J. M. Guerra, L. Gerardo-Giorda, Is a single lethal electric field threshold sufficient to characterize the lesion size in computational modeling of cardiac pulsed-field ablation?, Heart Rhythm O2 6 (5) (2025) 671–677. doi:10.1016/j.hroo.2025.02.014.

[49] J. G. Stinstra, B. Hopenfeld, R. S. MacLeod, On the passive cardiac conductivity, Annals of Biomedical Engineering 33 (2005) 1743–1751. doi:10.1007/s10439-005-7257-7.

[50] O. Tovar, L. Tung, Electroporation and recovery of cardiac cell membrane with rectangular voltage pulses, American Journal of Physiology 263 (4) (1992). doi:10.1152/ajpheart.1992.263.4.H1128.

[51] M. Leguebe, Modélisation de l'électroperméabilisation à l'échelle cellulaire, Theses, Université de Bordeaux (Sep. 2014).
URL https://theses.hal.science/tel-01148925

[52] H. Ammari, J. Garnier, L. Giovangigli, W. Jing, J. K. Seo, Spectroscopic imaging of a dilute cell suspension, Journal de Mathématiques Pures et Appliquées 105 (5) (2016) 603–661. doi:10.1016/j.matpur.2015.11.009.
URL https://hal.sorbonne-universite.fr/hal-01436816

[53] O. Kavian, Introduction à la théorie des points critiques et applications aux problèmes elliptiques, Springer Berlin, Heidelberg, 1991.

[54] P. Grisvard, Elliptic Problems in Nonsmooth Domains, Society for Industrial and Applied Mathematics, 2011. doi:10.1137/1.9781611972030.

[55] A. Evans, Partial Differential Equations, American Mathematical Society„ 1998.

[56] R. Lipton, Heat conduction in fine scale mixtures with interfacial contact resistance, SIAM Journal on Applied Mathematics 58 (1) (1998) 55–72. doi:10.1137/S0036139995295153.

[57] H. Ene, C. Timofte, Microstructure models for composites with imperfect interface via the periodic unfolding method, Asymptotic Analysis 89 (1-2) (2014) 111–122. doi:10.3233/ASY-141239.

[58] J. C. Neu, W. Krassowska, Homogenization of syncytial tissues., Critical reviews in biomedical engineering 21 2 (1993) 137–99.
URL https://api.semanticscholar.org/CorpusID:41260592

[59] M. Deville, Mathematical modeling of enhanced drug delivery by mean of electroporation or enzymatic treatment, Ph.D. thesis, Université de Bordeaux ; Università degli studi di Roma "Tor Vergata" (Nov. 2017).
URL https://theses.hal.science/tel-01699066

[60] F. Bader, M. Bendahmane, M. Saad, R. Talhouk, Derivation of a new macroscopic bidomain model including three scales for the electrical activity of cardiac tissue, Journal of Engineering Mathematics 131 (1) (Oct. 2021). doi:10.1007/s10665-021-10174-8.
URL http://dx.doi.org/10.1007/s10665-021-10174-8

[61] H. I. Ene, D. Poliševski, Model of diffusion in partially fissured media, Zeitschrift für angewandte Mathematik und Physik ZAMP 53 (6) (2002) 1052–1059. doi:10.1007/PL00013849.

[62] M. Amar, D. Andreucci, P. Bisegna, R. Gianni, On a hierarchy of models for electrical conduction in biological tissues, Mathematical Methods in the Applied Sciences 29 (7) (2006) 767–787. doi:10.1002/mma.709.

[63] J.-L. Auriault, H. I. Ene, Macroscopic modelling of heat transfer in composites with interfacial thermal barrier, International Journal of Heat and Mass Transfer 37 (18) (1994) 2885–2892. doi:10.1016/0017-9310(94)90342-5.

[64] M. A. Peter, M. Böhm, Different choices of scaling in homogenization of diffusion and interfacial exchange in a porous medium, Mathematical Methods in the Applied Sciences 31 (11) (2008) 1257–1282. doi:10.1002/mma.966.

[65] P. Donato, K. H. Le Nguyen, Homogenization of diffusion problems with a nonlinear interfacial resistance, Nonlinear Differential Equations and Applications 22 (5) (2015) 1345–1380. doi:10.1007/s00030-015-0325-2.

[66] G. Allaire, M. Briane, M. Vanninathan, A comparison between two-scale asymptotic expansions and Bloch wave expansions for the homogenization of periodic structures, SeMA Journal: Boletin de la Sociedad Española de Matemática Aplicada 73 (3) (2016) 237–259. doi:10.1007/s40324-016-0067-z.

[67] G. Allaire, A. Damlamian, U. Hornung, Two-scale convergence on periodic surfaces and applications, Mathematical Modelling of Flow through Porous Media (09 1995).

[68] F. Hecht, New development in Freefem++, Journal of Numerical Mathematics 20 (3-4) (2012) 251–265.
URL https://freefem.org/

[69] D. Šel, D. Cukjati, D. Batiuskaite, T. Slivnik, L. Mir, D. Miklavčič, Sequential finite element model of tissue electropermeabilization, IEEE Transactions on Biomedical Engineering 52 (5) (2005) 816–827. doi:10.1109/TBME.2005.845212.

[70] S. Nati Poltri, Mathematical modeling of cardiac tissue response after pulsed field ablation, Ph.D. thesis, Université de Bordeaux (Dec. 2024).
URL https://theses.hal.science/tel-04891219